THE STUDY OF APO-ENZYME/PROSTHETIC GROUPS AND THEIR APPLICATIONS IN CHEMICAL ANALYSIS

by

Dongxuan Shen

A dissertation submitted in partial fulfillment
of the requirements for the degree of
Doctor of Philosophy
(Chemistry)
in The University of Michigan
2009

Doctoral Committee:

Professor Mark E. Meyerhoff, Chair
Associate Professor Shuichi Takayama
Associate Professor Nils G. Walter
Assistant Professor Kristina I. Håkansson

ACKNOWLEDGEMENTS

First of all, I would like to thank my advisor, Dr. Mark E. Meyerhoff, for his teaching and guidance, his patience, his continuous support and encouragement throughout my dissertation work. His enthusiasm toward scientific research and his truth-seeking attitude will be a lifetime example for myself in pursuing future careers. I would also like to thank Dr. Hakansson, Dr. Takayama, and Dr. Walter for their service on my doctoral committee, especially Dr. Walter for the discussion and suggestions with synthetic PQQ work in Chapter 4.

Special thanks go to my collaborators at Berry & Associates. Without their expertise in the organic synthesis, one of my PQQ projects would be impossible to advance. I want to thank specifically Dr. Jack Hodges for the preparation of PQQ derivatives and collaboration on the project described in Chapter 4.

I also feel indebted to my past and present group members. I want to give special thanks to Dr. Hyoungsik Yim for his encouragement, support, and his help with starting my thesis research; Dr. Jeremy Mitchell-Koch, and Dr. Stacey Buchanan for their help during my rotation research; Dr. Sangyeul Huang for his helpful discussions with my organic synthesis work; Dr. Youngjea Kang and Dr. Wansik Cha for their insightful research idea discussions and interesting culture talks. I would also like to thank all other group members: Dr. Yiduo Wu, Dr. Zhengrong Zhou, Dr. Hairong Zhang, Dr. Fenghua

Zhang, Dr. Jason Bennet, Jun Yang, Lin Wang, Biyun Wu, Qinyi Yan, Laura Zimmerman, Natalie Walker. You all have made my life in Michigan very enjoyable.

I also appreciate all the support from my friends in JiaYin Chiristian Fellowship and AACCC: Pastor Teo, Shouchin and Michael Man, Paul and Alice Chao, Jinzhong and Yuanyuan, Xinen and Ji Fang, and all of the rest that I can't list all of your names. Thanks for your support and prayers!

Finally, I would like to thank my wife, Shiyan, my daughter, Noelle, and my mother, Okran Yang. Without their long lasting support and love, none of my work would be possible.

TABLE OF CONTENTS

LIST OF FIGURES

FIGURE

LIST OF TABLES

TABLE

LIST OF ABBREVIATIONS

AbCRP	Anti-CRP antibody
ABTS	2,2'-Azino-bis(3-ethylbenzothiazoline-6-sulfonic acid)
AlaOMe	Alanine Methyl Ester
ARIS	Apo-enzyme Reactivation Immunoassay System
Biotin-sulfo-NHS	N-Hydroxysulfosuccinimide ester of biotin
Boc-C6-COOH	N-(tert-butoxycarbonyl)glycine 6-(boc-amino)hexanoic acid
BSA	Bovine Serum Albumin
BtAbCRP	Biotinylated CRP antibody
CRP	C-reactive protein
DCC	N,N'-dicyclohexylcarbodiimide
DCM	Dichloromethane
DCPIP	2,6-Dichlorophenoindophenol
DIPEA	Diisopropylethylamine
DMF	Dimethylformamide
DNA	Deoxyribonucleic Acid
DOS	Bis(2-ethylhexyl) sebacate
ECL	Electrochemiluminescence
EDC	N-Ethyl-N'-(3-dimethylaminopropyl)carbodiimide
EIA	Enzyme Linked Homogeneous Immunoassay
ELISA	Enzyme Linked ImmunoSorbent Assay
EMIT	Enzyme Multiplied Immunoassay Technology
ESI	Electrospray Ionization
FAD	Flavin Adenosine Dinucleotide
FRET	Fluorescence Resonance Energy Transfer
FT-IR	Fourier Transform-Infrared Spectroscopy
G6PDH	Glucose-6-phosphate Dehydrogenase
GDH	Glucose Dehydrogenase
GOx	Glucose Oxidase
HABA	2-(4'-Hydroxyazobenzene) Benzoic acid
HOBt	1-Hydroxybenzotriazole
HPLC	High Pressure Liquid Chromatography
HRP	Horseradish Peroxidase
IPQ	Imidazolopyrroloquinoline
LOD	Limit of Detection

MALDI-TOF	Matrix Assisted Laser Desorption Ionization-Time of Flight
MDH	Methanol Dehydrogenase
MeCN	Acetonitrile
MIP	Molecularly Imprinted Polymer
MS	Mass Spectrometry
MWCO	Molecular Weight Cut-Off
NAD^+	Nicotinamide Adenine Dinucleotide
NHS	N-hydroxysucciniimide
NMR	Nuclear Magnetic Resonance Spectroscopy
PCR	Polymerase Chain Reaction
PEO	Polyethyleneoxide
PMMA	Polymethylmethacrylate
PMS	Phenazine Methosulfate
PQQ	Pyrroloquinoline Quinone
PVC	Poly(vinyl chloride)
QCM	Quartz Cystal Microbalance
RIA	Radioimmunoassay
SEM	Scanning Electron Microscopy
SWV	Square Wave Voltametry
T3	Triiodothyronine
T4	Thyroxine
TDMA	Tridodecylmethylammonium
TFA	Trifluoroacetic acid
THF	Tetrahydrofuran
TIS	Triisopropylsilane
TMB	3,3',5,5'-Tetramethylbenzidine
TNT	Trinitrotoluene
TRF	Time Resolved Fluorescence
Tris	Tri(hydroxylmethyl)aminomethane

CHAPTER 1

INTRODUCTION

1.1. Introduction

Since ancient times, enzymes have been used in people's everyday life such as in brewing, bread-making and cheese production. They remained as mystery matter until the first systematic study on a cell-free yeast extract, where the result suggested a chemical species other than whole cells was responsible for the fermentation of sugar to alcohol and carbon dioxide (1). The first crystal structure of the enzyme urease from Jack beans was proposed in 1926, resulting in widespread interest in the field of enzymology (2). Enzymes are highly efficient catalysts employed in numerous biochemical reactions in living cells including metabolism, biosynthesis, detoxification, and information storage (3). Just like its counterpart, the chemically synthesized catalyst, an enzyme works by lowering the activation energy of a reaction by stabilizing the transition state structure via complex formation (4). Further, an enzyme acts only on certain specific molecules, otherwise known as substrates, and catalysis occurs in the three-dimensional structure of the substrate-binding pocket known as the active site of the enzyme. The high efficiency and high specificity, on one hand, makes the enzyme an ideal target for drug discovery (5). On the other hand, researchers routinely utilize

enzymes as a tracer for quantifying a particular biological event such as antibody-antigen interactions, complementary DNA binding, protein-ligand interactions, etc..

Recent developments in molecular biology, biochemistry and instrumental methods, such as X-ray crystallography, have enabled researchers to examine the mechanism of an enzyme at the atomic level. Elucidation of enzyme structures and their related functions provided a path for chemists to possibly devise new strategies to employ enzymes in signal transduction. When redox enzymes, such as oxido-reductases, are catalyzing reactions, electron transfer occurs between the oxidized substrate and the enzyme. The electrons generated will be either further transferred to surrounding molecular oxygen or other electron mediators/acceptors. In order to be thermodynamically favorable, the redox potential of an electron acceptor needs to be higher than its precedent partners during the electron relay process. A scale describing the redox potential of some important biological electron carriers is shown in Figure 1.1 (1). The measurement of redox potential is carried out electrochemically by dissolving an oxidizing agent in water and measuring the voltage required to reduce it to a stable product.

Being mostly a cluster of polypeptide chains in nature, the interior of enzymes, including the active center, is naturally an insulator. The ability of electron transfer from the interior of the proteins to the outside environment is well explained by the theory of electron tunneling (6). However, there's a certain limit on the distance over which the electrons can travel. To facilitate this process, an electron mediator, which freely diffuses into the active site of the enzyme, is employed to carry the electrons over longer distance

until donating the electrons to an appropriate acceptor. The oxidized electron mediator is then ready for another round of electron shuttling.

1.2. Enzymes and Prosthetic Groups

Enzyme prosthetic groups, also called enzyme cofactors, were discovered in the late 19^{th} and early 20^{th} centuries (4). These small organic molecules, many of them vitamins, showed remarkable importance in curing certain dietary disorders. Over many years these coenzymes were identified with their chemical structures elucidated. Some representative cofactors and their enzymatic functions are summarized in Table 1.1 (4). In most cases, the cofactor and the enzyme associate with each other using weaker noncovalent interactions such as hydrogen bonding, electrostatic interaction, as well as dipole-dipole or hydrophobic interactions. In some cases, however, the cofactors are covalently bonded to an amino acid residue of the enzyme, forming thioester bonds with cysteine residues (7) or Schiff bases with lysine residues (8). If an enzyme requires a cofactor to be functional, the protein portion of the enzyme is referred to as the apo-enzyme, and holo-enzyme when the small molecular cofactor is included. The apo-enzyme can be prepared by physically extracting the prosthetic group out of its mother protein body after a denaturation process using acid or organic solvents, usually followed by chromatographic separations (9). Another way of preparing apo-enzymes is based on recombinant DNA technology by purposely expressing the genes regulating the production of solely the apo-form of the enzyme (10). The prosthetic groups can be added back later to reconstitute enzyme activity. The regeneration of the enzyme activity through the recombination of enzyme and its prosthetic group formed the basis for this

dissertation. Two enzyme-prosthetic group pairs employed in this work are described in detail below.

1.2.1. Glucose Dehydrogenase (GDH) and Pyrroloquinoline Quinone (PQQ)

The discovery of PQQ can be traced back to the year of 1964, when Hauge (11) reported that in a bacterial glucose dehydrogenase existed a dissociable cofactor that was neither a pyridine nucleotide (NAD^+) nor a flavin. However, the structure of PQQ, as shown in Figure 1.2, remained unknown until the late 1970s (12-14). There are two types of PQQ containing enzymes, quinoproteins and quino-hemo-proteins. Quinoproteins, such as GDH, aldose dehydrogenase (15), and glycerol dehydrogenases (16), contain only PQQ in the active center. Quino-hemo-proteins, such as fructose dehydrogenase (17) and alcohol dehydrogenase (18), contain PQQ and one or more heme groups. These enzymes are produced by gram-negative bacteria such as *Acinetobacter calcoaceticus* in the case of GDH and are located in either the periplasmic space or on the outer surface of the cytoplasmic membrane. Two types of functional GDH have been found: a soluble GDH (sGDH), which exists in the cytoplasm, and a membrane bound GDH (mGDH). It has been shown that these two enzymes have different molecular weights, pH optima, substrate specificity, and enzyme kinetics (19, 20).

PQQ, an ortho-quinone, is noncovalently bound to apo-GDH through ionic interactions between its carboxylic groups and basic amino acid residues at the active center of the enzyme (21). In the presence of calcium ions, sGDH can form a dimer, as shown in Figure 1.3; further, the calcium ions interact with the ortho-quinone groups on the PQQ to help facilitate glucose oxidation (22). PQQ supports two- or one-electron transfers and involves two half-reactions as shown in Figure 1.4. The reductive half-

reaction involves the formation of the reduced quinone coenzyme, while the oxidative half-reaction is characterized by transfer of electrons from the reduced quinone coenzyme to an electron acceptor, such as ubiquinones as in the case of the membrane bound GDH (23), cytochrome c as in the case of alcohol dehydrogenases (24) or molecular oxygen such as in copper amine oxidase (25). The reports on the identity of the natural electron acceptor for soluble GDH have been controversial, and the electron acceptor remains unknown although electrons can be transferred from $PQQH_2$ to cytochrome b-562 (26, 27). Soluble GDH can oxidize a wide range of pentose and hexose sugars, as well as mono- and disaccharides, to their corresponding lactones. Two possible reaction mechanisms, hydride transfer and addition–elimination mechanisms (see Figure 1.5) (25, 28, 29), have been proposed for methanol dehydrogenase (MDH) and sGDH. However, more recent molecular dynamics simulation suggested that MDH and sGDH catalyze their respective redox reactions via the same hydride transfer mechanism and not by a covalent addition-elimination mechanism (30).

The redox potentials of quinone coenzymes are generally in the range of 0.06-0.13 V (versus normal hydrogen electrode, pH 6.8-7.5) (31), with the PQQ having an E^0 value of 90 mV (32). Another commonly used electron mediator, phenazine methyl sulfate (PMS) with a reported E^0 value of 63 mV (33), is also employed in this dissertation. The redox potential of dichlorophenol indophenol (DCPIP), a redox dye used in most of the present study to accept electrons from reduced PQQ bound to the GDH active site, is about 270 mV (34), making it an excellent electron sink.

1.2.2. Horseradish Peroxidase (HRP) and Heme

Heme, as shown in Figure 1.6a, is a metallo-compound made up of an iron ion coordinated to the tetrapyrrole ring system, known as the protoporphyrin moiety, through its four nitrogen atoms (35). The iron in the heme of hemoglobin is in the ferrous state (Fe^{2+}) to allow reversible binding with oxygen (35). Iron is oxidized to ferric form (Fe^{3+}) when hemoglobin is oxidized to methemoglobin. Release of heme from globin leads to the oxidation of heme to hematin (Figure 1.6b) and in the presence of chloride ions, heme is converted to hemin (Figure 1.6c). Heme is a prosthetic group for a large number of cellular proteins as summarized in Table 1.2 (36) and these proteins carry out diverse biological functions such as respiration (37), signal transduction (38), regulation of cell growth (39), and gene expression (40).

HRP, as shown in Figure 1.7, is isolated from horseradish roots (*Amoracia rusticana*) and belongs to the ferroprotoporphyrin group of peroxidases. HRP readily combines with hydrogen peroxide (H_2O_2) and the resultant [HRP-H_2O_2] complex can oxidize a wide variety of chromogenic hydrogen donors such as pyrogallol, trimethylbenzidine (TMB) and 2,2′-azino-bis(3-ethylbenzothiazoline-6-sulfonic acid) (ABTS). HRP has also found wide applications in immunoassays, immunoblotting, and immunohistochemistry, where it has been used exclusively as a label for immunoglobulins or protein A (41).

1.3. Enzyme-linked Homogeneous and Heterogeneous Binding Assays

Since Yallow and Berson's introduction of radioimmunoassays (RIA) (42), immunoassays have received wide acceptance as an analytical tool in various fields including clinical analysis (43), environmental monitoring (44), study of biochemical activity (45), and the development of warning systems for homeland security (46).

Immunoassays take advantage of the highly specific recognition event between antibody and antigen (analyte). The utilization of radioisotopic labels gives the technique high sensitivity and wide applicability. However, the drawbacks of using a radioisotope are also apparent, including the potential health hazards and cost of appropriate waste disposal. Hence, the utilization of enzymes as tracers has been a preferred method of labeling for immunoassays for the past 35 years.

1.3.1. Enzyme-linked Homogeneous Binding Assays

Enzyme linked homogeneous immunoassay (EIA) (see principle shown in Figure 1.8) operates in a similar manner as RIA. A fixed concentration of enzyme labeled ligand (analyte of interest or its derivative forms) is mixed with a sample containing the analyte (free form) in the presence of a fixed and limiting concentration of an analyte specific antibody or binding protein. The competition between the enzyme labeled compound and free compound for the limited binding sites on the antibody or binding proteins determines the detection range and sensitivity of the assay format. Homogeneous competitive binding assays have found numerous applications in the field of clinical analysis because of their sensitivity and simplicity, with no washing step being required. The binding of the antibody with the enzyme-ligand conjugates results in a significant loss in enzyme activity due to steric interference or conformational changes in the enzyme structure. In the presence of the analyte, the enzyme activity is increased due to the competition for the antibody binding sites. An example of modern EIA is enzyme multiplied immunoassay technology (EMIT) (47), the first commercially available homogeneous EIA (48). One of the drawbacks of this technology is that the target

samples are usually limited to low molecular weight small molecules such as vitamins, drugs and hormones.

In 1981, Morris (49) demonstrated the concept that the enzyme prosthetic group could be modified and used as an enzyme signal modulator. Flavin adenosine dinucleotide (FAD), the prosthetic group of apo-glucose oxidase (apo-GOx), was successfully derivatized and the resulting FAD derivative was coupled to various analytes such as theophiline and trinitrotoluene (TNT) (50), in the development of a novel immunoassay technology called apo-enzyme reactivation immunoassay system (ARIS). Very similar to the enzyme based homogeneous competitive binding assay (EMIT), the detection scheme of ARIS is illustrated in Figure 1.9, where FAD is covalently conjugated with a hapten (analyte) and the resulting conjugate is able to reactivate the apo-GOx. The binding of the conjugate with an antibody to the analyte triggers the total inhibition of enzyme reactivation. In the presence of free analyte, however, the enzyme activity is regenerated due to the competition for the antibody binding sites between the free analyte and the conjugated analyte. Thus, the free analyte activity is correlated with the degree of the apo-GOx reactivation. A portion of the studies presented in this thesis is dedicated to investigating other available enzyme-prosthetic group pairs in hope of further extending the scope of their analytical applications in homogeneous binding assays.

1.3.2. Enzyme-linked Heterogeneous Binding Assays

Non-competitive binding assays are also referred to as immunometric or sandwich assays. In 1971, Engvall and Perlman (51) introduced a technique termed enzyme linked immunosorbent assay (ELISA), which was also described by Addison and Hales (52) in

the same year. In contrast to a homogeneous assay, it utilizes a solid support as a platform on which the immunochemical reactions are carried out. Therefore, multiple washings are required after the equilibration of the binding events between the antibody, the antigen, and an enzyme labeled agent. These heterogeneous binding assays have become the gold standard for sample analysis in the clinical chemistry field, in spite of long incubation times and intensive labor required. The reasons for the popularity of the ELISAs are the high sensitivity associated with this assay method, the ability of analyzing samples from complex matrices such as blood, and the high throughput afforded by 96 well (or greater) microtiter plates in which such ELISAs are carried out.

1.3.3. Nanospheres as Sensitive Tracers for Heterogeneous Binding Assays

Despite the wide applications of enzyme labeled binding assays, more sensitive or "PCR-like" amplification methods are desired for detecting even lower levels of biomolecules. With the advancement of nanotechnology, micro/nano materials including quantum dots (53), gold nanoparticles (54), nanotubes (55), nanowires (56) and polymeric particles or silica particles (57) have gained more and more interest in the development of diagnostic assays for biological analytes such as proteins and DNA. These novel materials not only aid in constructing the appropriate signal transduction platforms (nanowires used as field effect transistor (58), gold nanoparticles used for surface plasmon enhancement (59) and silver particles for surface enhancement Raman detection (60)), but also provide improved sensitivity by acting as a carrier for numerous reporter molecules. Dequaire demonstrated a sensitive immunoassay for IgG using gold nanoparticles as an antibody label, where the signal was detected by stripping voltammetry after gold dissolution with acid (61). Wang's group developed a sensitive

electrochemical assay based on the bar coding type technology using various inorganic semiconductor nanoparticles (CdS, PbS, ZnS) for the detection of multiple proteins or DNA (62). Lin's group at PNNL also developed highly sensitive immunoassays using apoferritin-templated metallic phosphate labels or poly[guanine] coated silica nanoparticles with electrochemical detection, e.g., square wave voltammetry (SWV) (63). Besides these, functionalized liposomes (64), polymeric microspheres loaded with electrochemiluminescent agents (65) and enzyme modified silica particles (66) have also been applied successfully in the development of novel binding assays.

1.4. Development of a Novel Homogeneous Cleaving Enzyme Assay

At present, proteolytic enzyme activities are assessed in a variety of ways including quantification of end-products of substrate reactions or via direct colorimetric/fluorescence changes when the enzymes act on given chromogenic substrates. Different methods for quantification of a proteolytic end-products include assays based on reversed phase HPLC (67, 68) and monitoring end-product concentration by UV-Vis spectrophotometry or fluorescence (69). Labeled biological oligomer substrates can be employed in such assays. Synthesized or engineered probes/substrates contain one or more specific cleavage sites for the target enzymes, and chromogenic (70) or fluorogenic (71, 72) species attached to the ends of the oligomers serve as signal generators. Current methods usually depend on the accumulation of "marker" intensity of the end-product via the proteolysis activity. Intramolecularly quenched fluorescent probes based on FRET (Fluorescence Resonance Energy Transfer) have also been widely used for the purpose of achieving greater sensitivity and lower detection limits (73-75).

Some highly sensitive enzymatic assays employ radio-labeled substrates, which can either be attached to 96 microwell plates (76) or linked to magnetic beads (77). In these assays, radiation emitting reaction products need to be separated from unreacted substrates before quantification via suitable radiation detection. Therefore, these types of assay methods are discontinuous and a high disposal cost is associated with the radioactive materials. HPLC or HPLC-MS based assays can quantify and identify the end-products from undigested oligomer substrates. However, these methods are also time consuming, discontinuous and not suitable for high throughput screening procedures.

The first steps in developing real-time continuous spectroscopic enzyme activity assays include the design of both chromogenic or fluorogenic probes and specific detection schemes. This is done by attaching dye molecules to one end of the substrate, allowing for the measurement of a chromogenic product (e.g., nitroaniline, etc.). The information regarding enzyme kinetics is obtained indirectly by monitoring increasing intensity of dye molecules as they are liberated (in a form that yields significant absorbance or fluorescence) by the catalytic reaction. In contrast, methods based on FRET employ probes containing a fluorescent donor and a quenching acceptor on opposite ends of the oligomer. As the proteolytic or nuclease action begins, the donor and acceptor are separated resulting in increased fluorescence. The fluorescence-based methods are very sensitive due to intrinsic characteristics of fluorescence itself; however, even in FRET, there is already a significant background fluorescence signal owing to the inability of the acceptor species to fully quench the luminescence, and this limits the

ultimate detection limits. Further, none of these methods have ever employed any additional amplification mechanisms to obtain even greater sensitivity.

Other assays that do not require the use of fluorogenic, chromogenic or radio-labeled substrates include enzyme-coupled assays (78) and assays using surface plasmon resonance spectroscopy (79). These methods monitor proteolytic action of enzymes, but have a relatively narrow detection range, poor sensitivity, or require complicated instrumentation, which are major limitations. Other than these methods, a general assay format using calorimetry (80) to measure the heat generated during enzymatic activity has also been reported.

1.5. Statement of Research

The present dissertation work focuses on the design and development of a novel signal amplification system based on the reconstitution of an enzyme with its prosthetic group. The remarkable signal generation ability of these two entities enables the development of ultra-sensitive measurements for chemical analysis. Two major directions are pursued in this study. In the first approach, an ultra-sensitive immunoassay system is developed, wherein either a PQQ doped polymeric nanosphere will be used as an antibody label (heterogeneous immunoassay), as illustrated in Figure 1.10, or a ligand conjugated apo-GDH will be investigated for its potential advantage as a signal modulator (homogeneous binding assay). The second approach is to evaluate the chemically modified derivatives of PQQ and hemin for their ability to reconstitute the apo-GDH and apo-HRP, respectively. The optimized derivatives are then investigated for their potential usability as novel biological probes for the development of a protease assay and an ARIS type assay.

In Chapter 2, a high-sensitivity immunoassay system using PQQ doped polymeric nanospheres as a sensitive tracer is demonstrated and its analytical performance is evaluated for the detection of a small molecule, e.g. biotin, as well as a bio-macromolecule, e.g. C-reactive protein (CRP). A lipophilic version of a PQQ salt is prepared using a simple two-phase extraction method followed by a screening study in search of the optimum polymeric material to be compatible with this lipophilic PQQ salt. The organic solvent tolerance of apo-GDH is also studied with buffers containing varying percentages of organic solvents and the optimum solvent is chosen for the subsequent PQQ release study. It should be noted that the content of this chapter has been published as a full paper in *Analytical Chemistry* (81).

The primary goal of Chapter 3 is the evaluation of a biotinylated apo-GDH for use as a signal modulator in the development of a homogeneous competitive binding assay. In the presence of the binder protein, e.g. avidin, the electron transfer efficiency from biotin-GDH is inhibited compared to the case of a holo-enzyme where the binder protein prevents the access of the substrate only. The ratio of biotin to GDH is optimized and the lowest possible concentration of the avidin for the maximum inhibition of biotinylated apo-GDH is used in order to obtain the best limit of detection for biotin.

Chapter 4 focuses on the chemical modification of PQQ and the evaluation of the best possible strategy to link an oligomer substrate with minimum loss of the activity when reconstituted with apo-GDH. The reconstitution assay, together with HPLC and mass spectrometry (MS), suggest the optimum conjugation site of PQQ for future assay development.

In Chapter 5, hemin conjugation to a hormone thyroxine, a small amino acid and a 15-mer peptide is demonstrated. The synthetic derivatives are characterized with HPLC and MS followed by the evaluation of biological activity in the presence of apo-HRP. The hemin-peptide conjugate is further investigated as a probe for a protease assay and the hemin-thyroxine conjugate is studied as a potential probe in an ARIS type assay for the detection of free thyroxine.

Finally in Chapter 6, the versatility and advantages of using apo-enzyme/prosthetic group reconstitution assay systems are summarized. Some critical improvements needed to enhance the utility of such assay systems are also addressed. The future direction of the research in utilizing PQQ derivatives for the application of real-time PCR and ultrasensitive assay for small drug molecules is then suggested.

Cofactor	Enzymatic Use	Examples of Enzyme
Flavins	Redox center - proton transfer	Glucose oxidase, succinate dehydrogenase
Hemes	Redox center - ligand binding	Cytochrome oxidase, cytochrome P450s
NAD and NADP	Redox center - proton transfer	Alcohol dehydrogenase, ornithine cyclase
Pyridoxal phosphate	Amino group transfer	Aspartate transaminase, arginine racemase
Quinones	Redox center - hydrogen transfer	cytochrome b_0, dihydroorotate dehydrogenase
Coenzyme A	Acyl group transfer	Pyruvate dehydrogenase

Table 1.1. Selected examples of enzyme cofactors and their enzymatic functions. (4)

Hemoproteins (proteins containing heme as prosthetic group)
Respiratory cytochromes (Cytochrome c, Cytochrome c oxidase, Cytochrome reductase)
Cytochromes P450
Catalases
Nitrophorins
Peroxidases
Heme-responsive transcription factors (NPAS2, mPER2, and Bach1)
Globin-like coupled sensors
Histidine kinases
eIF2α-kinase (translational initiation factor)
Nitric oxide synthases (NOS): heme based sensors (~50 members)
Soluble guanylate cyclases (SGC): heme-based sensors
Cyclic nucleotide phosphodiesterases
Hemoglobins (heme based sensors)
Myoglobins (heme based sensors)
Nitrite reductase
δ-Aminolevulinic acid synthase
Hydroxylamine oxidoreductase

Table 1.2. Proteins/enzymes with heme as prosthetic group (22).

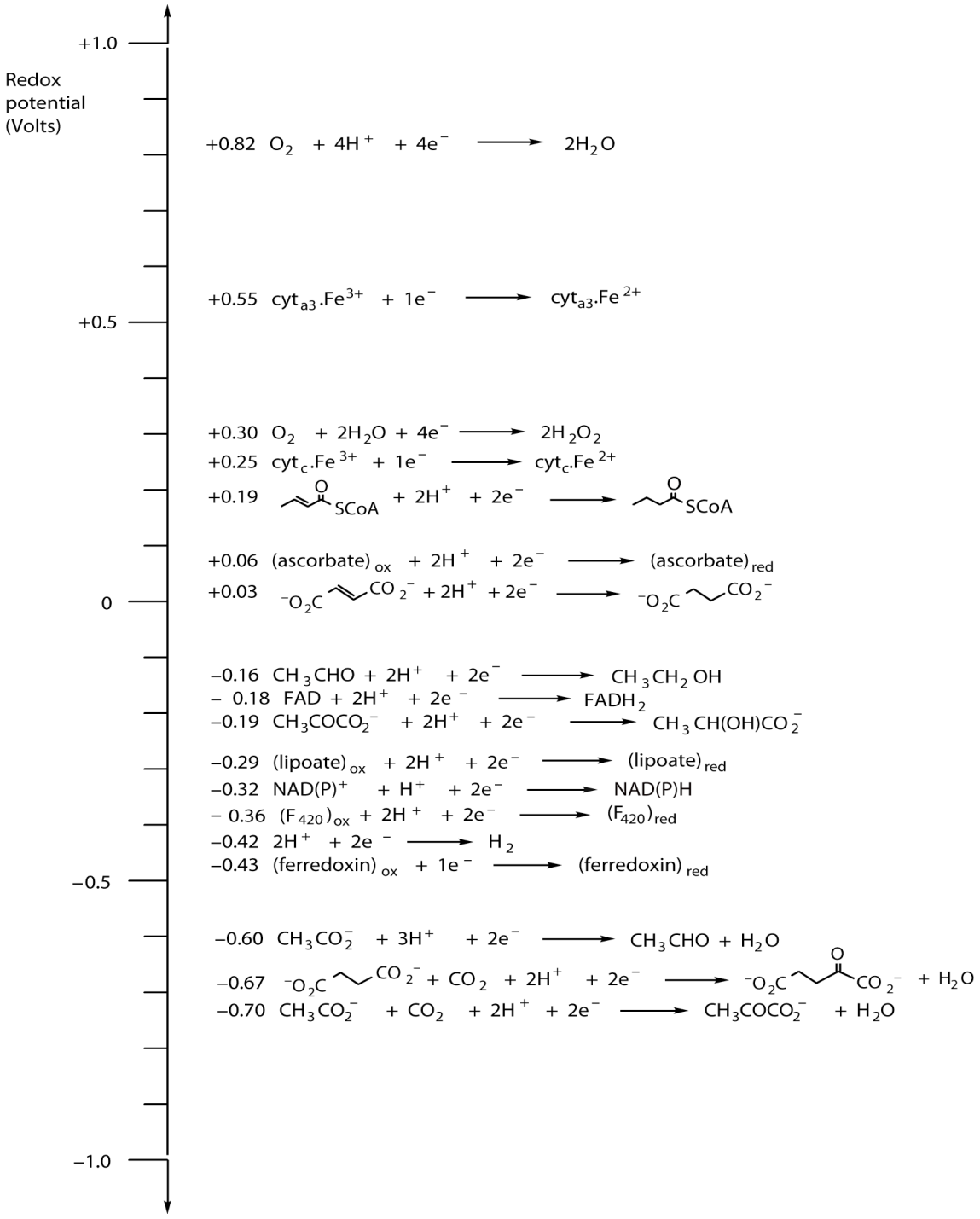

Figure 1.1. Some biologically important redox potentials. (1)

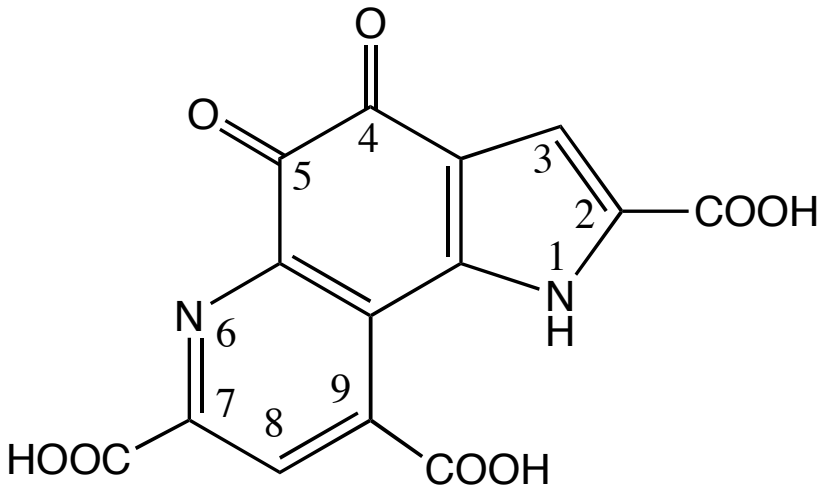

Figure 1.2. Structure of PQQ.

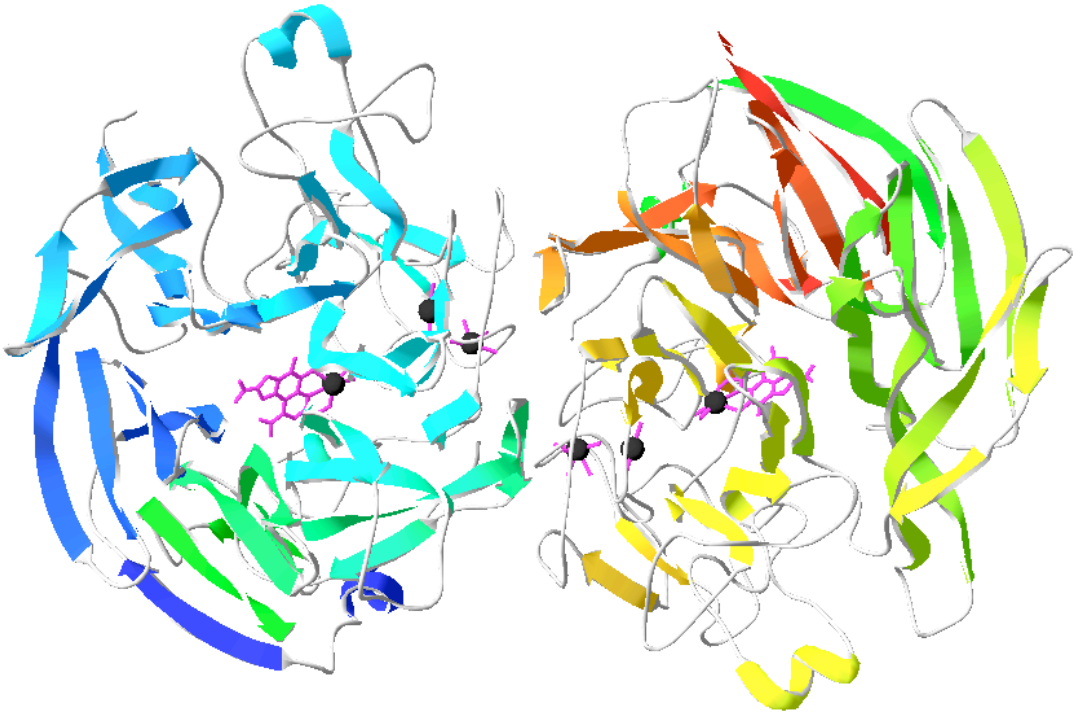

Figure 1.3. Crystal structure of the dimeric GDH with PQQ bound at the active center in the presence of calcium ions (black spheres) (The picture was generated using DeepView with the data of PDB ID: 1C9U).

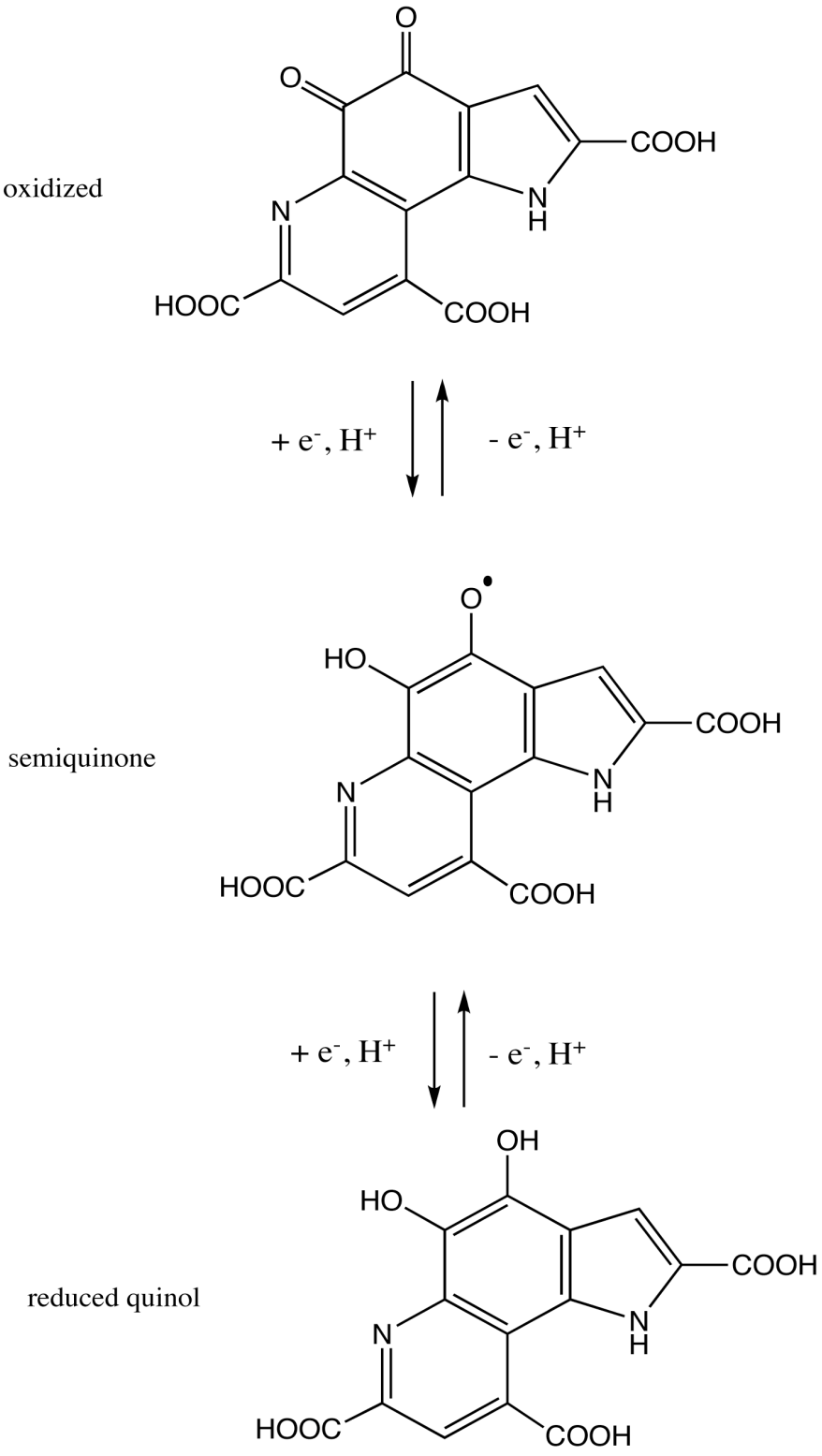

Figure 1.4. Redox states of PQQ.

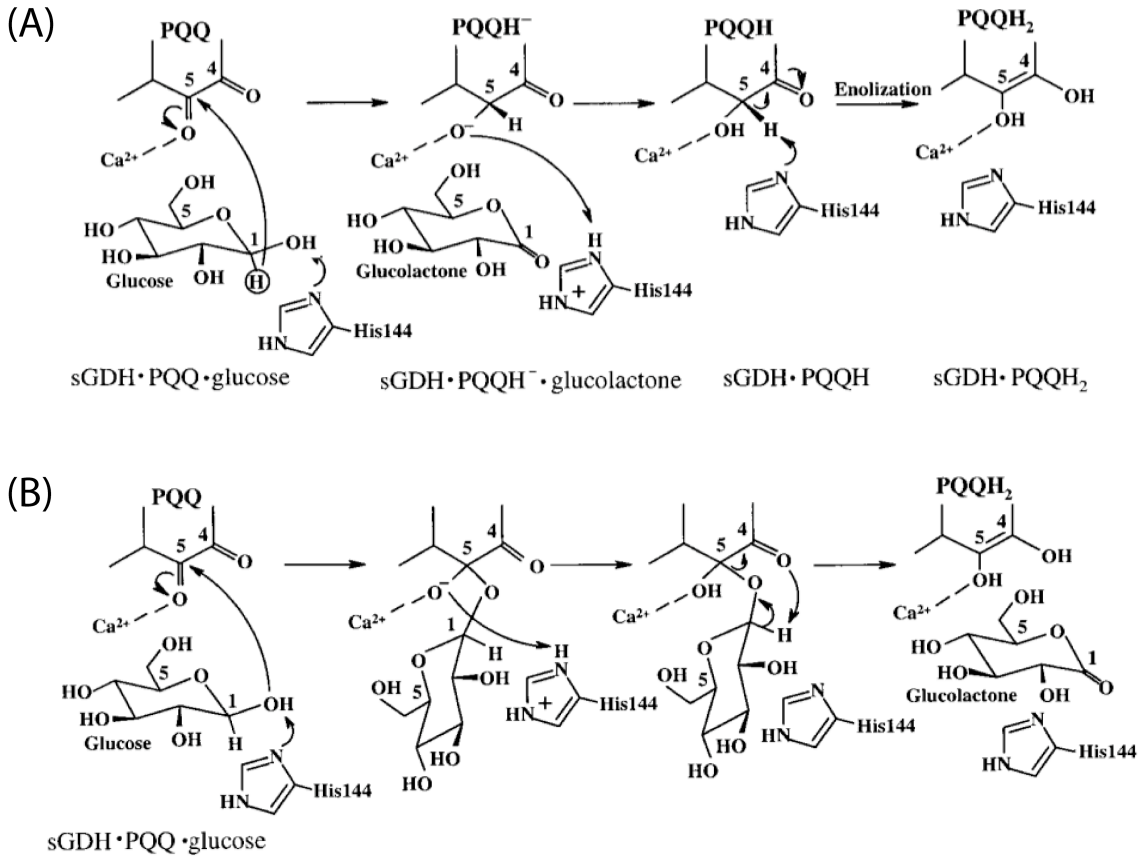

Figure. 1.5. Proposed glucose oxidation mechanisms by sGDH: (A) hydride transfer; (B) addition-elimination. (28)

(a)

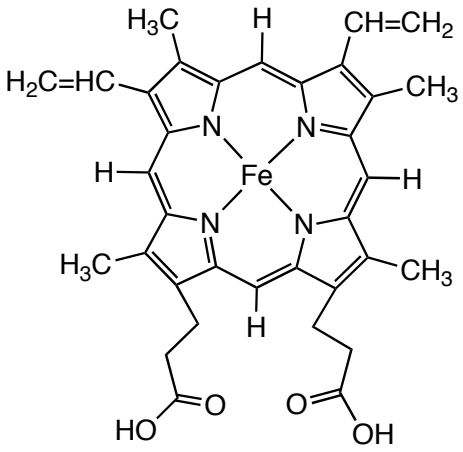

(b)

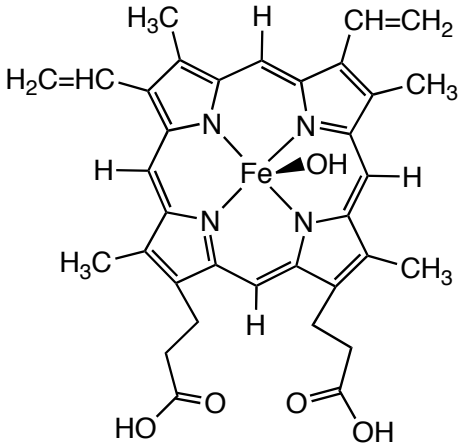

(c)

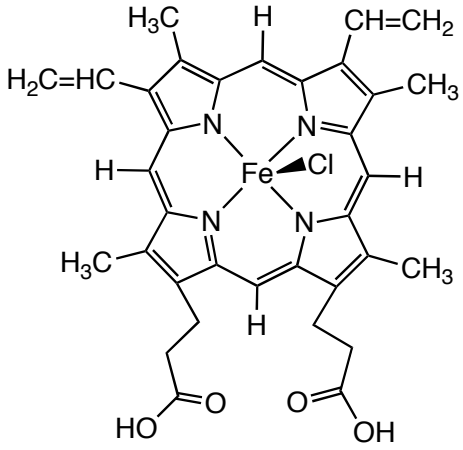

Figure 1.6. Structures of heme, hematin and hemin.

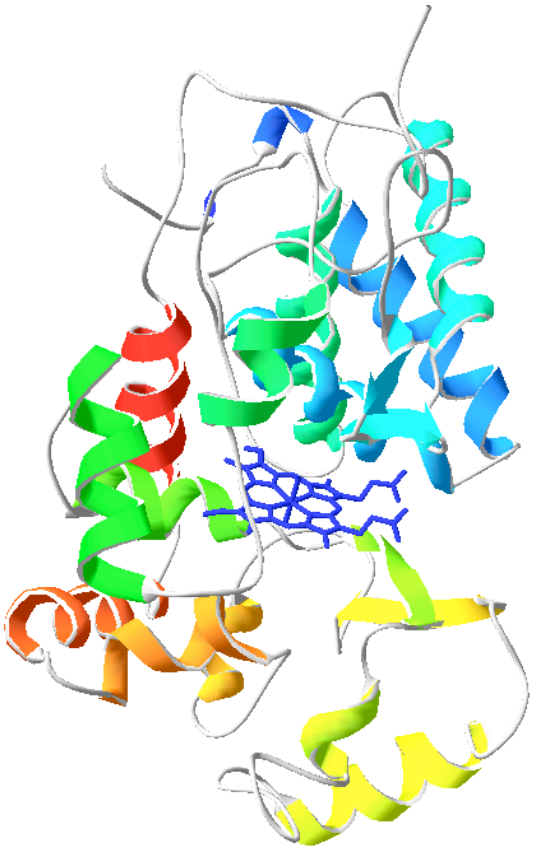

Figure 1.7. Crystal structure of HRP with heme bound at the active center (The picture was generated using DeepView with the data of PDB ID: 1W4W).

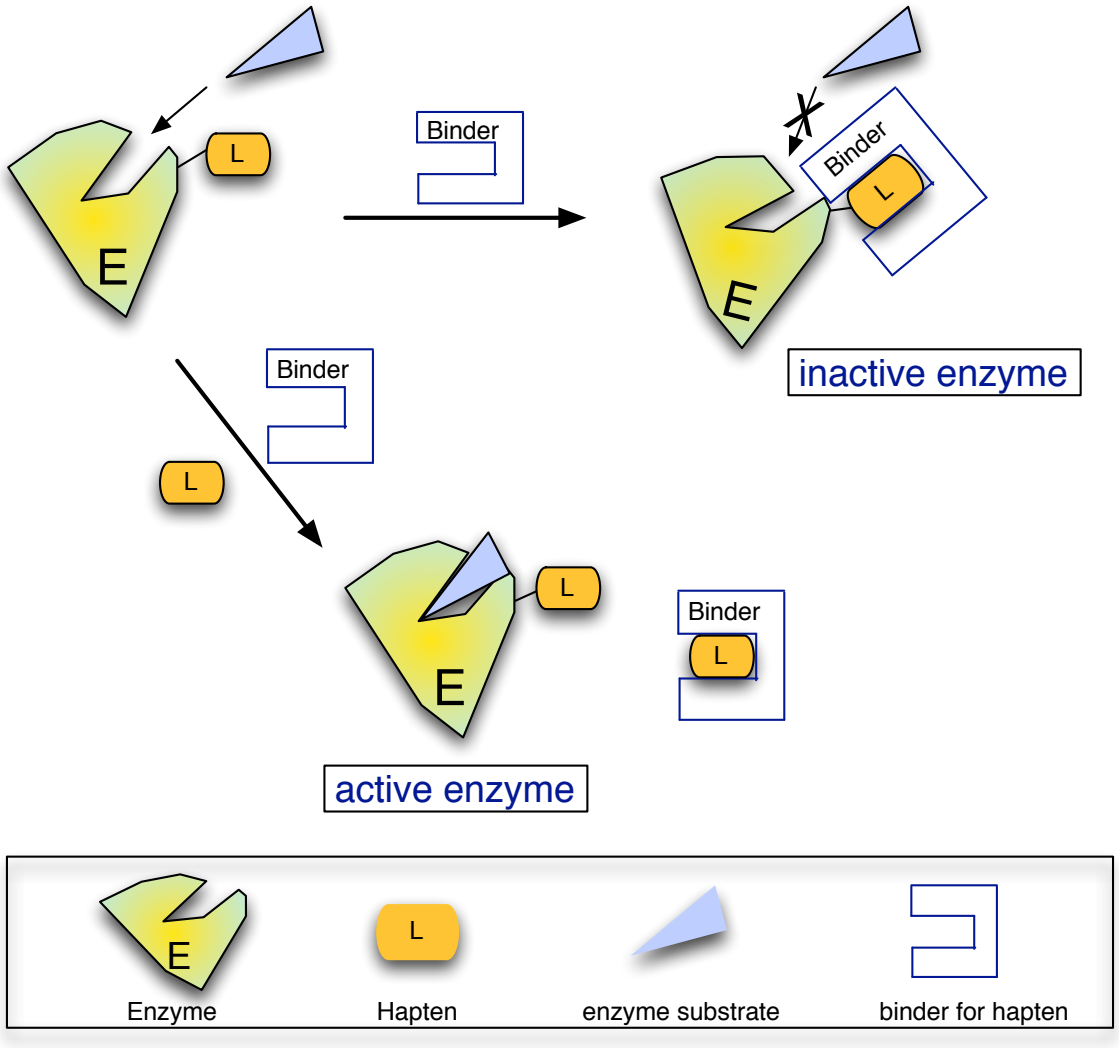

Figure 1.8. The working principle of homogeneous enzyme-linked immunoassay (EIA).

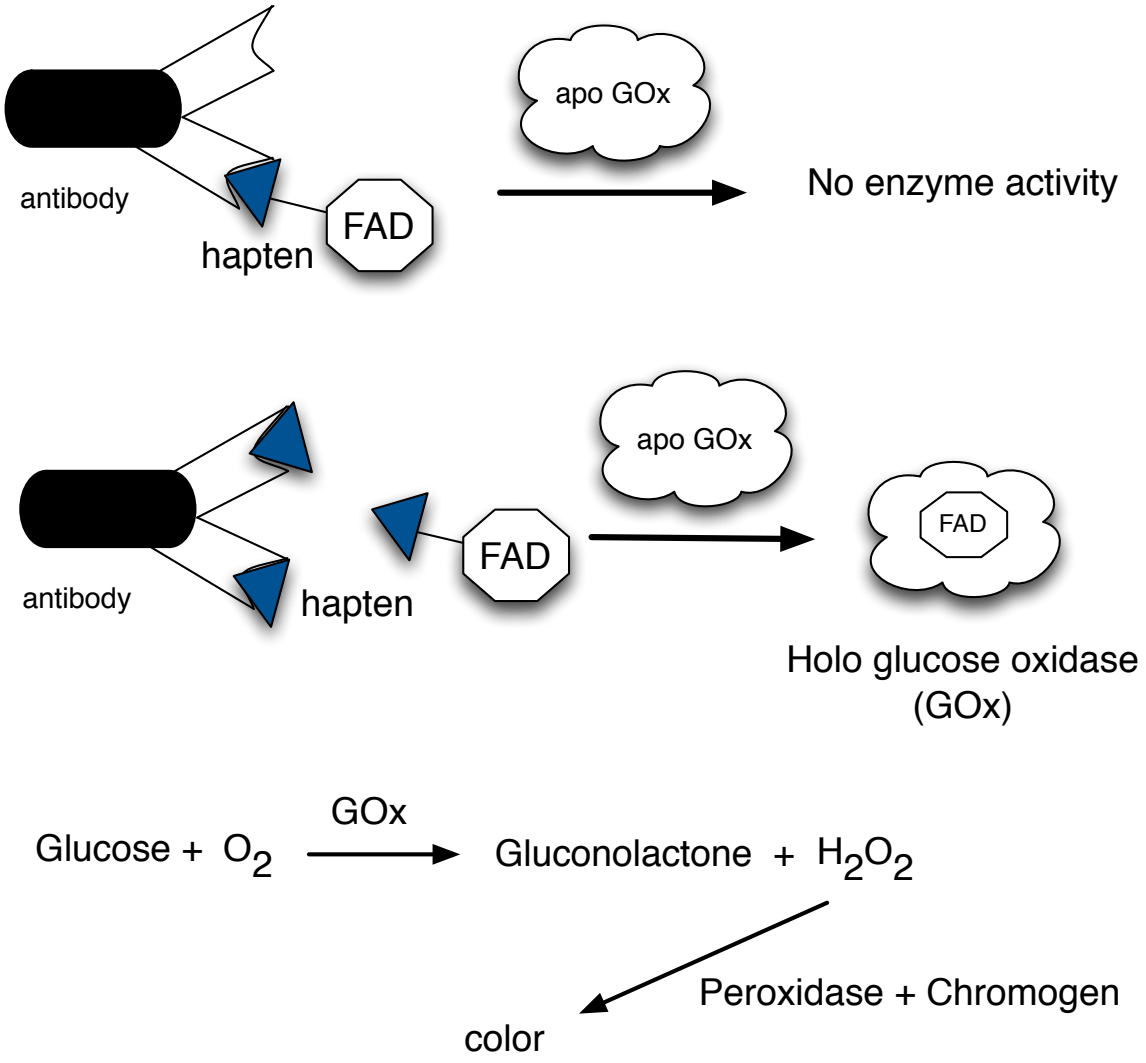

Figure 1.9. The working principle of ARIS.

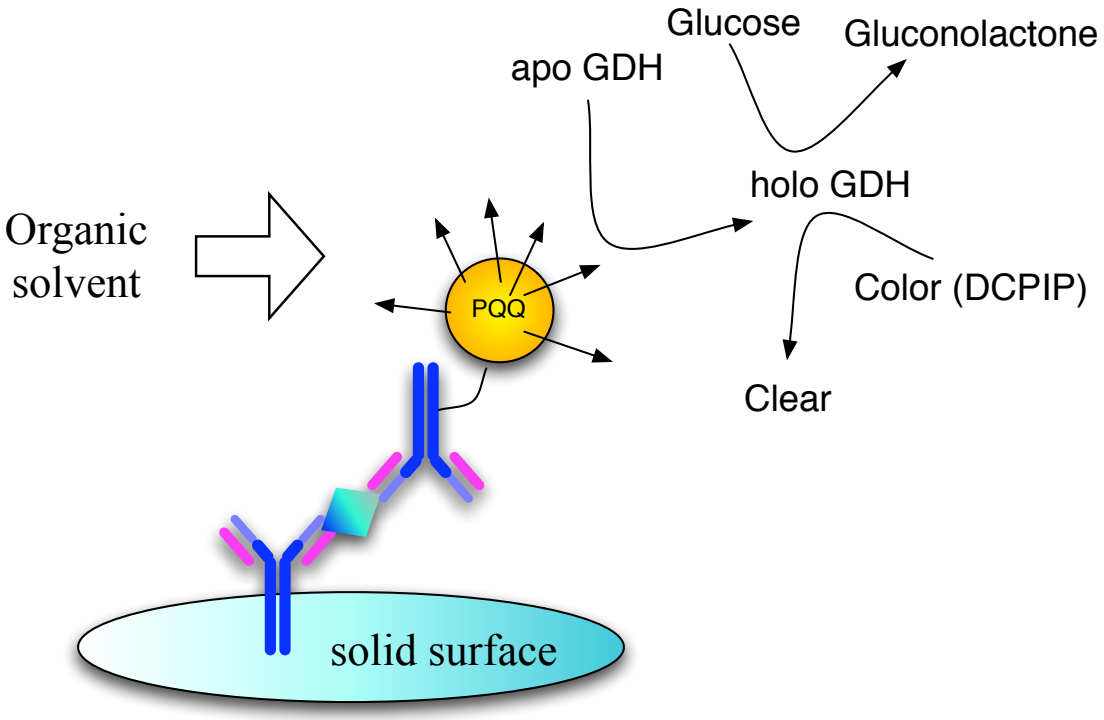

Figure 1.10. Illustration of a "sandwich" type immunoassay system with a prosthetic group doped nanosphere as a label.

1.6. References

(1) Bugg, T. *Introduction to Enzyme and Coenzyme Chemistry*, Blackwell Publications; 2004.

(2) Bugg, T.D.H. *Nat. Prod. Rep.* **2001,** *18*, 465-493.

(3) Voet, D.; Voet, J.G. *Biochemistry, 3rd ed.;* John Wiley & Sons, Inc.; 2004.

(4) Copeland, R.A. *Enzymes: A Practical Introduction to Structure, Mechanism, and Data Analysis*, Wiley - VCH, 2000.

(5) Raghavan, A.; Hang, H. *Drug Discov. Today* **2009,** *14*, 178-184.

(6) Hay, S.; Scrutton, N. *Photosynth. Res.* **2008,** *98*, 169-177.

(7) Jiang, Y.; Trnka, M.;Medzihradszky, K.;Ouellet, H.;Wang, Y.;De, M., PRO. *J. Inorg. Biochem.* **2009,** *103*, 316-325.

(8) Yoshikane, Y.; Yokochi, N.; Ohnishi, K.; Hayashi, H.; Yagi, T. *Biochem. J.* **2006,** *396*, 499-507.

(9) Kilty, C.G.; Maruyama, K.; Forrest, H.S. *Arch. Biochem. Biophys.* **1982,** *218*, 623-625.

(10) Olsthoorn, A.J.J.; Duine, J.A. *Arch. Biochem. Biophys.* **1996,** *336*, 42-48.

(11) Hauge, J. *J. Biol. Chem.* **1964,** *239*, 3630-&.

(12) Salisbury, S.; Forrest, H.; Cruse, W.; Kennard, O. *Nature* **1979,** *280*, 843-844.

(13) Westerling, J.; Frank, J.; Duine, J. *Biochem. Biophys. Res. Commun.* **1979,** *87*, 719-724.

(14) Duine, J.A.; Frank, J.; Vanzeeland, J.K. *FEBS Lett.* **1979,** *108*, 443-446.

(15) Southall, S.; Doel, J.; Richardson, D.; Oubrie, A. *J. Biol. Chem.* **2006,** *281*, 30650-30659.

(16) Matsushita, K.; Toyama, H.; Yamada, M.; Adachi, O. *Appl. Microbiol. Biotchnol.* **2002,** *58*, 13-22.

(17) Khan, G.; Shinohara, H.; Ikariyama, Y.; Aizawa, M. *J. Electroanal. Chem.* **1991,** *315*, 263-273.

(18) Ikeda, T.; Matsushita, F.; Senda, M. *Biosens. Bioelectron.* **1991,** *6*, 299-304.

(19) Davidson, V. *Princeples and Applications of Quinoproteins* Chapter 3 (p. 47-50), Marcel Dekker Inc., 1993.

(20) Iswantini, D.; Kano, K.; Ikeda, T. *Biochem. J.* **2000,** *350*, 917-923.

(21) Oubrie, A.; Rozeboom, H.; Kalk, K.; Olsthoorn, A.; Duine, J.; Dijkstra, B. *EMBO J.* **1999,** *18*, 5187-5194.

(22) Sato, A.; Takagi, K.; Kano, K.; Kato, N.; Duine, J.; Ikeda, T. *Biochem. J.* **2001,** *357*, 893-898.

(23) Matsushita, K.; Shinagawa, E.; Adachi, O.; Ameyama, M. *Biochemistry* **1989,** *28*, 6276-6280.

(24) Davidson, V. *Arch. Biochem. Biophys.* **2004,** *428*, 32-40.

(25) Anthony, C. *Biochem. J.* **1996,** *320*, 697-711.

(26) Dokter, P.; Vanwielink, J.; Vankleef, M.; Duine, J. *Biochem. J.* **1988,** *254*, 131-138.

(27) Okuda, J.; Wakai, J.; Yuhashi, N.; Sode, K. *Biosens. Bioelectron.* **2003,** *18*, 699-704.

(28) Frank, J.; Dijkstra, M.; Duine, J.; Balny, C. *Eur. J. Biochem.* **1988,** *174*, 331-338.

(29) Itoh, S.; Kawakami, H.; Fukuzumi, S. *J. Am. Chem. Soc.* **1997,** *119*, 439-440.

(30) Reddy, S.; Bruice, T. *Protein Sci.* **2004,** *13*, 1965-1978.

(31) Banerjee, R. *Redox biochemistry*, Wiley-Interscience, 2008.

(32) Bergethon, P. *Anal. Biochem.* **1990,** *186*, 324-327.

(33) Yabuki, S.; Mizutani, F.; Asai, M. *Biosens. Bioelectron.* **1991,** *6*, 311-315.

(34) Kumar, S.; Acharya, S. *Anal. Biochem.* **1999,** *268*, 89-93.

(35) Kaplan, B.; Tricoche, M.; Vanderhog. *Ann. NY. Acad. Sci.* **1974,** *241*, 334-346.

(36) Tsiftsoglou, A.; Tsamadou, A.; Papadopoulou, L. *Pharmacol. Therapeut.* **2006,** *111*, 327-345.

(37) Tanaka, R.; Tanaka, A. *Annu. Rev. Plant Biol.* **2007,** *58*, 321-346.

(38) Hsu, H.Y.; Chu, L.C.; Hua, K.F.; Chao, L. *J. Cell. Physiol.* **2008,** *215*, 603-612.

(39) Edison, E.; Bajel, A.; Chandy, M. *Eur. J. Haematol.* **2008,** *81*, 411-424.

(40) Kapitulnik, J.; Maines, M. *Trends Pharmacol. Sci.* **2009,** *30*, 129-137.

(41) Arakawa, H.; Maeda, M.; Tsuji, A. *Anal. Biochem.* **1979,** *97*, 248-254.

(42) Yalow, R.; Berson, S. *J. Clin. Invest.* **1960,** *39*, 1157.

(43) Todd, J.; Freese, B.;Lu, A.; Held, D.; Morey, J.; Livingston, R.; Goix, P. *Clin. Chem.* **2007,** *53*, 1990-1995.

(44) Li, X.M.; Yang, X.; Zhang, S. *Trend Anal. Chem.* **2008,** *27*, 543-553.

(45) Jaroszewicz, J.; Rogalska, M.; Flisiak, R. *Biomarkers* **2008,** *13*, 478-485.

(46) Regan, J.; Makarewicz, A.; Hindson, B.; Metz, T.; Gutierrez, D.; Corzett, T.; Hadley, D.; Mahnke, R.; Henderer, B.; Breneman, J.; Weisgraber, T.; Dzenitis, J. *Anal. Chem.* **2008,** *80*, 7422-7429.

(47) Gooch, J.; Caldwell, R.; Turner, G.J.; Colbert, D. *J Immunoassay* **1992,** *13*, 85-96.

(48) Rubensteke, U., EF; SCHNEIDERS. *Biochem. Bioph. Res. Co.* **1972,** *47*, 846.

(49) Morris, D.L.; Ellis, P.; Carrico, R.; Yeager, F.; Schroeder, H.; Albarella, J.; Boguslaski, R.; Hornby, W.; Rawson, D. *Anal. Chem.* **1981,** *53*, 658-665.

(50) Dosch, M.; Weller, M.; Bückmann, A.; Niessner, R. *Fresenius. J. Anal. Chem.* **1998,** *361*, 174-178.

(51) Engvall, E.; Jonsson, K.; Perlmann, P. *Biochim. Biophys. Acta* **1971,** *251*, 427.

(52) Addison, G.; Hales, C. *Horm. Metab. Res.* **1971,** *3*, 59-60.

(53) Medintz, I.; Mattoussi, H.; Clapp, A. *Int. J. Nanomed.* **2008,** *3*, 151-167.

(54) Taton, T.A.; Mirkin, C.A.; Letsinger, R.L. *Science* **2000,** *289*, 1757-1760.

(55) Komaba, S.; Mitsuhashi, T.; Shraishi, S. *Electrochemistry* **2008,** *76*, 619-624.

(56) Brunker, S.; Cederquist, K.; Keating, C.D. *Nanomedicine* **2007,** *2*, 695-710.

(57) Jain, T.K.; Roy, I.; De, T.K.; Maitra, A. *J. Am. Chem. Soc.* **1998,** *120*, 11092-11095.

(58) Lee, H.S.; Kim, K.S.; Kim, C.J.; Hahn, S.; Jo, M.H. *Biosens. Bioelectron.* **2009,** *24*, 1801-1805.

(59) Choi, S.; Kim, H.S.; Kang, W.; Kim, J.H.; Cho, Y.J.; Kim, J.H. *J. Nanosci. Nanotechnol.* **2008,** *8*, 4569-4573.

(60) Seney, C.; Gutzman, B.; Goddard, R. *J. Phys. Chem.* **2009,** *113*, 74-80.

(61) Dequaire, M.; Degrand, C.; Limoges, B. *Anal. Chem.* **2000,** *72*, 5521-5528.

(62) Liu, G.D.; Wang, J.; Kim, J.; Jan, M.R.; Collins, G. *Anal. Chem.* **2004,** *76*, 7126-7130.

(63) Liu, G.D.; Wang, J.; Wu, H.; Lin, Y.Y.; Lin, Y.H. *Electroanalysis* **2007,** *19*, 777-785.

(64) Kumada, Y.; Tomioka, K.; Katoh, S. *J. Chem. Eng. Jpn.* **2001,** *34*, 943-947.

(65) Miao, W.J.; Bard, A.J. *Anal. Chem.* **2004,** *76*, 7109-7113.

(66) Wu, Y.F.; Chen, C.; Liu, S.Q. *Anal. Chem.* **2009,** *81*, 1600-1607.

(67) Gehringer, H., Von Der Helm, K.; Seelmeir, S.; Weiβbrich, B.; Eberle, J.; Nitschko, H. *J. Virol. Methods* **2003,** *109*, 143-152.

(68) Jewell, D.; Swietnicki, W.; Dunn, B.; Malcolm, B. *Biochemistry* **1992,** *31*, 7862-7869.

(69) Sinicropi, D.; Baker, D.L.; Prince, W.S.; Shiffer, K.; Shak, S. *Anal. Biochem.* **1994,** *222*, 351-358.

(70) Badalassi, F.; Nguyen, H.; Crotti, P.; Reymond, J. *Helv. Chim. Acta* **2002,** *85*, 3090-3098.

(71) Tolun, G.; Myers, R.S. *Nucleic Acids Res.* **2003,** *31*, e111.

(72) Tompa, P.; Schad, E.; Baki, A.; Alexa, A.; Batke, J.; Friedrich, P. *Anal. Biochem.* **1995,** *228*, 287-293.

(73) Grahn, S.; Ullmann, D.; Jakubke, H.D. *Anal. Biochem.* **1998,** *265*, 225-231.

(74) Li, J.J.; Geyer, R.; Tan, W. *Nucleic Acid Res.* **2000,** *28*, e52.

(75) Liu, L.; Tang, Z.; Wang, K.; Tan, W.; Li, J.; Guo, Q.; Meng, X.; Ma, C.; Meng C. *The Analyst* **2005,** *130*, 350-357.

(76) Gutierrez, O.A.; Salas, E.; Hernandez, Y.; Lissi, E.A.; Castrillo, G.; Reyes, O.; Garay, H.; Aguilar, A.; Garcia, B.; Otero, A.; Chavez, M.A.; Duarte, C.A. *Anal. Biochem.* **2002,** *307*, 18-24.

(77) Wu, Y.Q.; Abeles, R.H. *Anal. Biochem.* **1995,** *229*, 143-144.

(78) Cathers, B.E.; Schloss, J.V. *Anal. Biochem.* **1996,** *241*, 1-4.

(79) Steinrucke, P.; Aldinger, U.;Hill, O.; Hillisch, A.; Basch, R.; Diekmann, S. *Anal. Biochem.* **2000,** *286*, 26-34.

(80) Todd, M.J.; Gomez, J. *Anal. Biochem.* **2001,** *296*, 179-187.

(81) Shen, D. and Meyerhoff, M. E. *Anal. Chem.* **2009**, *81*, 1564-1569.

CHAPTER 2

PQQ-DOPED POLYMERIC NANOSPHERES AS SENSITIVE TRACER FOR BINDING ASSAYS

2.1. Introduction

Immunoassays and other bioaffinity assays (e.g., DNA) are now employed routinely in the areas of clinical diagnostics (1, 2), environmental monitoring (3) and homeland security (4). While earlier binding assays employed radioisotopes, enzymes, and fluorescent tracers, in recent years there has been a significant effort to utilize nanoparticles as tracers for such assays (5). For example, gold (6) or silver (7) metal spheres, inorganic nanocrystals (8) and nanowires (9), fluorescent nanocrystals (10) and fluorescent silica nanoparticles (11), and apoferritin nanospheres (12) have all been reported as potential labels for bioaffinity assays. However, in most instances, to achieve reasonably low detection limits (ng/mL for sandwich type immunoassays (13)), some type of fluorescence read-out instrumentation is necessary.

Recent work by Miao et al. has shown that polymeric microparticles can also be loaded with electrochemiluminescent ruthenium complexes, and that such particles can be utilized as labels in binding assays by releasing the electrochemical tracer from the particles after the binding reaction (5, 14). Detection limits on the order of sub-µg/mL for CRP were reported using electrochemically generated chemiluminescent method to measure the released ruthenium complex. Herein, we describe a new type of polymeric

nanospere label that contains pyrroloquinoline quinone (PQQ), and detection at low levels can be readily achieved with simple spectrophotometry or even via a visual read.

PQQ is a prosthetic group for a host of PQQ dependent redox enzymes. It was first discovered in the 1960's but its exact structure was not elucidated until 1979 (15-18). Proteins bearing PQQ molecules are classified as quinoproteins (18). Glucose dehydrogenase (GDH) is one such quinoprotein that is widely used for enzymatic detection of glucose (see Chapter 1). PQQ binds tightly to apo-GDH in the presence of calcium ions and this site serves as the catalytic center for the conversion of glucose to gluconolactone (19). Two electrons and two protons are transferred to PQQ with the oxidation of glucose as illustrated in Figure 2.1a. The binding of PQQ to apo-GDH in a GDH-PQQ reconstitution assay can be monitored electrochemically (20) or colorimetrically (21).

In the present work, we describe a method to dope PQQ within 450 nm sized polymethacrylate spheres and characterize these nanospheres with respect to PQQ content and potential utility for conducting binding assays of both low MW and macromolecular species. The GDH-PQQ reconstitution assay is evaluated, for the first time, in the presence of organic solvents so that loaded PQQ can be readily extracted for enzymatic detection after the nanosphere bioaffinity reaction. It will be shown that acetonitrile is the optimal added solvent for both retaining GDH activity and releasing PQQ from the polymeric nanosphere materials. Finally, the PQQ-doped particles are used as a tracer for devising competitive assays for low MW analyte (biotin), and also for devising a non-competitive sandwich type immunoassay to detect C-reactive protein

(CRP) at ng/mL levels in accordance with the general detection scheme illustrated in Figure 2.1b.

2.2. Experimental

2.2.1. Materials and Reagents:

PQQ was obtained from Iris Biotech GmbH (Marktredwitz, Germany). PQQ dependent apo-glucose dehydrogenase, pre-activated 96-well microtiter plates (NUNC amino) and polypropylene 96-well microtiter plates were purchased from Fisher Scientific. Trihydroxylmethylaminomethane base (Tris), Tween 20, ethanolamine hydrochloride, tridodecylmethylammonium chloride (TDMA), bovine serum albumin (BSA), 2,6-dichlorophenolindophenol (DCPIP), glucose, C-reactive protein (CRP) standards, poly(vinyl chloride) (PVC, high molecular weight), bis(2-ethylhexyl) sebacate (DOS), polystyrene (M.W. 1447000), polymethylmethacrylate (PMMA, low molecular weight), carboxylated poly(vinyl chloride) (1% wt carboxyl) and sulfosuccinimidyl biotin were all obtained from Sigma-Aldrich. Affinity purified goat anti-human CRP polyclonal antibodies were purchased from Immunology Consultants Laboratory (Newburg, OR). NeutrAvidin was a product of Invitrogen and PMMA nanospheres (450 nm in diameter) were obtained from Bang's Laboratory. All the solutions/buffers used were prepared in the laboratory from Milli-Q grade deionized water (18.2 MΩ, Millipore Corp., Billerica, MA).

2.2.2. Instruments: A MTX Lab Systems Inc. (Vienna, VA) 96-well microtiter plate reader was utilized to record the activity of apo-GDH after reaction with PQQ released from the nanospheres. The instrument was equipped with a filter to monitor the optical absorbance of the test solution at 590 nm.

2.2.3. Preparation of PQQ-doped PMMA Nanoparticles

Preparation of PQQ-TDMA Complex

A 0.75 mM PQQ solution was prepared in 2 mM NaOH and a separate solution containing 4 mg of TDMA was dissolved in 2 mL dichloromethane. Two mL of the PQQ solution was mixed with 2 mL of the TDMA solution and the mixture was shaken vigorously. After two minutes, the lower dichloromethane layer was carefully separated from the upper aqueous layer and the dichloromethane was evaporated. The resulting PQQ-TDMA salt was redissolved in 1 mL of tetrahydrofuran (THF) or methanol.

Screening of Polymeric Materials for PQQ Loading

Several hydrophobic polymers such as PVC (plasticized with DOS), polystyrene, carboxylated PVC, and PMMA were chosen for an initial screening study to assess the best material for PQQ loading. For these tests, 100 mg of polymer was dissolved in 1 mL of freshly distilled THF with 10 µL of 0.5 mM PQQ-TDMA complex added. Then, 20 µL of this "cocktail" solution was added dropwise into each well of a polypropylene 96 well plate. After the coated plate was dried under a ventilation hood overnight, the wells were incubated with either Tris-Sulfate buffer or in Tris-Sulfate buffer containing 40% acetonitrile for 10 min followed by the GDH-PQQ reconstitution assay (see below).

Loading of PQQ-TDMA into PMMA Nanoparticles

The PQQ-TDMA salt was dissolved in a solvent mixture of 850 µL methanol and 50 µL acetonitrile. A 100 µL aqueous suspension of PMMA particles was added into the PQQ-TDMA solution and the mixture was sonicated briefly for 10 s before it was placed on a shaker. After 1 h of incubation, the particles were centrifuged and the supernatant was discarded. The particles were then redispersed and washed with 50 mM Tris-Sulfate

buffer, pH 7.0 and then deionized water. The washing steps continued until no PQQ leaking was confirmed by the GDH-PQQ reconstitution assay. Finally, the particles were dispersed in 1 mL of Tri-Sulfate buffer.

2.2.4. Preparation of NeutrAvidin Coated PQQ Doped PMMA Nanoparticles

To a 100 µL aliquot of PQQ doped PMMA nanoparticles (PMMA-PQQ) (~ 200 million particles/mL in Tris-Sulfate buffer) was added 50 µL of 0.5 mg/mL NeutrAvidin and 850 µL Tris-Sulfate buffer. After 1 h of incubation, 50 µL of 5 wt% BSA was added and the mixture was incubated for another hour. The particles (PMMA-PQQ-N) were washed with Tris-Sulfate buffer twice and then were dispersed in 1 mL of Tris-Sulfate buffer.

GDH-PQQ Reconstitution Assay and Organic Solvent Assisted PQQ Release from PMMA Particles

The GDH-PQQ reconstitution assay was partially adapted from a procedure reported in the literature (22). Briefly, in 200 µL of Tris-Sulfate buffer, 5 µL of 0.5 mg/mL apo-GDH, 20 µL of dye mix (1 mM DCPIP containing 20 mM calcium chloride), 20 µL of 80 mM glucose and 20 µl of a solution of varying concentrations of PQQ were mixed together in wells of a 96-well microtiter plate. Absorbance changes were monitored at 590 nm and the data points were obtained every 20 s. To measure PQQ release from the PMMA nanoparticles, the PQQ doped PMMA particles were incubated with 100 µL of Tris-Sulfate buffer containing 40% acetonitrile for 20 min. Then, the addition of apo- GDH, DCPIP and glucose was followed by the absorbance readings on a 96-well plate reader. A dose-response curve for free PQQ reconstitution was constructed based on the method of fixed time analysis. The initial absorbance was fixed using the

average absorbance value from each well. Then the absorbance change during the first two minutes was plotted against the varying PQQ concentrations.

2.2.5. Competitive Binding Assay for Small Molecules Using Biotin-Avidin as a Model System

Preparation of Biotinylated BSA: A lightly conjugated biotinylated-BSA (biotin-BSA) was prepared using pre-activated sulfosuccinimidyl biotin (initial mole ratio, biotin:BSA = 15:1). The resulting biotin-BSA conjugate (2 mg/mL) was dialyzed/centrifuged with a Millipore dialysis centrifuge tube (molecular weight cut-off = 5,000).

Preparation of Biotinylated NUNC Plate: The biotin-BSA was reacted with the surface of NUNC amino plate wells by adding 5 μL of 2 mg/mL biotin-BSA into 95 μL of 100 mM sodium carbonate buffer, pH 9.6 (conjugation buffer) for 2 h and then another 1 h of reaction after adding 20 mM ethanolamine to cap any unreacted sites on the surface of the plates.

Competitive Binding Assay: An aliquot of 10 μL of PMMA-PQQ-N was added into the biotin-BSA plate wells containing varying concentrations of biotin in 5% BSA. The plate was shaken for 30 min and the plate was then washed thoroughly with wash buffer (50 mM Tris-Sulfate, pH 7.0, containing 0.05% Tween 20). Then, 100 μL of 40% acetonitrile containing Tris-Sulfate buffer was added into each well and incubated for 20 min before the GDH-PQQ reconstitution assay was carried out.

2.2.6. Solid-phase Sandwich CRP Immunoassay

Capture anti-CRP antibody (AbCRP) was covalently linked to the surface of NUNC amino plate wells following the manufacturer's recommended procedure. Briefly, 2.5 μg/mL AbCRP was incubated with 100 μL of sodium carbonate conjugation

buffer, pH 9.6, in each well for 2 h. Then, 150 µL of 20 mM ethanolamine in the same sodium carbonate buffer was added into each well and incubated for another hour. The plate was then washed two times with washer buffer. Varying concentrations of CRP calibrators in 100 µL of Tris-Sulfate buffer were then incubated for 1 h under ambient conditions. The plate was then washed twice with wash buffer. A 5 µL aliquot of 10 µg/mL biotinylated CRP antibody (btAbCRP) was then incubated with Tris-Sulfate buffer for one hour. Finally, 10 µL of PMMA-PQQ-N particles was added along with 90 µL 5% BSA to each well and the plate was incubated on a shaker for another hour. The plate was washed with wash buffer 5 times before the PQQ release and GDH reconstitution assay was carried out.

2.3. Results and Discussion

2.3.1. Evaluation of GDH-PQQ Reconstitution Assay

The GDH-PQQ reconstitution assay has been used as a standard biochemical tool for quantitatively determining the activity of PQQ present in bacteria culture media during cultivation (22). In our experiments, various assay conditions were optimized to maximize the performance of this assay, e.g., lowering the detection limit. The optimized assay showed excellent reproducibility in detecting PQQ concentrations down to sub-nM levels (see Figure 2.2a). The main advantage of the enzyme reconstitution assay is that excess amount of apo-enzyme and its substrate glucose can be utilized to achieve the maximum electron transfer rate. Therefore, the variation of PQQ concentration will be the only species that dictates the rate of color change of the solution. The compatibility of this assay with various organic solvents was also examined because of the ultimate requirement to release PQQ from the polymeric nanoparticles in the proposed binding

assay experiments. As shown in Figure 2.2b, 20% acetonitrile was found to be the best candidate with the least activity loss of GDH-PQQ reconstitution. The GDH-PQQ reconstitution assay with 20% acetonitrile present lost ca. 50% of its sensitivity; however, the limit of detection (based on blank measurement plus three times its standard deviation) was actually found to be somewhat better than the assay performed in buffer without acetonitrile (100 pM vs. 280 pM). This is due to the improved precision of the blank measurements in the presence of the added acetonitrile. In addition, the detection process can be monitored visually, as shown in Figure 2.3, without the need of any instrumentation.

2.3.2. Screening of Polymeric Materials for PQQ Loading

Unlike other particle-based detection methods using fluorescence (11) or electrochemiluminescence (23) tracers, where often a hydrophobic dye or electroactive compound is the component encapsulated, PQQ is very soluble in aqueous media due to the three carboxyl groups and one quinone group within its structure. The strong reactivity of the quinone groups toward nucleophiles such as amines also makes PQQ less compatible with some amine containing buffers. Therefore, the conversion of PQQ into a hydrophobic ion-pair with TDMA using simple extraction was carried out first (see Figure 2.4). The prepared PQQ-TDMA ion-pair in chloroform was equilibrated with deionized water and various pH 7.0 buffers, and no significant loss of PQQ from the organic phase was observed (as determined by reconstitution assay of GDH activity using the equilibrated aqueous phase; data not shown).

To screen the ability to remove PQQ efficiently from polymers that could be obtained or prepared as nanoparticles, films of various polymers containing a known

amount of added PQQ-TDMA were initially cast in microtiter plate wells. The goal was to examine the swelling properties of the polymers and the release of PQQ using the working Tris-Sulfate buffer, pH 7.0, containing 40% acetonitrile. As shown in Figure 2.5, all four polymeric materials tested exhibited good release of PQQ, as determined from the assay of PQQ present in the wells after incubation with the buffer containing acetonitrile. However, carboxylated PVC and polystyrene also yielded a relatively significant activity response when incubating with Tris-Sulfate buffer without the acetonitrile, suggesting that extraction of PQQ was occurring from these matrices even in the absence of organic solvent as a swelling agent. Based on the data presented in Figure 2.5, PMMA was found to be the optimal polymeric material for entrapping PQQ without observing significant extraction into aqueous buffer phase, and also for fast release of PQQ when organic solvent is present in the primarily aqueous phase assay buffer.

2.3.3. PQQ Release from PMMA Nanoparticles

The PQQ-doped PMMA particles (PMMA-PQQ) were characterized using scanning electron microscopy (SEM). There were no observable changes, as shown in Figure 2.6, in the shape or size of the nanospheres after their loading with the PQQ-TDMA salt. These particles were also evaluated in the Tris-Sulfate buffer alone and the same buffer containing acetonitrile. As shown in Figure 2.7, when a suspension of PMMA-PQQ nanoparticles is incubated with buffer alone (no acetonitrile), and then the supernatant is assayed for PQQ by the reconstitution enzymatic assay, very low catalytic activity is observed. However, in the presence of 40 % acetonitrile in the PMMA-PQQ particle incubation buffer, significant amounts of PQQ are extracted into the surrounding solution, resulting in a dramatic increase in catalytic enzymatic activity in the

reconstitution assay. A calibration curve for quantifying the number of particles in the test suspension was constructed based on a turbidity measurement. Based on the known calibration for PQQ concentrations via the reconstitution assay, and the number of particles present based on turbidity measurements, the number of PQQ molecules released from a single particle in a given period of time (20 min in this incubation experiment) is estimated to be approximately 20,000 (based on the concentration of PQQ detected in the incubation solution after 20 min; data now shown).

2.3.4. Evaluation of NeutrAvidin Coating and Binding Capacity

The adsorption of proteins onto the surface of the PMMA nanoparticles occurs rapidly (24). To further facilitate the adsorption process, a buffer with a pH close to the isoelectric point of NeutrAvidin was chosen for incubation. To finalize the coating procedure, BSA was added as a "filler" to coat any portion of the particles not coated by the NeutrAvidin. Further, the presence of BSA may also help maintain a thermodynamically stable layer of proteins on the surface of the particles (25).

To evaluate the binding capability of the PMMA-PQQ-N nanoparticles, the particles were tested with a biotinylated BSA coated microtiter plate, where varying amounts of biotinylated BSA were covalently coupled onto the surface of the wells. Upon incubation with the biotinylated microtiter plate wells, the number of PMMA-PQQ-N particles bound to the well surface via biotin-NeutrAvidin binding was dependent on the number of biotins available on the surface immobilized biotin-BSA layer. As shown in Figure 2.8, the more biotin-BSA used to coat the plate, the greater the amount of PQQ detected after washing the wells and incubating the wells with the buffer containing 40% acetonitrile.

2.3.5. Heterogeneous Competitive Binding Assay for Biotin

In a competitive assay format, the presence of free biotin in the assay mixture competes with the biotins immobilized on the plate for the available avidin binding sites on PMMA-PQQ-N particles. Although sequential saturation method as described by Zettner et al. (26) could lead to more sensitive detection of biotin, an equilibrium method (all reagents added simultaneously) was used instead for simplicity. The results, shown in Figures 2.9a and 2.9b, illustrate a detection range from 2 nM to 10 nM of biotin. Depending on the number of NeutrAvidins on the PMMA particles or the number of biotin sites on the plate, the detection range for free biotin, as shown in Figure 2.10, could be shifted to a higher or lower concentration range.

2.3.6. CRP Sandwich Immunoassay

To further investigate the practical application of the novel prosthetic group loaded PMMA-PQQ-N nanoparticles, CRP was chosen as a macromolecule target and a "sandwich" type of immunoassay was developed. A schematic of this assay design is illustrated in Figure 1b. A pre-activated NUNC-amino plate (reactive toward primary amines) is available commercially and the capture antibody toward human CRP was covalently attached to the plate well surfaces via a PEO linker as described by the manufacturer (27).

As in any immunoassay system, nonspecific adsorption can yield problems of high background noise and poor detection limits. In this study, ethanolamine was employed to cap the reactive sites left over after the conjugation reaction of the surface with the capture antibody. Hydroxyl groups on ethanolamine also help minimized nonspecific adsorption of CRP and anti-CRP reporter antibody (labeled with biotin) in

the subsequent incubations. Because of the hydrophobic nature of PMMA-PQQ-N particles, even after coating with layers of NeutrAvidin and BSA, they tend to stick to the surface of the protein coated polymeric materials. For this reason, 0.05 vol% Tween 20 and BSA up to 5 wt% were used in the incubation and wash buffers to minimize these nonspecific interactions.

As shown in Figure 2.11a, use of the PMMA-PQQ-N nanoparticles as a tracer yields a dose-response curve toward CRP in the range from 0 to 10 ng/mL with a detection limit of about 220 pg/mL. The limit of detection (LOD) is defined as a CRP concentration value equivalent to an absorbance rate change value that is three times the standard deviation of zero-dose blank. The LOD obtained is comparable to or better than other sandwich assays reported for CRP that utilize either enzyme (28) or fluorescent labels (1).

The density of the immobilized capture antibody in the wells of the plate was found to be crucial to obtain a high sensitivity CRP assay. For comparison purposes, as shown in Figure 2.11b, when a 20-fold increase in the amount of capture antibody was used during the immobilization step, a nearly 20-fold higher LOD (~ 3.1 ng/mL) was obtained. The improvement of LOD when using lower capture antibody levels likely arises from both the smaller standard deviation of zero-dose blank and better binding of PMMA-PQQ-N particles at low CRP concentrations owing to a less crowded capture surface. Indeed, the decreased antibody density on the surface of the wells also helps minimize the nonspecific adsorption and enables better accessibility of PMMA-PQQ-N particles to bind to the biotin attached to the anti-CRP reporter antibody.

2.4. Conclusions

A novel nanoparticle tracer that encapsulates the redox prosthetic group species PQQ has been prepared and utilized for developing sensitive bioaffinity assays. Detection of bound nanoparticles was realized by employing a GDH reconstitution assay coupled with an indicator dye to detect PQQ released from the particles via use of acetonitrile added to the working buffer. The rate of signal change can be readily recognized visually or read on simple microtiter plate reader. The new PQQ-doped nanoparticles can be utilized as a tracer in both competitive and non-competitive assays. The detection limits obtained for CRP as a model macromolecule were in the range reported for fluorescent nanosphere-based assays. The ability to detect PQQ at extremely low levels (< 100 pM) with short assay times via enzymatic amplification using apo-GDH reconstitution makes the use of this approach quite attractive. If enhanced loading of the nanospheres can be realized (beyond the 20,000 PPQ molecules per particle used herein), and if the non-specific adsorption/aggregation of the nanoparticles can be reduced further, the proposed PMMA-PQQ nanosphere tracers may prove to be an attractive tool for the design of high sensitivity screening assays that would need only a visual read of the final solution color changes to assess the presence or absence of the target analyte.

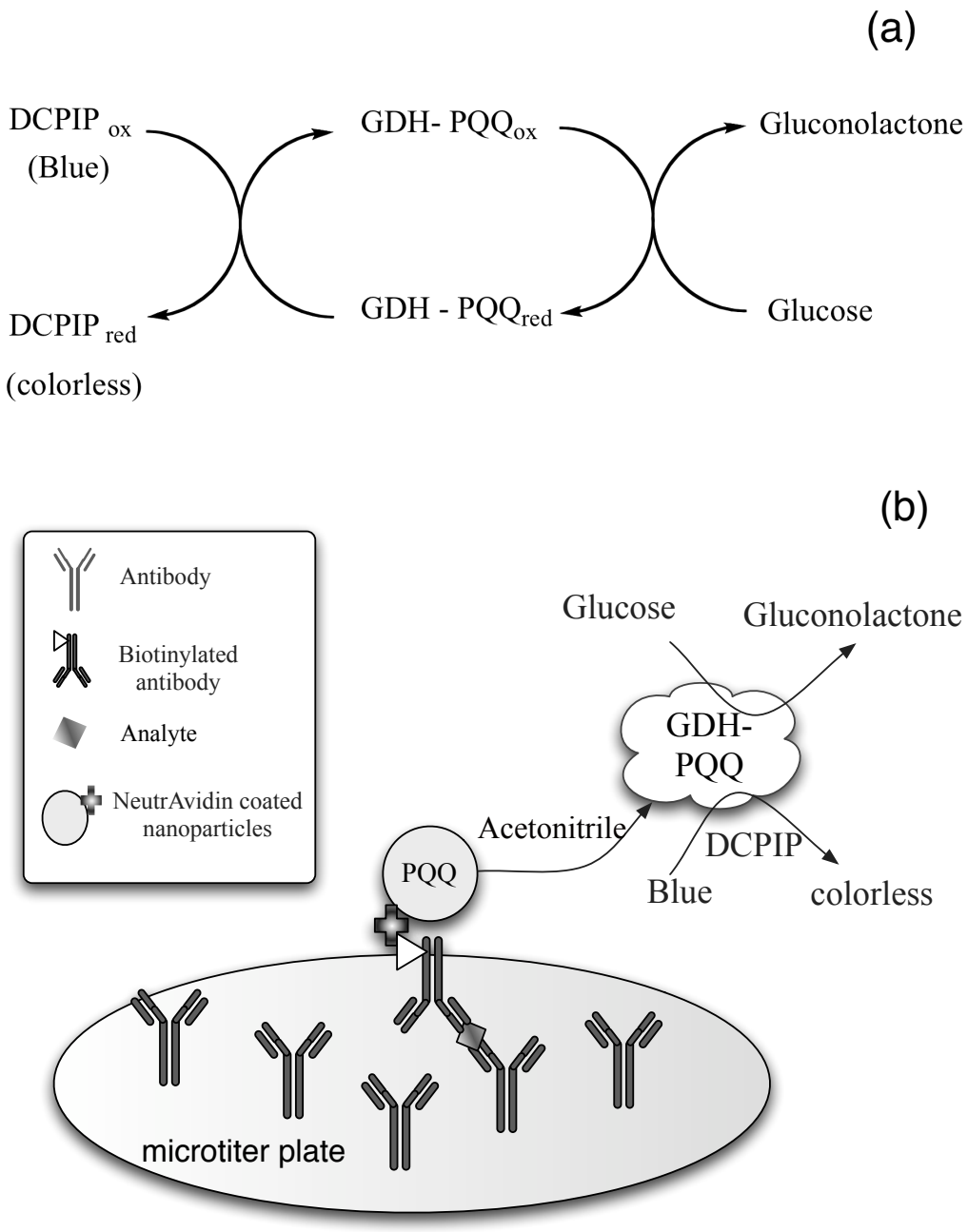

Figure 2.1. (a) GDH-PQQ reconstitution assay with DCPIP as an indicator (ox: oxidized form; red: reduced form). (b) Scheme of "sandwich" type immunoassay arrangement utilizing the new PQQ-doped PMMA nanoparticles as a tracer and biotin-avidin linkage to bind the nanoparticles to the reporter antibody of the assay.

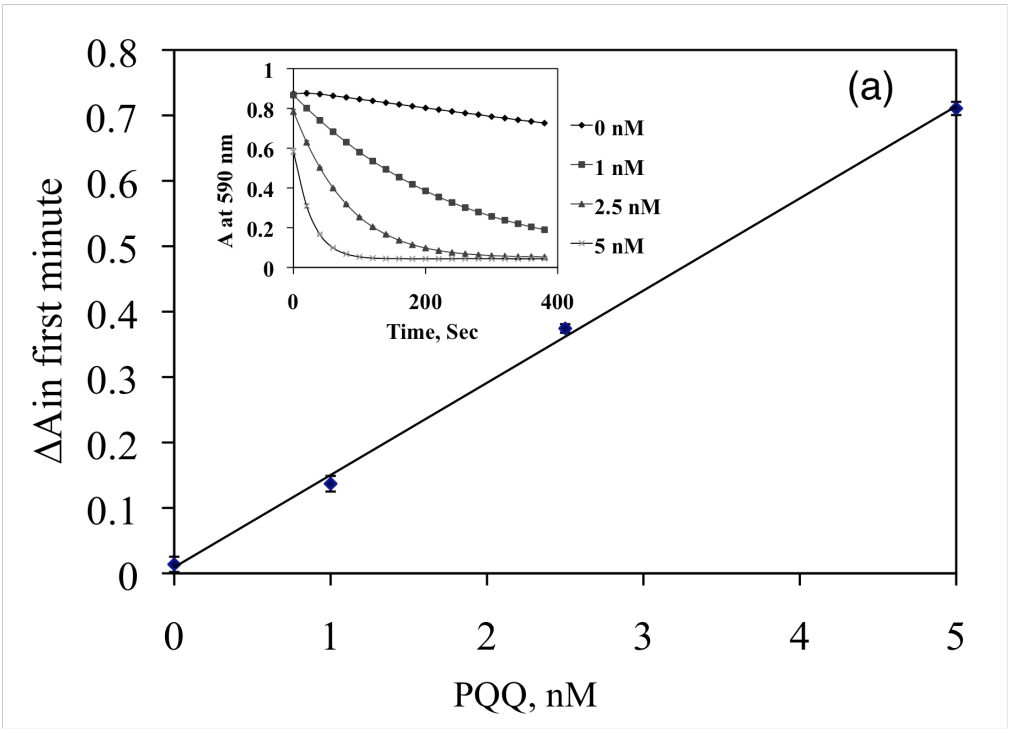

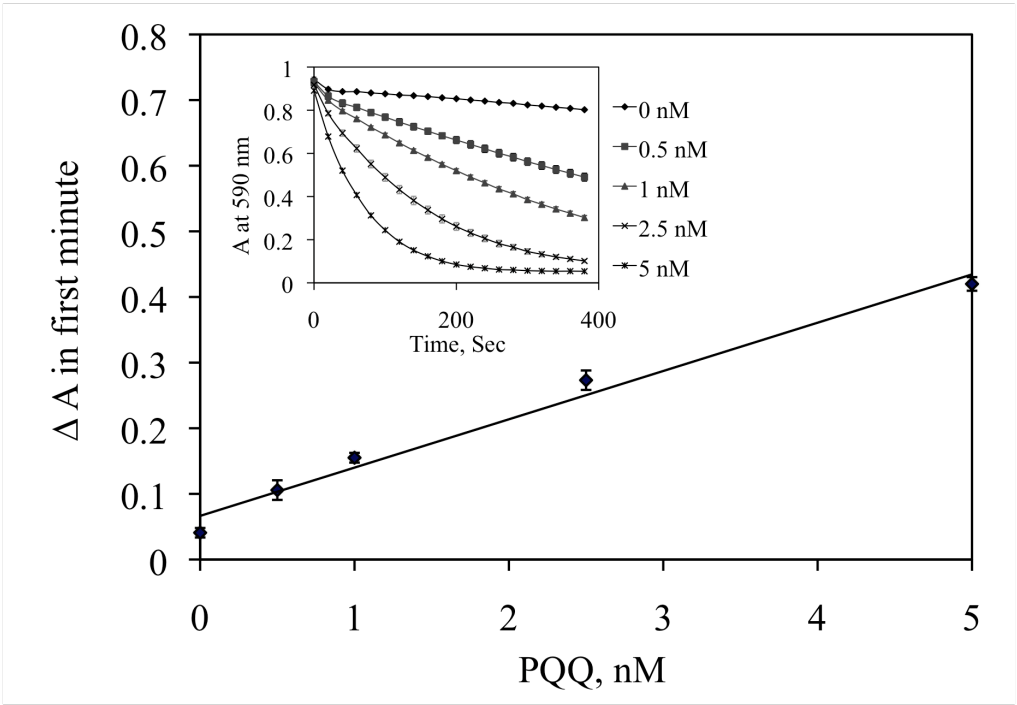

Figure 2.2. (a) PQQ dose response in GDH-PQQ reconstitution assay in Tris-Sulfate buffer (insert: real time monitoring of DCPIP reduction at 590 nm).
(b) PQQ dose response in GDH-PQQ reconstitution assay in Tris-Sulfate buffer containing 20% acetonitrile (insert: real time monitoring of DCPIP reduction at 590 nm)

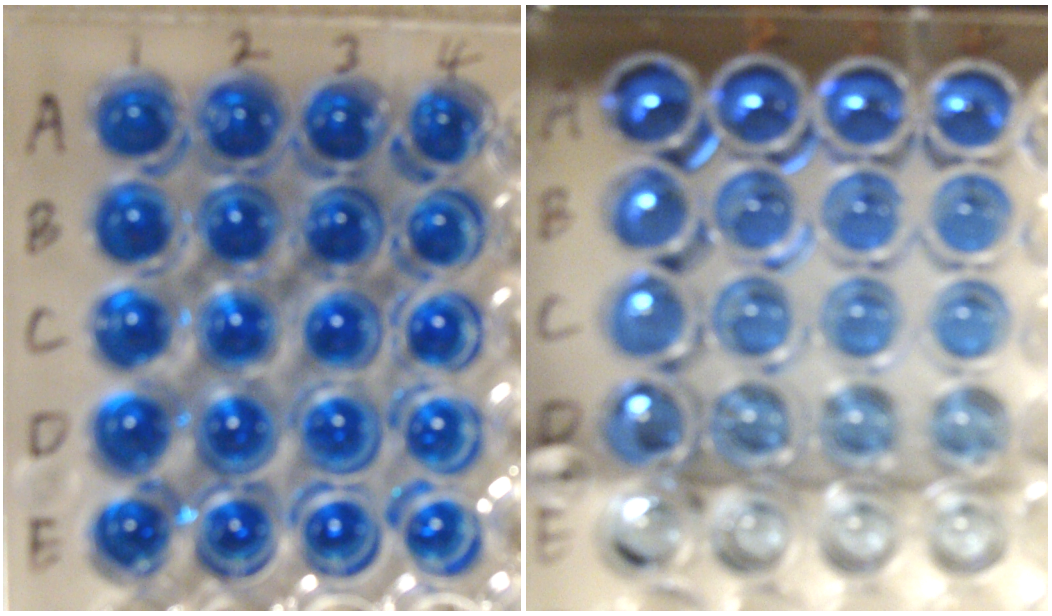

Figure 2.3. Digital picture of PQQ assay showing visual determination.
For every 4 wells from A to E, there contains PQQ of varying concentrations: 0 nM, 0.5 nM, 1 nM, 2.5 nM and 5 nM; Left: GDH-PQQ assay mixture at 0 min; Right: GDH-PQQ assay mixture at 3 min after the addition of glucose, which will trigger the start of the assay and the change of color.

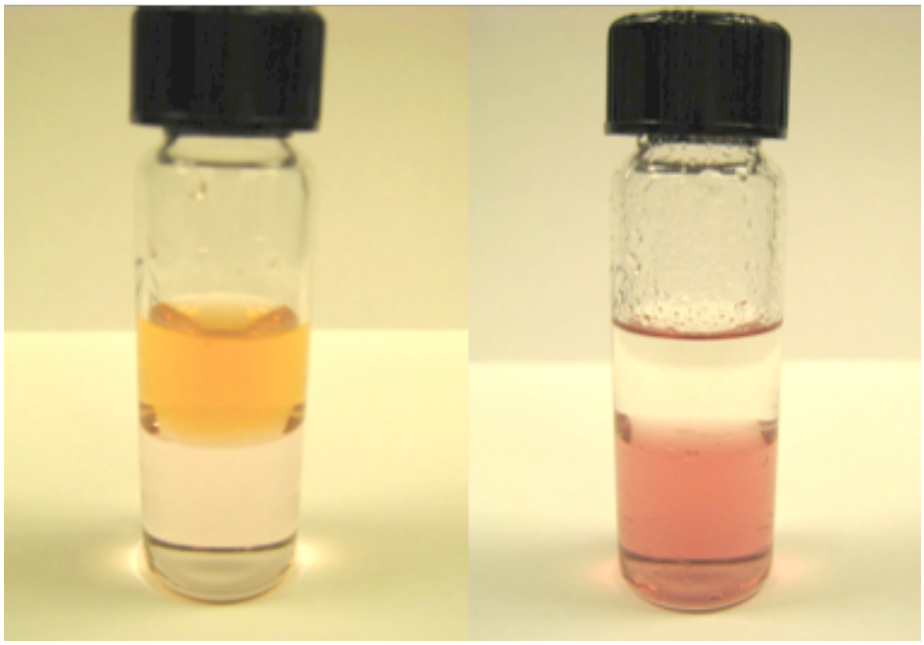

Figure 2.4. Preparation of PQQ-TDMA lipophilic salt. Left: before extraction, PQQ stays in the upper aqueous layer containing 1 mM NaOH; Right: after extraction, PQQ was drawn into lower chloroform layer with the aid of TDMAC.

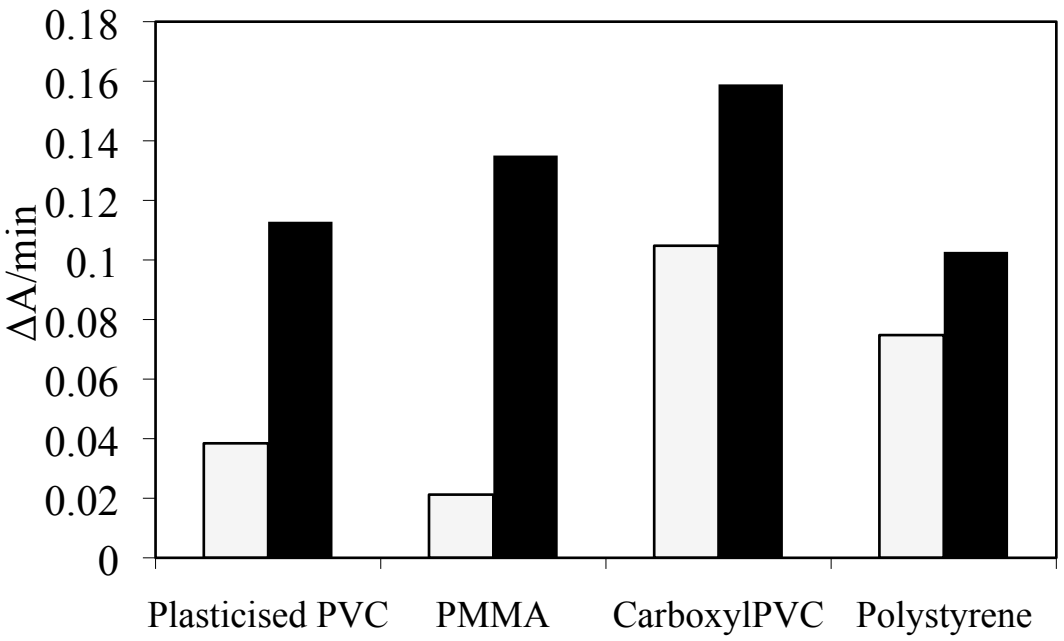

Figure 2.5. Results of screening studies of different polymeric materials for encapsulating and releasing PQQ-TDMA salt into the polymer bulk phase. White bars are relative activity of PQQ in soaking solution of polymer films without acetonitrile, and black bars are relative PQQ activity found after incubation of films with buffer containing 40% acetonitrile.

Before PQQ loading:

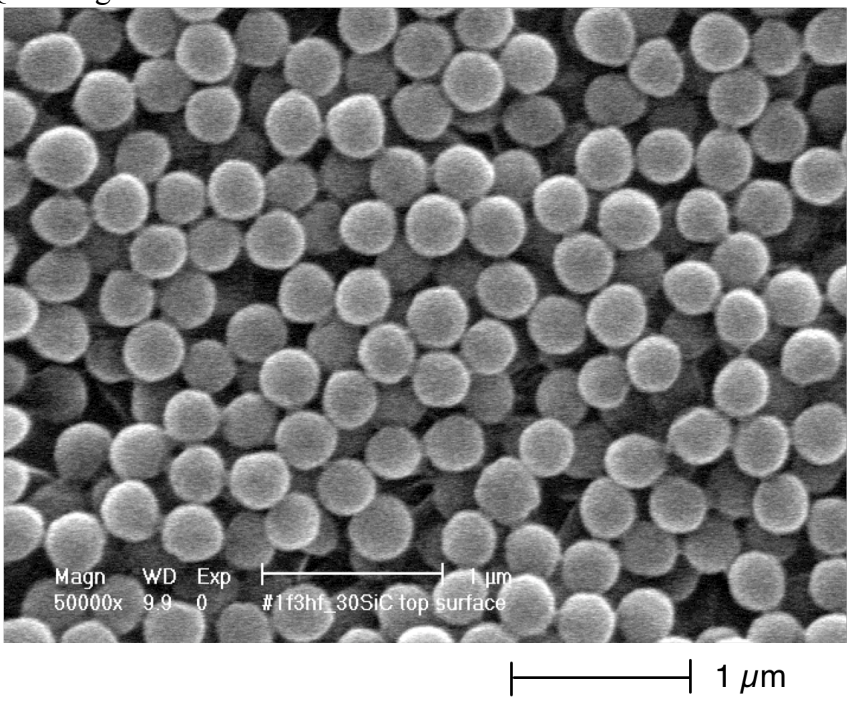

After PQQ loading:

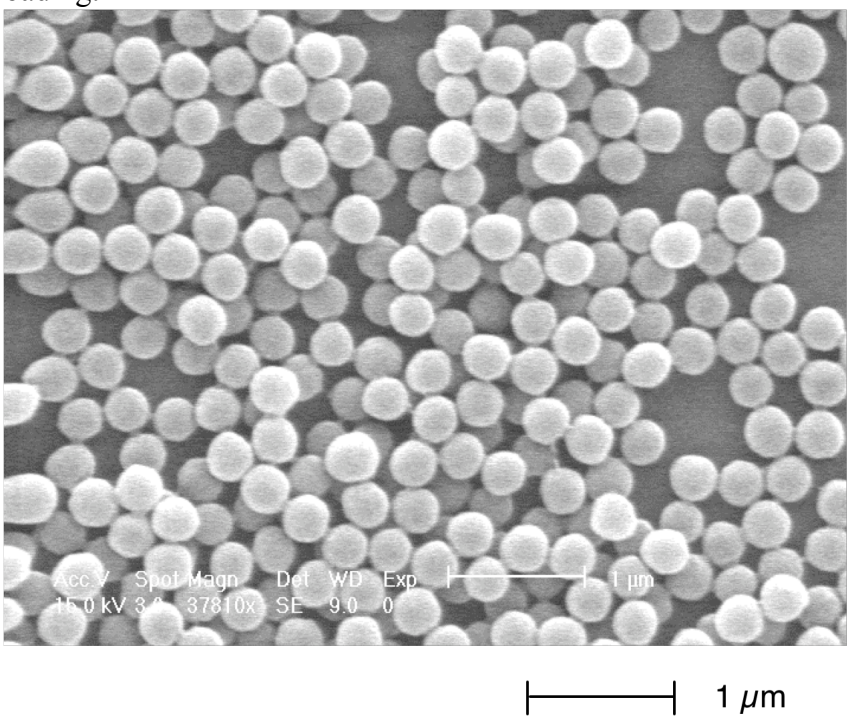

Figure 2.6. SEM pictures of PMMA nanoparticles before and after PQQ loading.

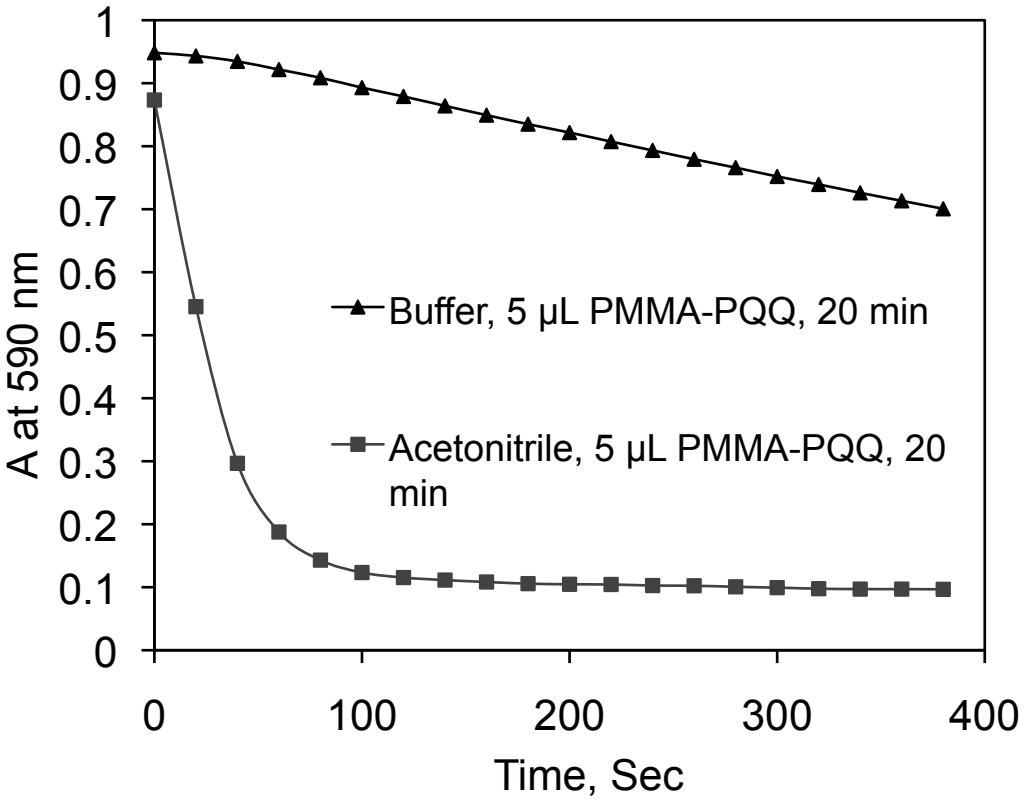

Figure 2.7. Characterization of PMMA-PQQ particles by measuring released PQQ from an aliquot of 5 µL particles after 20 min incubation with Tris-Sulfate buffer and the same buffer containing 40% acetonitrile.

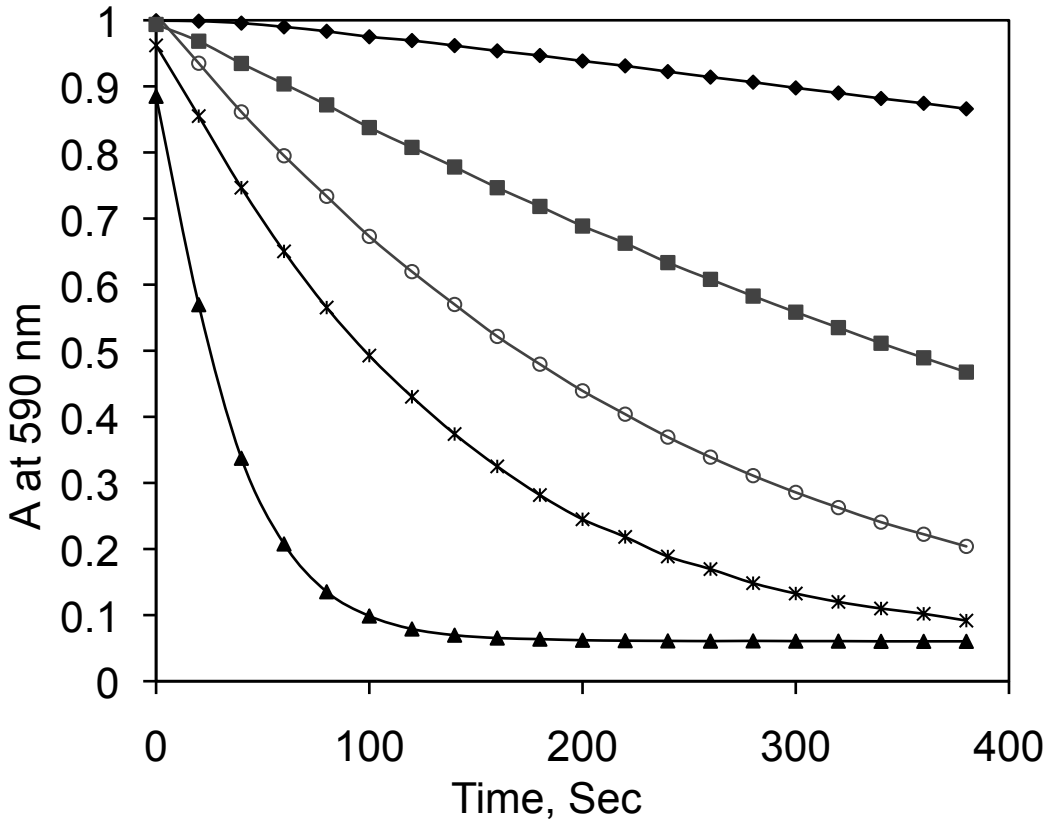

Figure 2.8. PMMA-PQQ-N particles binding with varying levels of biotin-BSA immobilized on the surface of NUNC amino microtiter plate wells. Initial amounts of biotin-BSA used for the immobilization: (♦) 0 µg/well (blank); (■) 0.5 µg/well; (O) 5 µg/well; (✱) 10 µg/well; (▲) commercial biotinylated plate.

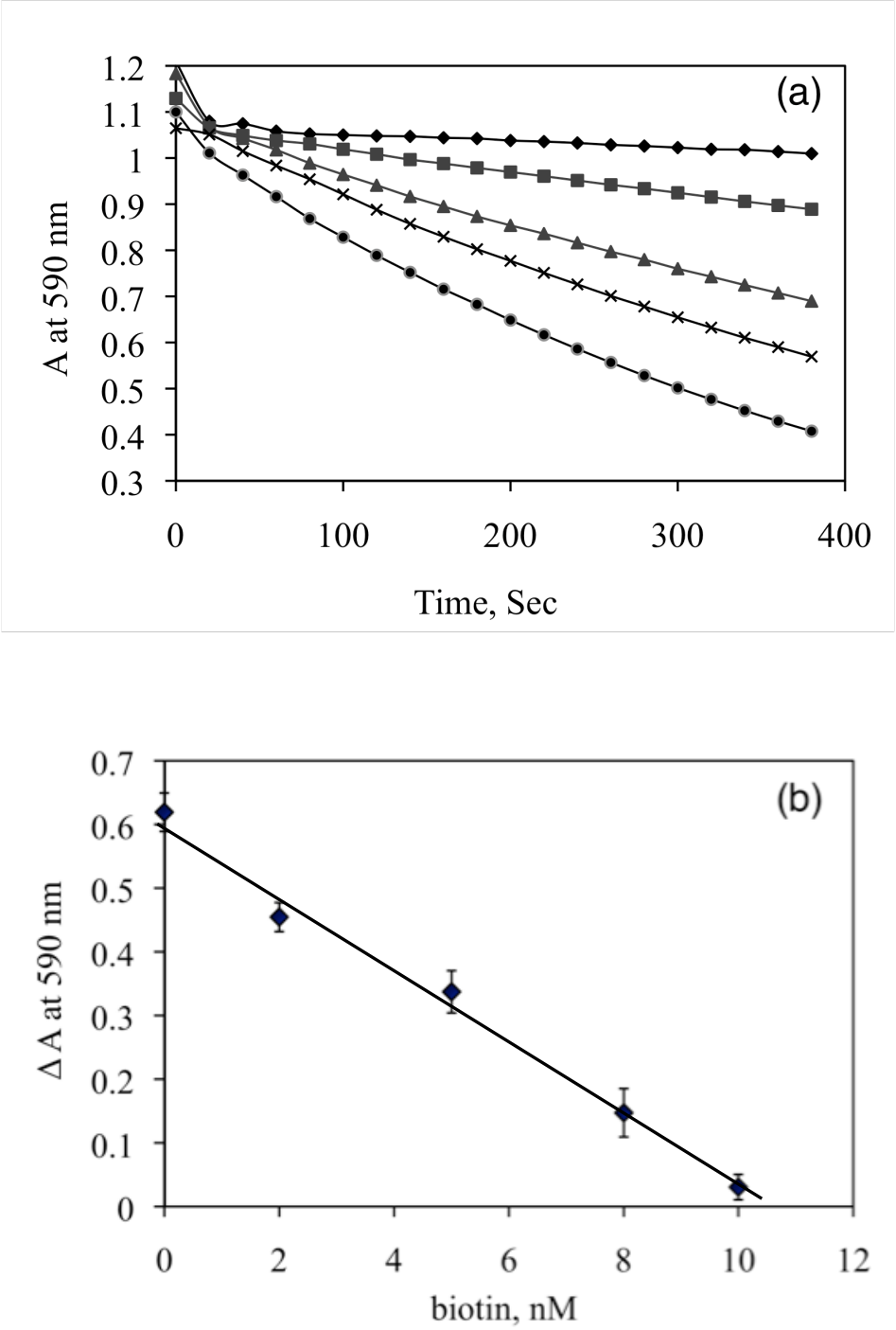

Figure 2.9. Detection free biotin levels in a heterogeneous competitive assay format using PMMA-PQQ-N particles: (a) Real time monitoring of PQQ released from the bound particles after washing as a function varying level of free biotin concentrations: (♦) 10 nM; (■) 8 nM; (▲) 5 nM; (×) 2 nM; (●) 0 nM. (b) Biotin dose-response for data shown in (a).

(a)

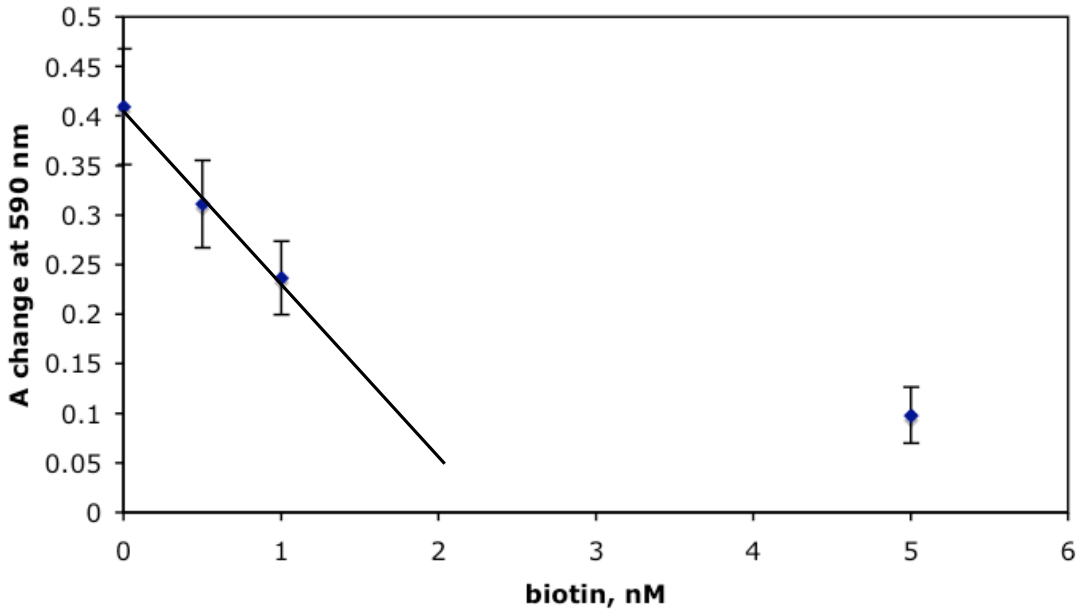

(b)

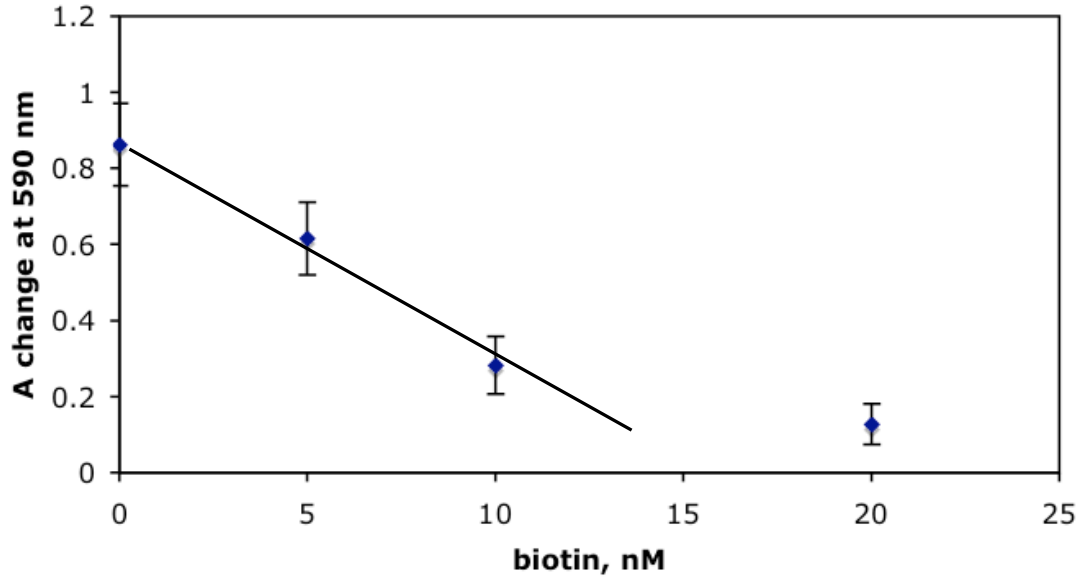

Figure 2.10. Biotin/Avidin competitive assay and shifting in the detection range as a function of NeutrAvidin level on PMMA-PQQ particles.
(a) with 5 µL of NeutrAvidin coated PMMA-PQQ particles (N = 3);
(b) with 20 µL of NeutrAvidin coated PMMA-PQQ particles (N = 3).

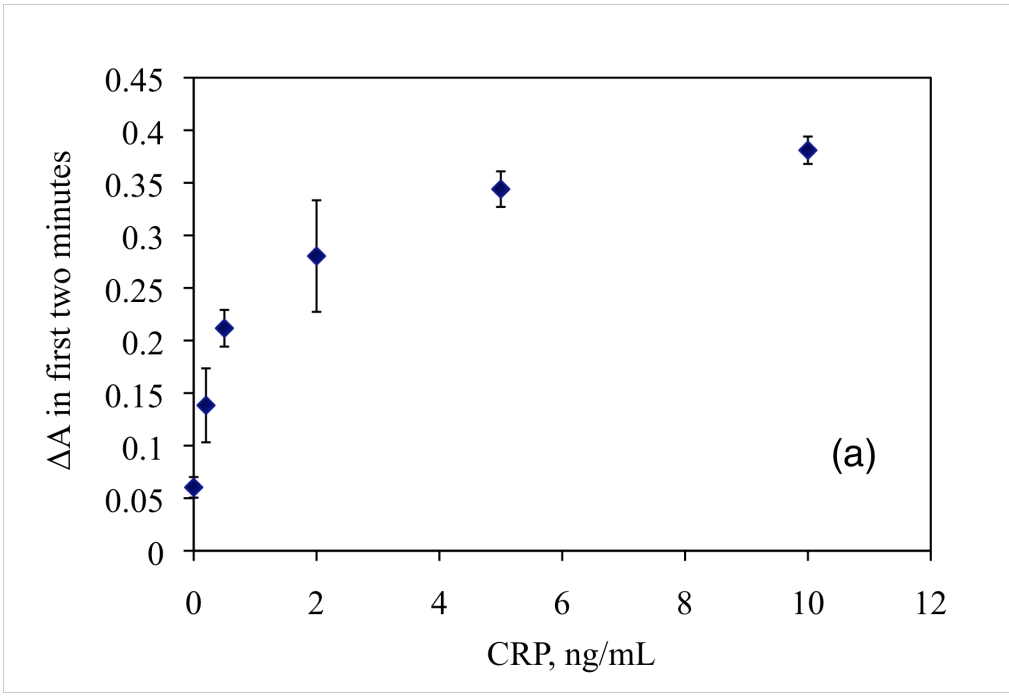

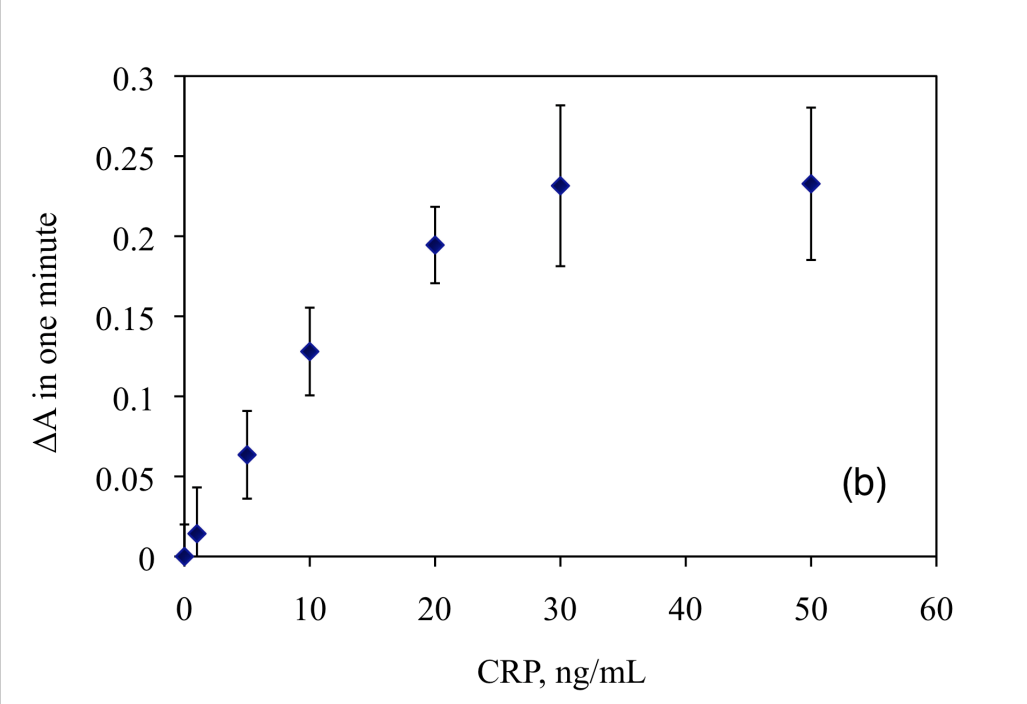

Figure 2.11. CRP dose-response curve for sandwich assay format; (a) with optimized capture antibody levels immobilized on the surface of NUNC amino microtiter plate wells; (b) with higher levels of capture antibody immobilized on the surface of NUNC amino microtiter plate wells.

2.5. References

(1) Tarkkinen, P.; Palenius, T.; Lovgren, T. *Clin. Chem.* **2002,** *48*, 269-277.

(2) Yu, H.; Diamandis, E.P. *Clin. Chem.* **1993,** *39*, 2108-2114.

(3) Liang, C.; Jin, R.; Gui, W.; Zhu, G. *Environ. Sci. Technol.* **2007,** *41*, 6783-6788.

(4) Andreotti, P.E.; Ludwig, G.V.; Peruski, A.H.; Tuite, J.J.; Morse, S.S.; Peruski, L.F. *Biotechniques* **2003,** *35*, 850-859.

(5) Miao, W.J.; Bard, A.J. *Anal. Chem.* **2004,** *76*, 7109-7113.

(6) Dequaire, M.; Degrand, C.; Limoges, B. *Anal. Chem.* **2000,** *72*, 5521-5528.

(7) Wang, J.; Polsky, R.; Xu, D.K. *Langmuir* **2001,** *17*, 5739-5741.

(8) Thurer, R.; Vigassy, T.; Hirayama, M.; Wang, J.; Bakker, E.; Pretsch, E. *Anal. Chem.* **2007,** *79*, 5107-5110.

(9) Wang, J.; Liu, G.D.; Zhu, Q.Y. *Anal. Chem.* **2003,** *75*, 6218-6222.

(10) Chan, C.P.Y.; Bruemmel, Y.; Seydack, M.; Sin, K.K.; Wong, L.W.; Merisko-Liversidge, E.; Trau, D.; Renneberg, R. *Anal. Chem.* **2004,** *76*, 3638-3645.

(11) Zhao, X.J.; Hilliard, L.R.; Mechery, S.J.; Wang, Y.P.; Bagwe, R.P.; Jin, S.G.; Tan, W.H. *Proc. Natl. Acad. Sci. U. S. A.* **2004,** *101*, 15027-15032.

(12) Liu, G.D.; Wang, J.; Wu, H.; Lin, Y.H. *Anal. Chem.* **2006,** *78*, 7417-7423.

(13) Tian, D.; Duan, C.; Wang, W.; Li, N.; Zhang, H.; Cui, H.; Lu, Y. *Talanta* **2009,** *78*, 399-404.

(14) Miao, W.J.; Bard, A.J. *Anal. Chem.* **2004,** *76*, 5379-5386.

(15) Duine, J.A.; Frank, J.; Vanzeeland, J.K. *FEBS Lett.* **1979,** *108*, 443-446.

(16) Corey, E.J.; Tramontano, A. *J. Am. Chem. Soc.* **1981,** *103*, 5599-5600.

(17) Kilty, C.G.; Maruyama, K.; Forrest, H.S. *Arch. Biochem. Biophys.* **1982,** *218*, 623-625.

(18) Duine, J.A. *J. Biosci. Bioeng.* **1999,** *88*, 231-236.

(19) Dewanti, A.R.; Duine, J.A. *Biochemistry* **1998,** *37*, 6810-6818.

(20) Ikebukuro, K.; Kohiki, Y.; Sode, K. *Biosens. Bioelectron.* **2002,** *17*, 1075-1080.

(21) Missetsmits, M.; Oltshoorn, A.J.J.; Dewanti, A.; Duine, J.A. *Methods Enzymol. (vit. Coenzymes, Part J)* **1997,** *280*, 89-98.

(22) Biville, F.; Mazodier, P; Gasser, F.; Van Kleef, M.A.G.; Duine J.A. *FEMS Microbiol. Lett.* **1988,** 53-58.

(23) Wei, H.; Liu, J.; Zhou, L.; Li, J.; Jiang, X.; Kang, J.; Yang, X.; Dong, S.; Wang, E. *Chemistry, Eur. J.* **2008,** *14*, 3687-3693.

(24) Li, W.; Li, Songjun. *Colloids Surf.* **2007,** 159-164.

(25) Minton, A.P. *Biophys. J.* **1999,** *76*, 176-187.

(26) Zettner, A.; Duly, P. E. *Clin. Chem.* **1974,** *20*, 5-14.

(27) *www.NUNCBRAND.com Technote #56*,

(28) Zhang, H.R.; Meyerhoff, M.E. *Anal. Chem.* **2006,** *78*, 609-616.

CHAPTER 3

APO-GLUCOSE DEHYDROGENASE BASED HOMOGENEOUS COMPETITIVE BINDING ASSAY FOR SMALL MOLECULES USING BIOTIN/AVIDIN AS A MODEL SYSTEM

3.1. Introduction

The use of enzyme labels in immunoassays (antibody-antigen) or other biological binding assays (e.g., DNA) has been extensively exploited (1, 2). Although heterogeneous methods such as ELISA (3-6) have excellent detection capabilities, homogeneous assay formats are usually preferred because of their quick response, ease of adaptation for automation, and because they require no additional separation or washing (7). The homogeneous competitive binding assay is based on the inhibition/reactivation of enzyme-ligand conjugates by their interaction with the analyte (ligand) specific binding proteins or antibodies. When no free analyte is present in the assay mixture, enzyme inhibition occurs, and this inhibition is dependent on the amount of binder molecules available for binding with the enzyme-ligand conjugates. The observed inhibition of enzyme activity can be explained by two possible mechanisms: 1) enzyme substrates are prevented from accessing the enzyme catalytic center by the bulky antibody-ligand complex on the surface of the enzyme; 2) the conformational changes of the enzyme by the binding molecule induces a complete or partial inactivation of the enzyme.

Various enzyme labels have been successfully employed in homogeneous competitive binding assays, including glucose-6-phosphate dehydrogenase (G6PDH) (7-9), malate dehydrogenase (10), adenosine deaminase (11), pyruvate dehydrogenase (12), beta-galactosidase (13), alkaline phosphatase (14). The selection rules for an enzyme label are as follows: firstly, the enzyme should have high specific activity; secondly, the enzyme should be available in high purity at a reasonable cost; thirdly, the enzyme should be able to retain a high degree of its activity after undergoing appropriate conjugation reactions with analyte derivatives; and lastly, the resulting small molecule-enzyme conjugates should be inhibited upon binding to antibodies or binding proteins directed toward the small analyte molecules.

As demonstrated in Chapter 2, the GDH-PQQ reconstitution assay is very sensitive with a detection limit of sub-nanomolar concentrations of PQQ. The high sensitivity of the reconstitution assay translates to a low amount of apo-GDH required in the assay system, which is a critical component in optimizing a high sensitivity assay. Besides this, some additional advantages of this assay are the reconstitution process of PQQ with apo-GDH and the electron transfer process from reduced PQQ to the redox dye DCPIP, which happens right at the catalytic center of the enzyme. In this chapter, a highly sensitive homogeneous enzyme linked competitive binding assay using a biotin/avidin model system is described based on the GDH-PQQ reconstitution assay. A schematic of the proposed assay is illustrated in Figure 3.1. A well characterized biotin-apo-GDH conjugate was successfully prepared, and close to 100% inhibition was observed in the presence of the binding protein avidin. At least a one order of magnitude

better detection limit is obtained in dose-response toward free biotin as compared to the previous assays using G6PDH as an enzyme label (15).

3.2. Experimental

3.2.1. Apparatus. A labsystems Multiskan RC 351 microplate reader was used to monitor the color change as a result of the enzymatic reaction in a 96-well plate. An Eppendorf centrifugation system (5810R, 15 amp version) was used to centrifuge enzyme-ligand conjugates.

3.2.2. Reagents. All solutions were prepared with Millipore (18.2 MΩ Milli-Q) water. PQQ was obtained from Iris Biotech GmbH (Marktredwitz, Germany). PQQ dependent apo-glucose dehydrogenase and polypropylene 96-well microtiter plates were purchased from Fisher Scientific (Pittsburgh, PA). Tri(hydroxylmethyl)aminomethane base (Tris), Tween 20, 2,6-dichlorophenolindophenol (DCPIP), glucose, avidin and biotin were purchased from Sigma-Aldrich (St. Louis, MO). N-Hydroxysulfosuccinimide esters of biotin (biotin-sulfo-NHS) and 2-(4'-hydroxyazobenzene) benzoic acid (HABA) assay kit were purchased from Pierce (Rockford, IL).

3.2.3. Preparation of Biotin-GDH Conjugates

Reagents including apo-GDH and glucose were prepared in 0.1 M sodium bicarbonate buffer, pH 8.0. Biotin-sulfo-NHS was dissolved in DMSO at a concentration of 2 mg/mL right before the conjugation reaction. An aliquot of apo-GDH (0.1 mg) and 100 µL of 80 mM glucose (to block active center of the apo-GDH) were mixed with 400 µL of the bicarbonate buffer. The mixture was stirred at 4 ºC for 30 min. Then an appropriate amount of biotin-sulfo-NHS solution was added at an interval of 10 min while the mixture was being stirred. The ligand/enzyme ratio was varied from 100:1 to

1000:1. The conjugation reaction was run for 3 h at 4 ºC under constant stirring. Unreacted biotin-sulfo-NHS was filtered off using Amicon centrifuge tube equipped with a filter inset of 5000 MWCO (molecular weight cut-off). The mixture was repeatedly centrifuged 3 times at 4000 rpm for 20 min for each centrifugation. The conjugated enzyme (biotin-apo-GDH) was collected carefully and the volume was adjusted for a desired concentration with 50 mM Tris-sulfate buffer, pH 7.0.

3.2.4. Determination of Biotinylation Degree of Apo-GDH

The degree of biotinylation of apo-GDH was determined by employing commercially available 2-(4'-hydroxyazobenzene) benzoic acid (HABA) EZ-biotin quantitation kit. The principle of HABA assay (16, 17) utilizes the absorbance shift (348 nm to 500 nm) of HABA upon binding to avidin. Since the binding between HABA and avidin (K_d = 5.8 x 10^{-6} M) (18) is relatively weak compared to biotin and avidin (K_d = 1 x 10^{-15} M) (19), in the presence of biotin, biotin can easily displace HABA from the HABA/avidin complex and lead to a decrease in absorbance at 500 nm. The procedure was modified slightly to accommodate the filter available on the microplate reader. The absorbance at 490 nm was obtained instead of the manufacturer recommended 500 nm. Briefly, 100 µL of D.I. water was added to one microtube of HABA/Avidin premix. An aliquot of 20 µL of the HABA/Avidin solution was added into 160 µL of Tris-Sulfate buffer. The initial absorbance at 490 nm was recorded after mixing the solution for 20 s. Then another 20 µL of biotin-apo-GDH and biotin-HRP (positive control supplied in the kit, in a separate microplate well) were added. The final absorbance value was obtained in the same manner. The biotin to apo-GDH ratio was calculated based on these two

absorbance values using an empirical equation verified and provided by the manufacturer.

3.2.5. Determination of Residual Enzyme Activity and Maximum % Inhibition

The GDH-PQQ reconstitution assay, as described in detail in Chapter 2, was used to evaluate the residual enzyme activity for the biotin-GDH conjugates with varying degree of biotinylation. The biotin-GDH was diluted with Tris-Sulfate buffer to an appropriate concentration and in the presence of 15 nM PQQ, DCPIP/calcium chloride dye mix and glucose. The absorbance change at 590 nm was monitored and the result was compared to the assay with the same concentration of unconjugated apo-GDH.

In order to determine the maximum percent inhibition value for each biotin-GDH conjugate, 1 μg of avidin was added in aliquots to the wells containing 5 μg of the biotin-GDH conjugate. The mixture was incubated for 20 min, and then the GDH-PQQ reconstitution assay was carried out in the same manner as described above.

3.2.6. Association Kinetics Study of Avidin with Biotin-Apo-GDH

To determine the time dependence of association between avidin and biotin-apo-GDH, 10 μL of 10 μg/mL avidin and 10 μL of 5 μg/mL biotin-apo-GDH were mixed in 100 μL Tris-Sulfate buffer. The mixture was incubated for 0, 2, 5, 10, 20, and 30 min. Then GDH-PQQ reconstitution assay was carried out in the presence of 15 nM PQQ.

To determine the binding rate between avidin and biotin-apo-GDH, 10 μL of biotin-apo-GDH and 10 μL of avidin of varying concentration were mixed in 100 μL Tris-Sulfate buffer. The mixture was incubated for 20 min. Then the GDH-PQQ reconstitution assay was carried out in the presence of 15 nM PQQ.

3.2.7. Dose-Response Curve Toward Free Biotin

a) Equilibrium saturation mode: The free biotin solution of varying concentrations was prepared in assay buffer-Tris-Sulfate buffer. In equilibrium saturation mode, 10 µL of 10 µg/mL avidin, 10 µL of biotin with varying concentrations, and 10 µL of 5 µg/mL biotin-apo-GDH were mixed simultaneously and incubated for 30 min. Then the GDH-PQQ reconstitution assay was carried out in the presence of 15 nM PQQ.

b) Sequential saturation mode: In this mode, 10 µL of 10 µg/mL avidin and 10 µL of biotin with varying concentrations were incubated for 10 min before 10 µL of 5 µg/mL biotin-apo-GDH was added. The mixture was then incubated for 30 min. Then the GDH-PQQ reconstitution assay was carried out in the presence of 15 nM PQQ.

3.3. Results and Discussion

3.3.1. Biotin-Apo-GDH Conjugation

In an ideal homogeneous enzyme linked competitive binding assay, the ligand-enzyme conjugate should have as high a residual activity and as low a degree of ligand/enzyme conjugation as possible. The former determines the fast response and greatest modulation range upon binding with a binding protein. The latter not only ensures an active enzyme conjugate but also determines the lowest possible limit of detection.

In the present study, the biotin-apo-GDH conjugate was prepared with varying mole ratios of biotin to apo-GDH (see Table 3.1). Prior to the addition of activated biotin-sulfo-NHS, glucose was first mixed in the buffer solution containing apo-GDH and placed in the refrigerator (4 ºC) for 30 min. Glucose was added to protect the active site of apo-GDH from reaction with biotin-sulfo-NHS and the temperature control helped slow the kinetics the conjugation reaction. After repeated washings via the dialysis-

centrifugation tube, reconstituted biotin-apo-GDH was subject to a reactivation assay in the presence of free PQQ, glucose and a DCPIP/calcium chloride dye mix. The residual activities of the enzyme conjugates are summarized in Table 3.1. The starting mole ratio of 100:1 was found to be optimal in terms of the remaining activity as compared to unconjugated apo-GDH. This biotin-apo-GDH conjugate (GB-6) was further characterized with the HABA assay. The average number of biotin per GDH molecule was estimated to be 6.2. Essentially, under moderately basic condition (~ pH 8), biotin-sulfo-NHS reacts with side chain amino groups of lysine residues. GDH possesses 70 lysine residues (counted based on the amino acid sequence of the GDH (20)), of which at least 20-30 residues should be located in an accessible region, such as the outer surface of the enzyme molecule. It is believed that the number of biotin substitutions per enzyme molecule should follow a Gaussian distribution with a median/average at around 6 biotins/enzyme.

3.3.2. Avidin Association Study with Biotin-Apo-GDH Conjugates

Unlike antibodies which only have two binding sites for the antigens, a binding protein such as avidin has up to four binding sites for biotin (21). To evaluate the binding efficiency of the avidin with the biotin-apo-GDH conjugate, a time dependent kinetic study and a dose dependent study was carried out. As shown in Figure 3.2, in the presence of 100 ng avidin, the inhibition of biotin-apo-GDH was plotted against varying incubation times. The binding reaction occurred in two phases. The first phase involves the rapid change in enzyme activity and reached almost 80% maximum inhibition after 10 min incubation. The second phase showed a much slower rate change, indicating

further binding of avidins with biotins conjugated in certain regions of apo-GDH that may not be readily accessible. To study the dose dependent effect, the incubation time was fixed to be 20 min and varying amounts of avidin were incubated with 10 μL of 5 μg/mL of GB-6A. The avidin doses over 200 ng were shown to be the most efficient with inhibition close to 100% (see Figure 3.3). The avidin dose of 100 ng was chosen to be the "working dose" for the following competitive binding experiments for free biotin. This is because the lower the concentration of the binder present in the reaction mixture, the lower the number of free biotin molecules that are needed for the regeneration of the enzyme activity.

3.3.3. Competitive Binding Assays for Free Biotin

The competitive assays were evaluated with varying concentrations of free biotin present in the mixture containing the fixed amount of biotin-apo-GDH and avidin. In equilibrium saturation mode (22), avidin was added into the mixture of free biotin and biotin-apo-GDH, while in the sequential saturation mode (23), avidin was incubated with free biotin first for a period of time before the addition of biotin-apo-GDH. In both cases, PQQ was added after 30 min of the pre-incubations, i.e. after the formation of a relatively stable avidin-biotin-GDH complex. As shown in Figures 3.4 and 3.5, both assays showed excellent sensitivity toward free biotin detection. A "gate-like" response curve (24) indicated stronger binding between avidin and free biotin compared to avidin and the conjugate-biotin-GDH. In both cases, the detection limit was found to be less than 10 nM biotin with sequential saturation mode having a slight better sensitivity at the low concentration end. Theoretically (25), the detection range is dictated by the intrinsic catalytic efficiency of the enzyme and the interaction between the conjugate and the

binder. When a lower concentration of biotin-apo-GDH conjugate is used, a smaller amount of avidin is needed to completely inhibit the enzyme activity. Thus, a lower detection limit (< 5 nM) could be achieved (see Figure 3.6). Although it is attractive to continue lowering the detection limit by adjusting biotin-apo-GDH and avidin levels, it is not possible to do so because of the decreased enzyme activity and narrower modulation window (i.e., the biotin concentration range for 0% inhibition to 100% inhibition).

3.4. Conclusions

In this study, a homogeneous competitive binding assay was successfully demonstrated to detect free biotin concentrations using the apo-GDH/PQQ enzyme system. The assay utilized biotin-conjugated apo-GDH as an enzyme tracer which was then reconstituted with free PQQ to generate a signal in the presence of the redox dye DCPIP. An optimized biotin-apo-GDH conjugate was obtained by experimenting with varying starting mole ratios between biotin and apo-GDH. This was determined by examining the residual enzymatic activity of the biotin-apo-GDH conjugates and the maximum % inhibition of the enzyme conjugates in the presence of avidin. The dose dependence and incubation time effect of avidin toward biotin-apo-GDH conjugates were studied and optimized for the free biotin competitive binding assay. No distinguishable changes were found between the two different detection modes. This is probably because of the strong and fast binding/interaction of the avidin with the biotin-apo-GDH conjugates. A better detection limit could be achieved by lowering the concentration of avidin and biotin-apo-GDH; however, this is limited by the intrinsic enzymatic signal modulation range. Another option to accomplish this goal could be using a modified assay procedure, where an additional electron mediator – phenazine methosulfate (PMS)

could be coupled to the GDH-PQQ assay system as shown in Figure 3.7. If the avidin-biotin-apo-GDH complex is capable of preventing electrons from flowing to the DCPIP in the presence of PMS, a much more sensitive detection range could be readily achieved. Furthermore, it is also desired to have the site-specific biotinylation (26, 27) on the apo-GDH, possibly very close to the active site or at the substrate access region. Compared to the heterogeneous mixture of biotinylated apo-GDH prepared in this work, which gives an average enzymatic response in the presence or absence of binding of PQQ and glucose, a more homogeneous biotinylated apo-GDH is expected to be more sensitive to the change in the concentration of the binding molecule, avidin, e.g., less avidin needed for the inhibition of enzymatic response and thus possibly a lower detection range for free biotin. This could be accomplished by site-directed mutagenesis of the gene for apo-GDH that would make selective change of a single biotin molecule or other ligand on an amino acid site (arginine or cysteine) near the PQQ binding site of the enzyme.

	GB-6A	GB-9A	GB-10A	GB-11A	GB-7A
% activity, residual	32.5	7.1	5.8	5.0	3.3
Biotin/GDH	100: 1	200:1	300:1	400:1	500:1

	GB-6A, 1 µg avidin	GB-9A, 1 µg avidin	GB-10A, 1 µg avidin	GB-11A, 1 µg avidin	
% inhibition	81.1	96.4	97.6	97.7	

Table 3.1. Comparison of residual activity and avidin inhibition for biotin-apo-GDH conjugates with varying starting ratios of biotin to apo-GDH.

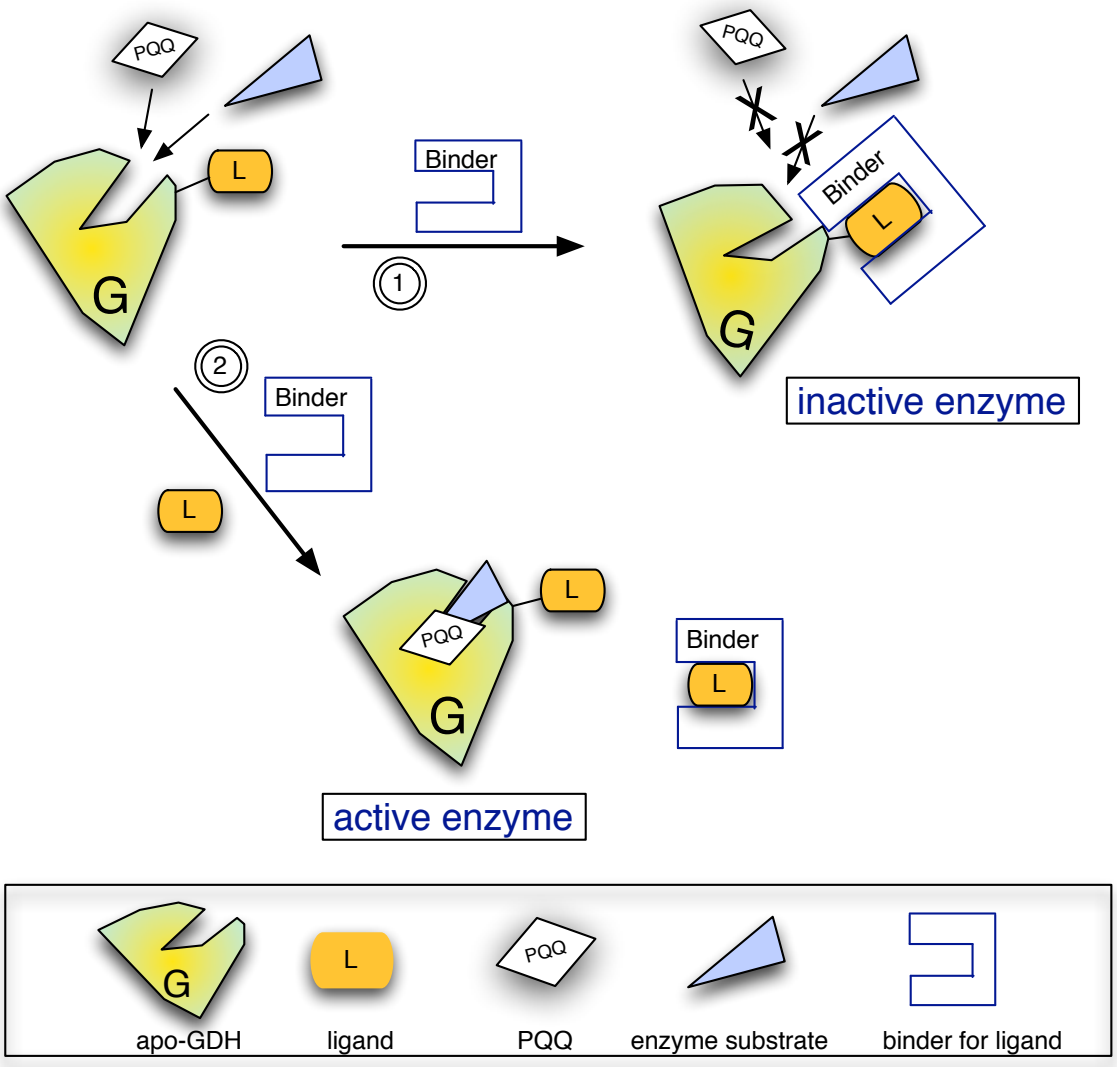

Figure 3.1. Enzyme-linked homogeneous competitive binding assay based on the GDH-PQQ reconstitution.

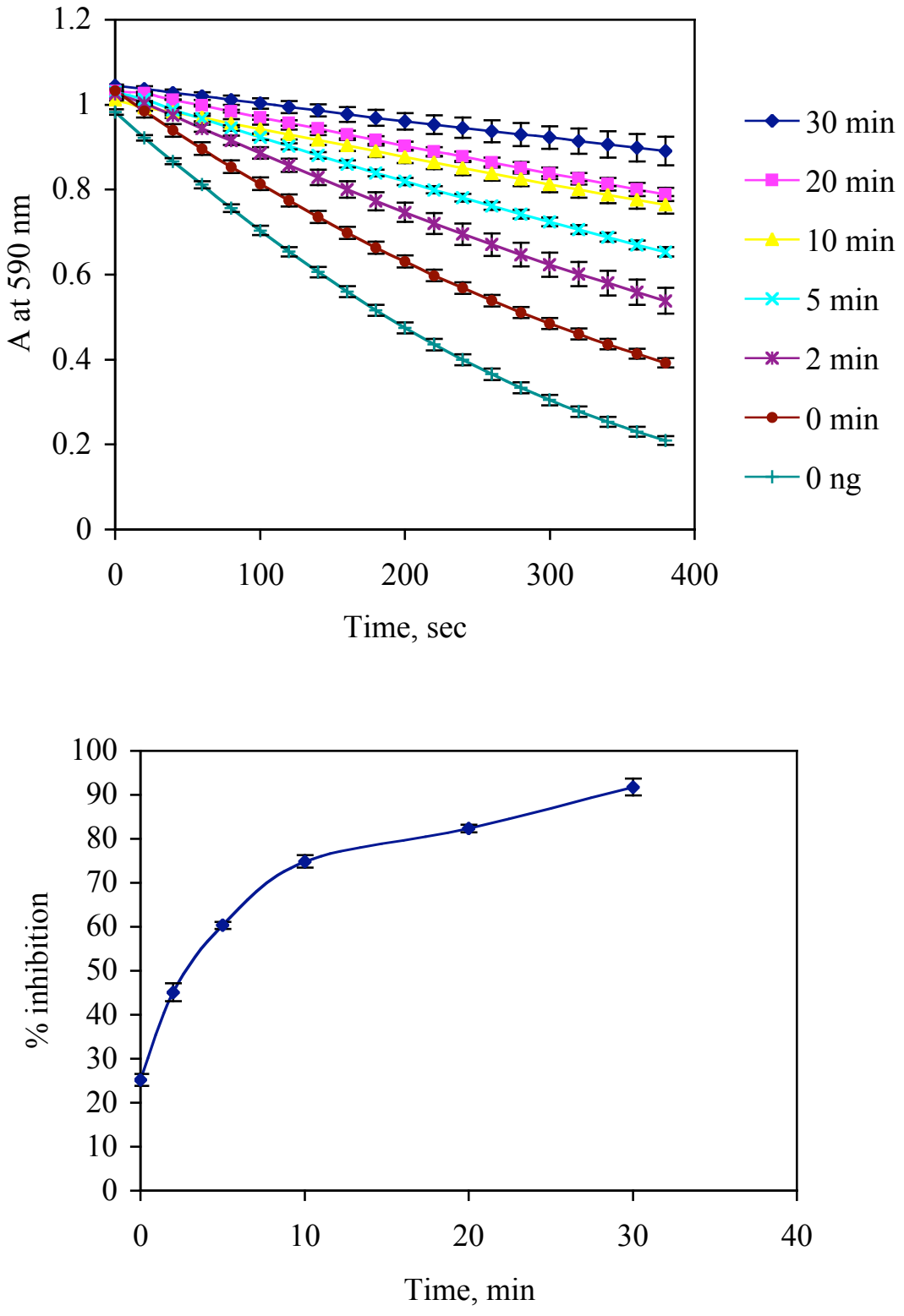

Figure 3.2. Real time data for monitoring the enzyme inhibition (above) and % inhibition reached with varying incubation times of 100 ng avidin with 10 µL of 5 µg/mL GB-6A.

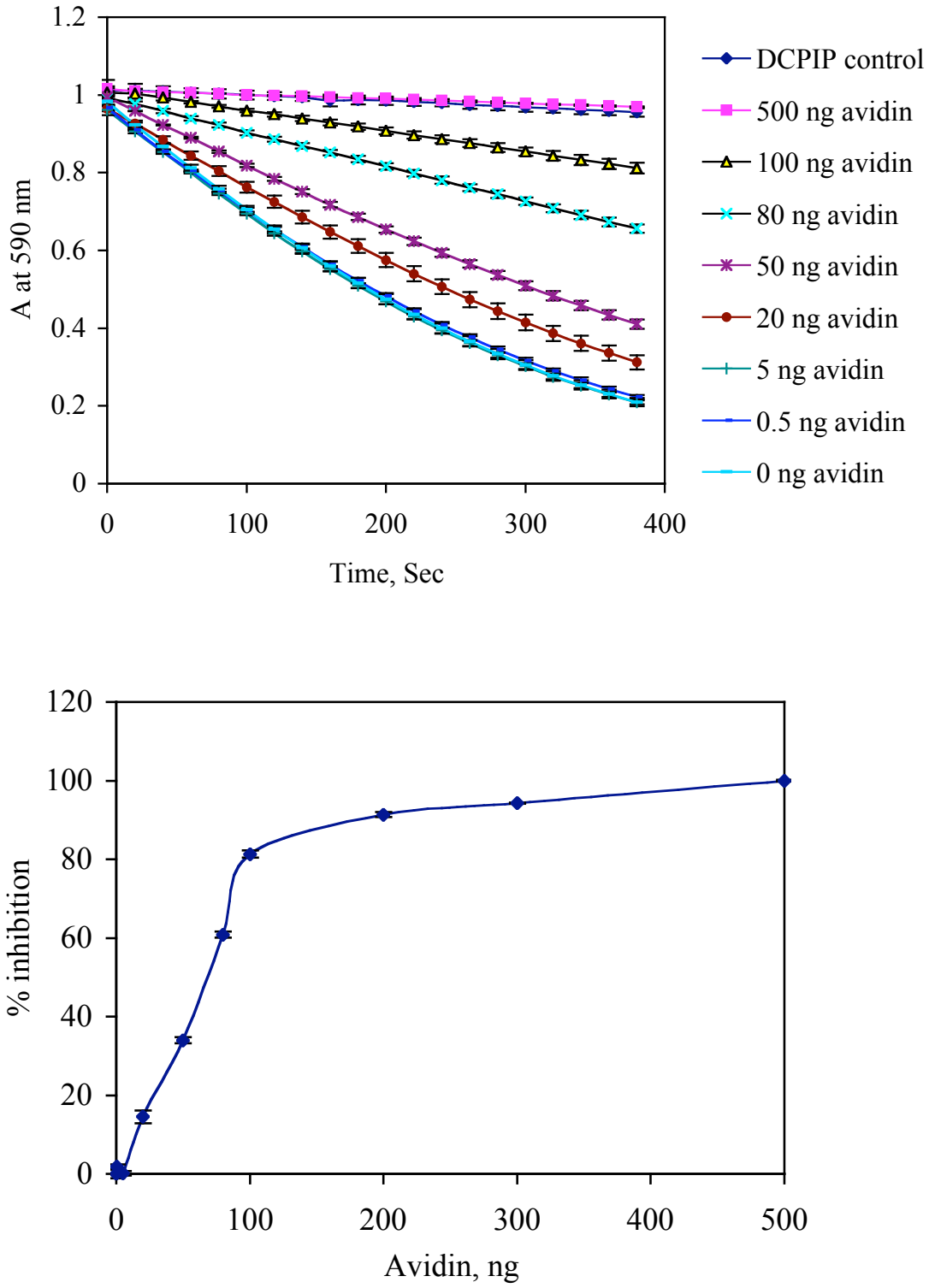

Figure 3.3. Real time data for monitoring the enzyme inhibition (above) and % inhibition reached with varying amounts of avidin with 10 µL of 5 µg/mL GB-6A at a fixed time of 20 min (below).

(a)

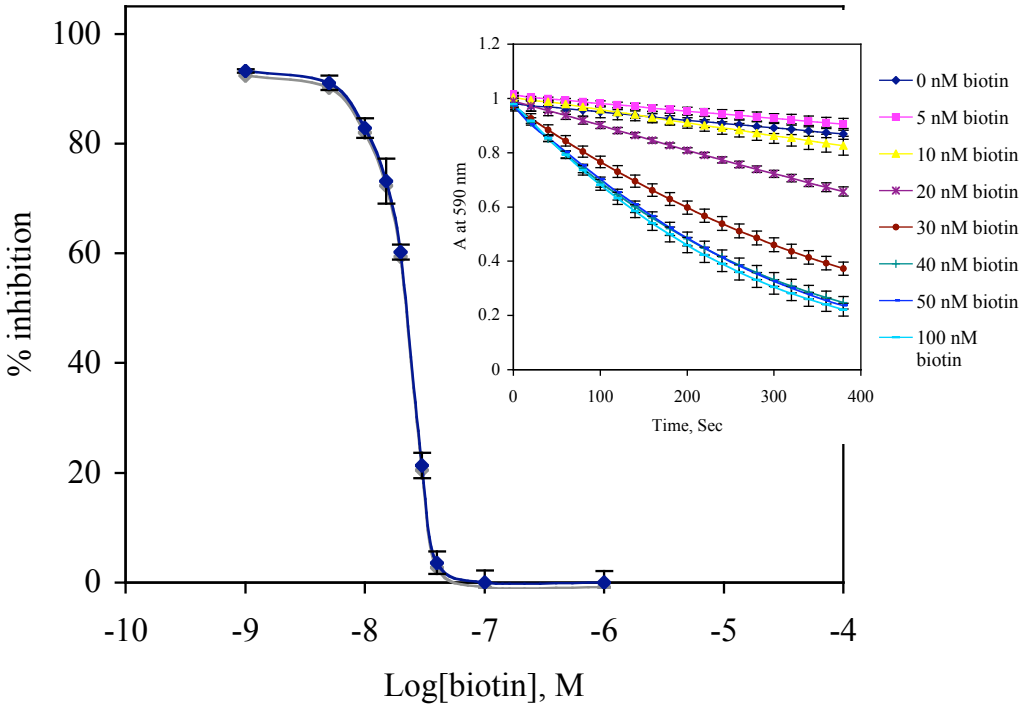

(b)

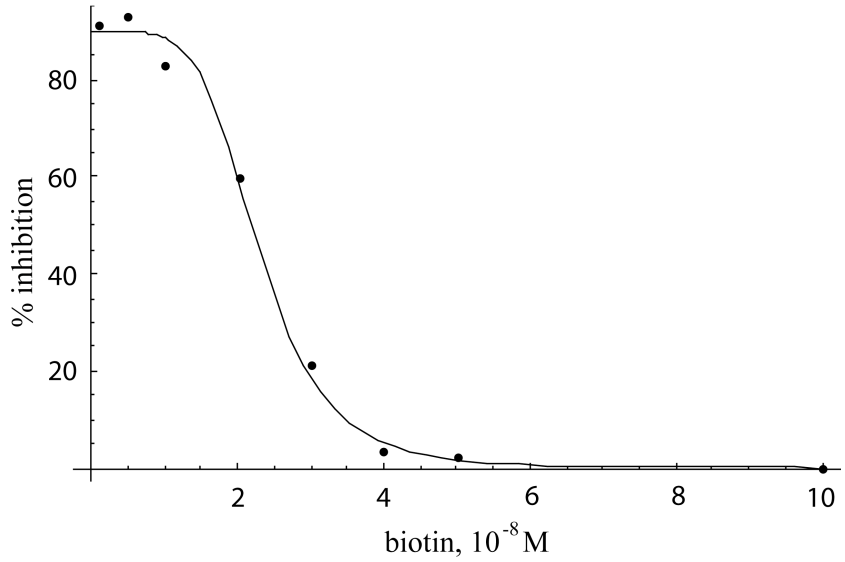

Figure 3.4. (a) Dose response curve of biotin in equilibrium saturation mode. (b) Curve fitting based on 4-parameter logistic model (28): Y= ((A-D)/1+(X/C)^B))+D, where A = 90 (zero concentration response), B = 5 (slope factor), C = 2.3 x 10^{-8} (inflection point), D = 0 (infinite concentration response).

(a)

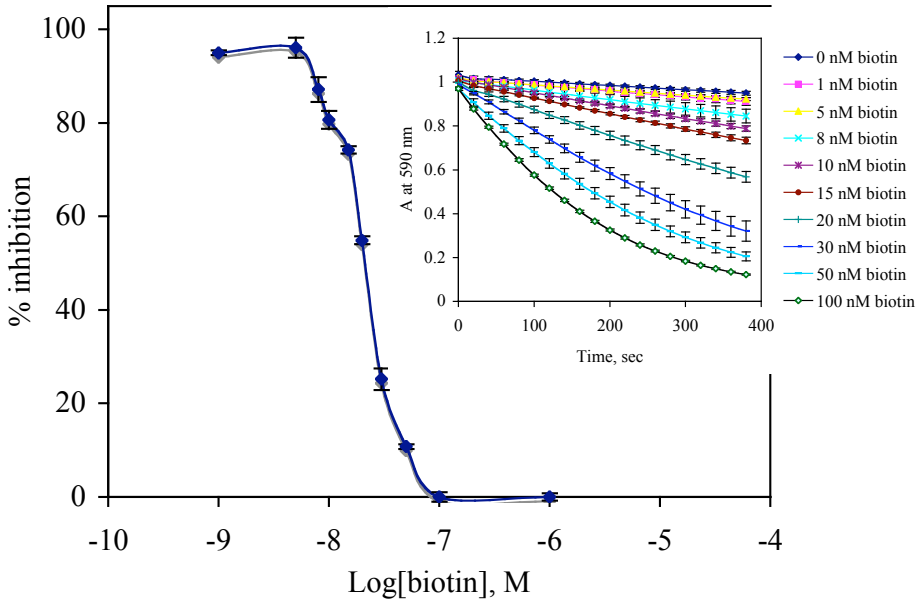

(b)

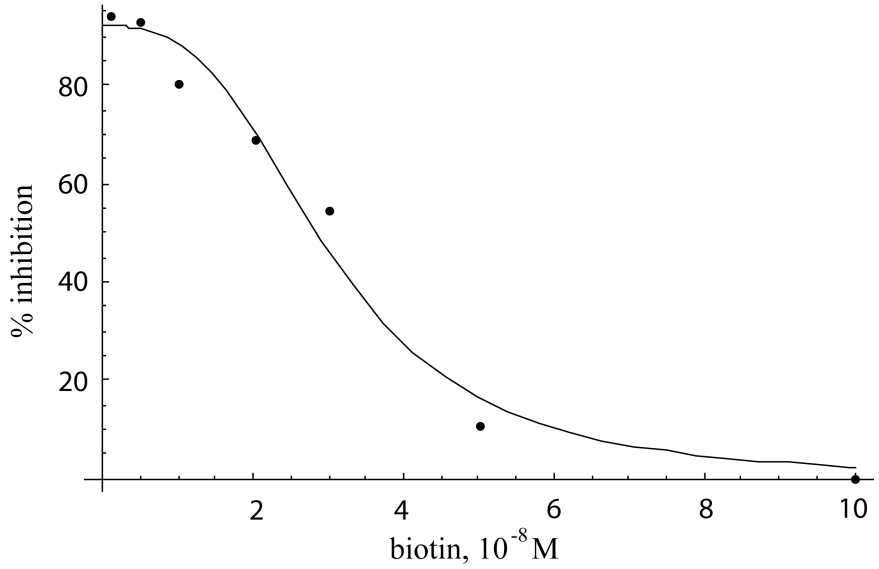

Figure 3.5. (a) Dose response curve of biotin in sequential saturation mode. (b) Curve fitting based on 4-parameter logistic model: Y= ((A-D)/1+(X/C)^B))+D, where A = 90 (zero concentration response), B = 3 (slope factor), C = 3 x 10^{-8} (inflection point), D = 0 (infinite concentration response).

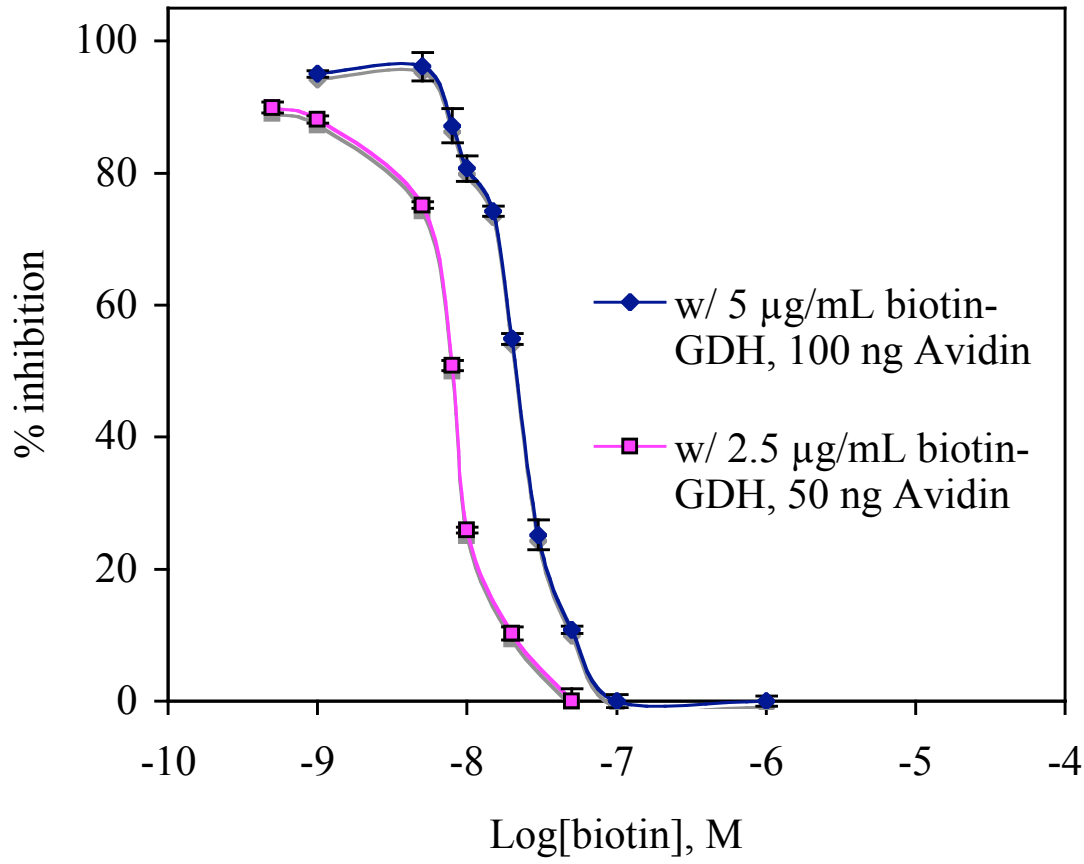

Figure 3.6. Shifting detection limit to lower concentration range by lowering concentration of signal modulator (biotin-apo-GDH).

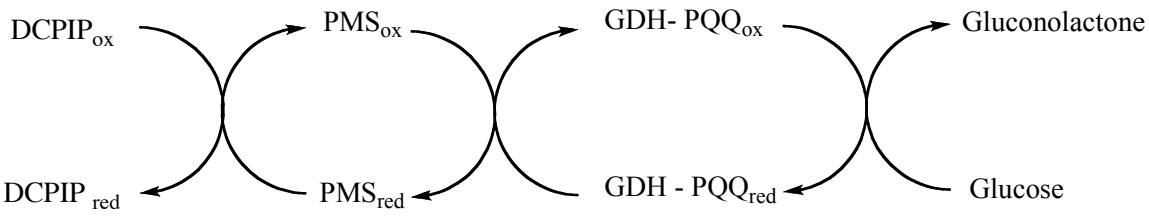

Figure 3.7. The electron transfer diagram of the GDH-PQQ reconstitution assay with PMS as a mediator.

3.5. References

(1) Bernhardt, P. *Aust. J. Chem.* **2006,** *59*, 233-256.

(2) Diaz-Gonzalez, M.; Gonzalez-Garcia, M.B.; Costa-Garcia, A. *Electroanalysis* **2005,** *17*, 1901-1918.

(3) Bizzaro, N.; Tampoia, M. *Clin. Rev. Allerg. Immunol.* **2008,** *34*, 16-20.

(4) Middelhoven, W.; Notermans, S. *Int. J. Food Microbiol.* **1993,** *19*, 53-62.

(5) Nielsen, U.; Geierstanger, B. *J. Immunol. Methods* **2004,** *290*, 107-120.

(6) Urlacher, A.; Tongio, M.; Mayer, S. *Pathol. Biol.* **1985,** *33*, 133-138.

(7) Bachas, L.; Meyerhoff, M. *Anal. Chem.* **1986,** *58*, 956-961.

(8) Cha, G.S.; Meyerhoff, M. *Anal. Chim. Acta* **1988,** *208*, 31-41.

(9) Daunert, S.; Bachas, L.; Meyerhoff, M. *Abstr Pap Am Chem S* **1987,** *194*, 165-ANYL.

(10) Guo, X.; Meyerhoff, M. *Appl. Biochem. Biotechnol.* **1997,** *68*, 41-56.

(11) Barbarakis, M.; Daunert, S.; Bachas, L. *Bioconjugate Chem.* **1992,** *3*, 225-229.

(12) Maclean, A.; Bachas, L. *Anal. Biochem.* **1991,** *195*, 303-307.

(13) Buckwalter, J.; Guo, X.; Meyerhoff, M. *Anal. Chim. Acta* **1994,** *298*, 11-18.

(14) Kim, H.J.; Kim, M.J.; Kim, J.M.; Cha, G.S. *Anal. Sci.* **1996,** *12*, 337-341.

(15) Daunert, S.; Bachas, L.; Meyerhoff, M. *Anal. Chim. Acta* **1988,** *208*, 43-52.

(16) Hofstetter, H.; Morpurgo, M.; Hofstetter, O.; Bayer, E.; Wilchek, M. *Anal. Biochem.* **2000,** *284*, 354-366.

(17) Livnah, O.; Bayer, E.; Wilchek, M.; Sussman, J. *FEBS Lett.* **1993,** *328*, 165-168.

(18) Green, N.M. *Spectrophotometric Determination of Avidin and Biotin.* Methods in Enzymol., Vol XVIII, 1970, Academic Press: New York, p. 418.

(19) Laitinen, O.; Hytonen, V.; Nordlund, H.; Kulomaa, M. *Cell Mol. Life Sci.* **2006,** *63*, 2992-3017.

(20) Oubrie, A.; Rozeboom, H.; Kalk, K.; Olsthoorn, A.; Duine, J.; Dijkstra, B. *EMBO J.* **1999,** *18*, 5187-5194.

(21) Neish, C.S.; Martin, I.; Henderson, R.; Edwardson, J. *Brit. J. Pharmacol.* **2002,** *135*, 1943-1950.

(22) Zettner, A. *Clin. Chem.* **1973,** *19*, 699-705.

(23) Zettner, A.; Duly, P.E. *Clin. Chem.* **1974,** *20*, 5-14.

(24) Tsalta, C.; Bachas, L.; Daunert, S.; Meyerhoff, M. *BioTechniques* **1987,** *5*, 148-151.

(25) Bachas, L.; Meyerhoff, M. *Anal. Biochem.* **1986,** *156*, 223-238.

(26) Cho, I.H.; Paek E.H.; Lee H.; Kang J.Y.; Kim T.S. and Paek S-H Anal. Biochem. 2007, 365, 14-23.

(27) Qiu X-Q; Jakes K.S.; Finkelstein, A. and Slatin, S.L. J. Biol. Chem. 1994, 10, 7483-7488.

(28) Findlay, J. W.A. and Dillard, R. F. *AAPS J.* **2007**, 9, Article 29, E260.

CHAPTER 4

CHARACTERIZATION OF PQQ DERIVATIVES AND EVALUATION OF THEIR BIOLOGICAL ACTIVITIES

4.1. Introduction

From single stranded nucleic acids to super coiled protein complexes, enzymes play important roles in the regulation of biochemical activities within living organisms (1). For this reason, it is necessary to quantitate the activity of specific enzymes such as proteases and nucleases, even via real-time measurements (2). Indeed, detection of enzymatic reactions in real-time is key to monitoring modern DNA assays, where exonuclease reactions can be employed for continuous PCR detection of a target DNA sequence. One important drawback of current enzymatic assays (3-8) includes long incubation times to achieve ultra-sensitive detection using simple analytical transduction methods such as spectrophotometry (9) and electrochemistry (10).

The long term goal of the research described in this chapter is to develop an enzyme amplification system that can be applied for the real-time detection of the activity of an oligomer cleaving enzyme by employing a specially designed substrate probe possessing a substrate cleavage site for a target enzyme. As illustrated in Figure 4.1, this approach can enable ultra-sensitive real-time enzyme activity assays based on a novel prosthetic group amplification mechanism. Both signal transduction and amplification will be realized through an electron transfer chain reaction based on the cleaving enzyme-

oligomer substrate reaction. The released prosthetic group will reactivate an apo-enzyme and the activity of this enzyme will serve as the signal generator as described earlier in this dissertation. Based on preliminary studies, the most promising system to implement such an assay is the apo-enzyme glucose dehydrogenase (GDH) and its prosthetic group, PQQ.

PQQ, the core group residing at the active center of GDH, however, has never been an easy molecule to derivatize. The quinone carbonyl group at the C-5 position (see structure shown in Figure 4.2) has been reported to be very reactive toward nucleophiles such as primary amines, aldehydes, thiols, and even acetone under weakly basic conditions (11). Water is also reported to be able to covalently attach to PQQ at both the C-5 and the C-4 positions to form a PQQ dihydrate, resulting in a green fluorescent species (12). Reduced forms ($PQQH_2$, $PQQH_4$), methyl derivatives and formation of other adducts greatly enhance the fluorescence signal. To better understand the reactivity and catalytic potency of PQQ, a number of studies have been carried out. A PQQ-butyraldehyde adduct was turned into a highly fluorescent compound after treatment with $NaBH_4$ (13). An aminophenol form of PQQ was prepared when PQQ trimethylester was reacted with ammonia (14). Model studies with PQQ analogues, such as 7,9-didecarboxyl PQQ (15), PQQ esters (mono-, di-, tri-esters), phenanthrene, and phenanthroline-dione (16), revealed the catalytic mechanisms of PQQ and investigated the residual activities of PQQ analogues when reconstituted with apo-GDH. It was also reported that PQQ forms oxazoles (17) or imidazolopyrroloquinoline (IPQ) (18) derivatives when incubated with amino acids.

In this chapter, a systematic study is undertaken toward developing an ultrasensitive assay with oligomer-PQQ conjugates. First, PQQ is covalently conjugated through an amide bond linkage with an amino acid residue. The possibility of direct reaction of carboxyl groups with molecules containing primary amines is investigated. Then, a variety of PQQ derivatives (see Figure 4.2) prepared by our collaborator, Berry & Associates, are further characterized with HPLC and MS and their biological activities are evaluated in the GDH reconstitution assay. Finally, the best strategy for attaching the oligomer substrate to PQQ molecules is suggested.

4.2. Experimental

4.2.1. Apparatus. A Perkin-Elmer dual beam spectrophotometer (Model: Lamda 35; Boston, MA) was used for recording UV-Vis spectra. A Micromass LCT Time-of-flight (TOF) interfaced with electrospray ionization (ESI) was used for obtaining sample mass spectra. A Varian Inova 500 (500 MHz) NMR spectrometer was used for the proton and carbon-13 NMR experiments. A Perkin-Elmer FT-IR spectrometer was used for PQQ conjugate characterization. An HP Agilent 1050 HPLC system equipped with a varying wavelength UV detector and a C-18 reversed phase column (Waters Symetry, 5 μm, 150 mm) was used for the PQQ analogue isolation and purification. A LABCONO freeze dry system (Model 7750000; Kansas city, MO) was employed for drying PQQ derivatives isolated from HPLC. A Labsystems Multiskan RC 351 microplate reader was used to monitor the color change as a result of the enzymatic reaction in a 96-well plate.

4.2.2. Reagents. All solutions were prepared with Millipore (18.2 MΩ Milli-Q) water. PQQ was obtained from Iris Biotech GmbH (Marktredwitz, Germany). PQQ dependent apo-glucose dehydrogenase, polypropylene 96-well microtiter plates and acetonitrile

were purchased from Fisher Scientific (Pittsburgh, PA). Esterase (from porcine liver), trihydroxylmethylaminomethane base (Tris), 2,6-dichlorophenolindophenol (DCPIP), glucose, trifluoroacetic acid, analine methylester, N-Ethyl-N′-(3-dimethylaminopropyl)carbodiimide (EDC), 1-hydroxybenzotriazole (HOBt), diisopropylethylamine (DIPEA) and sodium borohydride ($NaBH_4$) were purchased from Sigma-Aldrich (St. Louis, MO). The derivatives of PQQ triesters and their analogues were prepared by Berry & Associates (Dexter, MI).

4.2.3. Preparation, Isolation and Characterization of Alanine Methylester Conjugate of PQQ (PQQ-AlaOMe)

A sample of 10 mg of PQQ (26.7 μmole) was dissolved in about 1 mL of 50 mM phosphate buffer, pH 6.0, and the solution was transferred to a 2 mL air-tight vial. The solution was purged with Ar for 30 min before 5 mg of $NaBH_4$ (at least 10 eq.) was added. The reduction reaction was allowed to proceed for 1 h at room temperature. Using a modified procedure from the literature (19), 2 equivalents of AlaOMe, 1.1 equivalents of EDC, 0.1 equivalent of HOBt and 1 μL of DIPEA were mixed and purged with Ar thoroughly before injection into the reduced PQQ solution. The reaction mixture was stirred for another 6 h followed by subsequent purification using HPLC (acetonitrile and water with 0.1% TFA as mobile phase). A gradient method with 10% to 40% acetonitrile over 20 min was used. The organic solvent in the pooled sample after the HPLC separation was removed by the rotary evaporation system and the remaining aqueous portion was frozen with a “cold bath” containing 0.5 lb of dry ice and 200 mL of acetone. The frozen sample was immediately moved into one of the chambers of the

freeze dryer and remained there for 72 h until completely dried. The dried sample was further characterized with UV-Vis, FT-IR, MS and NMR for the identification of PQQ-AlaOMe.

4.2.4. GDH Reconstitution Assay for PQQ Derivatives

PQQ derivatives were dissolved in acetonitrile first and then further diluted with 50 mM Tris-sulfate buffer, pH 7.0, in varying concentrations for the GDH reconstitution assay. Briefly, in 200 µL of Tris-Sulfate buffer, 10 µL of 0.25 mg/mL apo-GDH, 50 µL of dye mix (0.4 mM DCPIP containing 8 mM calcium chloride), 40 µL of 40 mM glucose and 10 µl of a solution of PQQ derivatives (with or without incubation with sodium hydroxide as described below) were mixed together in a 96-well microtiter plate. Absorbance changes were monitored at 590 nm and the data points were obtained every 20 s.

4.2.5. Identification of the Hydrolyzed PQQ Esters Using HPLC and MS

One of the PQQ derivatives shown in Figure 4.2, DF40, was selected as a model compound for further investigation on the hydrolysis behavior of this class of PQQ esters. Sodium hydroxide and a general esterase were used for the hydrolysis experiments. Briefly, 0.7 mg of DF40 was dissolved in 0.4 mL of acetonitrile and 0.8 mL of D.I. water. The DF40 solution was then further diluted to the desired concentrations with Tris-Sulfate buffer. An aliquot of 200 µL of the prepared DF40 was mixed with an equal volume of 20 mM NaOH. After 5 min of incubation at room temperature, 10 µL of the mixture was used for the GDH reconstitution assay.

A 20 µL injection of the DF40 (with or without NaOH incubation) was performed on the HPLC with a gradient method (acetonitrile: 10% to 20% at 0-12min, then 70% at 20 min). Eluted peaks with retention time at 12.5 min, 18 min and 19 min were collected for the MS analysis. Molecular masses of the hydrolysis products were determined using the Micromass TOF mass spectrometer interfaced with an electrospray ionization module. The mobile phase was composed of methanol:water (50:50, v/v) delivered at 0.1 mL/min by an HPLC pump. A direct injection of 20 µL of sample was performed and the spectra were obtained in positive ion mode with a capillary voltage of 3.7 kV, a source temperature of 100 ºC and a cone voltage of 30 V.

A hydrolysis experiment was also performed with the esterase, where a sample containing 500 µL of 150 µM DF40 was incubated with 100 µL of 2 mg/mL esterase at 37 ºC for 1 h. The reaction was stopped by filtering off the esterase from the mixture using an Amicon centrifuge tube equipped with a filter inset of 5,000 MWCO (molecular weight cut-off). The filtrate was collected and 100 µL of it was injected onto the HPLC following the same elution method as described above. The MS analysis was performed with the pooled sample at the retention time of 15 min and the result was compared with the samples from the NaOH hydrolysis experiment.

4.3. Results and Discussion

4.3.1. Direct Conjugation Reaction with Alanine Methylester

The C-5 carbonyl group of PQQ is responsible for the catalytic conversion of glucose to gluconolactone at the active center of GDH via a proposed direct hydride transfer mechanism (20). In a similar fashion, this site also possesses the strong reactivity towards nucleophiles and it competes with any other reactions that induce a

nucleophilic attack mechanism to create desired derivatives. A reduction method using $NaBH_4$ has been shown to completely reduce the quinone groups at C-4 and C-5 positions to quinols (21) based on the UV-Vis analysis (see Figure 4.3). An anaerobic environment under Ar helps prevent the quinols from oxidizing back to quinones simply by oxygen dissolved in the solutions and from the ambient air. However, the in situ reactivation method using EDC and a catalytic amount of HOBt was not very successful in obtaining the desired PQQ conjugate of the alanine methyl ester via only one of the three PQQ carboxyl groups (see Figure 4.4a). As shown in the UV-Vis spectra (Figure 4.5), a strong red shift of the λ_{max} occurred from 260 nm (PQQ) to 296 nm (PQQ-AlaOMe), suggesting a possible reaction with the quinones. The FT-IR spectra, as shown in Figure 4.6, also suggested that one of the carbonyl groups was reacted, thus causing the disappearance of one carbonyl stretching and a shift of the other carbonyl stretching band from 1674 cm^{-1} to 1680 cm^{-1}. The comparisons of proton NMR and C-13 NMR spectra between PQQ and PQQ-AlaOMe, shown in Figures 4.7 and 4.8, indicated that the isolated PQQ-AlaOMe was a mixture of analogues, even though it appeared to be pure in the HPLC chromatogram (see Figure 4.9). The result from mass spectrometry, shown in Figure 4.10, further confirmed the identity of the PQQ derivative of alanine methyl ester, with an m/z of 488 (M+H+Methanol). In conclusion, it appears that alanine methylester was conjugated with one of the carboxyl groups of PQQ and it was also reacted with the C-5 quinone to form an IPQ adduct, as shown in Figure 4.4b.

4.3.2. Evaluation of Biological Activity of the PQQ Derivatives

The biological activities in terms of the reconstituted GDH activity for the PQQ derivatives prepared by Berry & Associates (see Figure 4.2), before and after NaOH hydrolysis, are shown in Figures 4.11a and 4.11b, respectively. The comparison of the activity loss before and after NaOH hydrolysis (also in comparison to free PQQ activity) is summarized in Table 4.1. Before NaOH hydrolysis, no PQQ triesters showed any activity in the GDH assay. A free carboxyl group at C-9 position gave ~0.04% of the activity compared to free PQQ and free carboxyl groups at C-2 and C-9 positions regained ~ 45% of the activity. These results reaffirmed the importance of the carboxyl groups, especially the ones at the C-2 and C-9 positions (22), in stabilizing the location of PQQ at the active center of the GDH. After NaOH hydrolysis, DF40 and DF60 regained their activities by about 5.4% and 0.009%, respectively. This could be explained by the difference of the ester groups at C-2 positions, with DF40 having an ethyl ester and DF60 having a hexyl ester. The esters on C-2 were not subject to hydrolysis even under more harsh conditions such as using higher concentrations of NaOH (data not shown). The activity of DF214 remained the same suggesting the amide bond was stable under such conditions. However, at this point, no conclusions could be drawn regarding which ester groups were most susceptible to the NaOH hydrolysis.

4.3.3. Characterization of the Hydrolysis Product of DF40

In order to further understand the results from the base hydrolysis experiment, DF40 was chosen for the subsequent HPLC/MS study. The pooled samples from the HPLC isolations (see Figure 4.12) were subjected to MS analysis, where the m/z or molecular weight of the samples was correlated, as shown in Figure 4.13, to the peaks in

the HPLC chromatograms. This allowed for the identification of the hydrolyzed products. Intact DF40 eluted at 19 min with an m/z of 387.1 (M+H). The NaOH hydrolysis products eluted at 18 min and 12 min. The m/z of 18 min peak was found to be 373.1 and it corresponded to the PQQ di-esters where one of the methyl esters was hydrolyzed. The ethyl ester at C-2 position remained the same as discussed earlier. The m/z of 12 min peak was found to be 269.1 and it appeared to be a product of PQQ mono-ester with only the ethyl ester on C-2 position left. The hydrolysis products after the esterase treatment were eluted at 19 min and 15 min, with 19 min peak being the unhydrolyzed DF40 and a new product different from those of the NaOH hydrolysis. The m/z of the 15 min peak was found to be 291.1, 301.0 and 327.2, each of which corresponded to the fragmentation patterns with the two possible structures shown in Figure 4.10. Given that the ethyl ester at the C-2 position was always robust and that the biological activity in the GDH assay for the esterase hydrolysis of DF40 was almost 0 (data not shown), it is believed that the 15 min peak corresponds to a di-ester with the ethyl ester at the C-2 position and one methyl ester at the C-9 position, both of which were confirmed to be critical in inhibiting the biological activities of PQQ in the GDH assay. The methyl ester at the C-7 position is also believed to be more accessible for the binding of the esterase. The 18 min peak found with NaOH hydrolysis is likely to be the one with a free carboxyl group at the C-9 position.

4.4. Conclusions

In this study, a direct conjugation method using a small amino acid was attempted with the reduction-protection for the quinone groups of the PQQ. The prepared conjugates were then characterized to be an IPQ form (Figure 4.4b) with one of the

carboxylic acid groups linked with the small molecule-alanine methylester. Then, the biological activities of PQQ derivatives obtained from Berry & Asscociates were evaluated in the GDH reconstitution assay. The esterification of carboxyl groups at the varying positions was demonstrated to weigh unevenly in reactivating the GDH and the order of their impact on the GDH activity was found to be as follows: C-2 ≥ C-9 > C-7. Sodium hydroxide enabled the fast hydrolysis of DF40 and the hydrolyzed product showed good regenerating activity (~5% compared to free PQQ). The hydrolysis experiments with NaOH and esterase, with HPLC separation and MS identification, concluded that the ester at the C-2 postion was the most stable from hydrolysis, followed by the ester at the C-9 position. The ester at the C-7 position was the most vulnerable upon exposure to hydrolysis conditions and it was also the most accessible to binding of the esterase to enhance the observed decomposition at this postition. Thus, the best linking strategy for further development of an appropriate PQQ-oligomer substrate should include the C-7 carboxyl group as the anchor point. The potential hydrolysis problems could be avoided if a linking chemistry, such as a hydroxamate bond (DF228), other than an amide bond is used.

	before NaOH hydrolysis	after NaOH hydrolysis
DF40	no activity	18.6 fold less (5.4 %)
DF60	no activity	11250 fold less (0.009%)
DF214	~2450 fold less	~2450 fold less
DF228	~45% of free PQQ	n/a

Table 4.1. Summary and comparison of the biological activities of PQQ derivatives (relative to free PQQ activity in the GDH reconstitution assay).

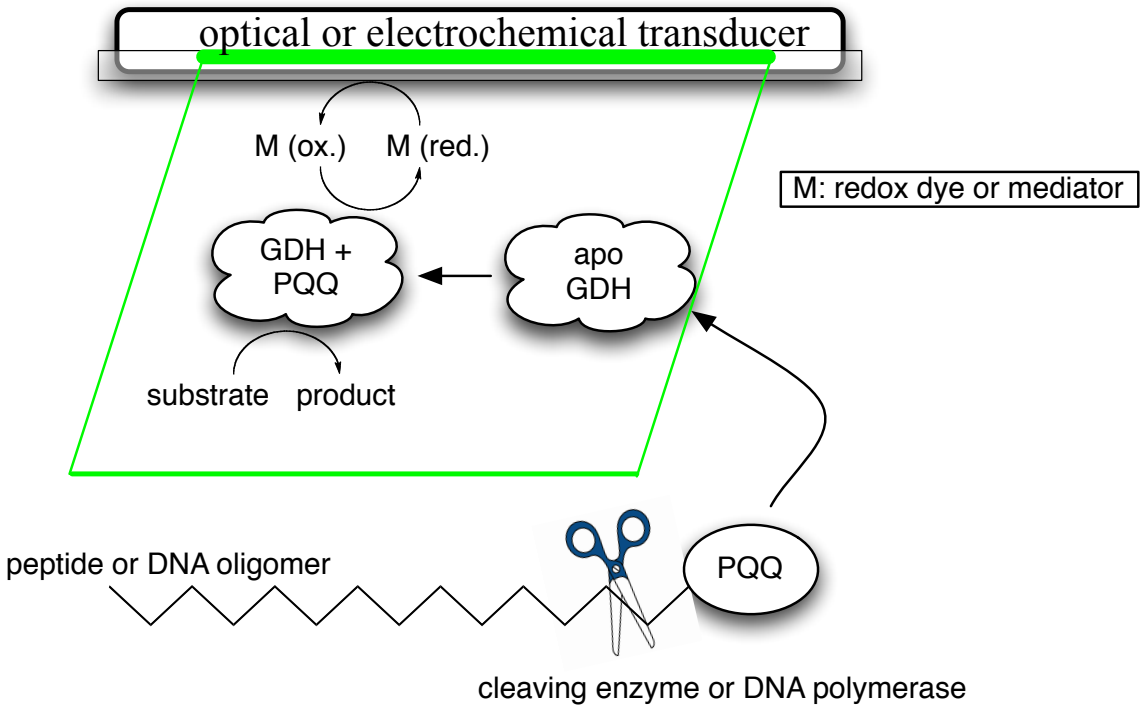

Figure 4.1. Homogeneous cleaving enzyme assay based on reconstitution of the PQQ fragment with apo-GDH after enzymatic cleavage.

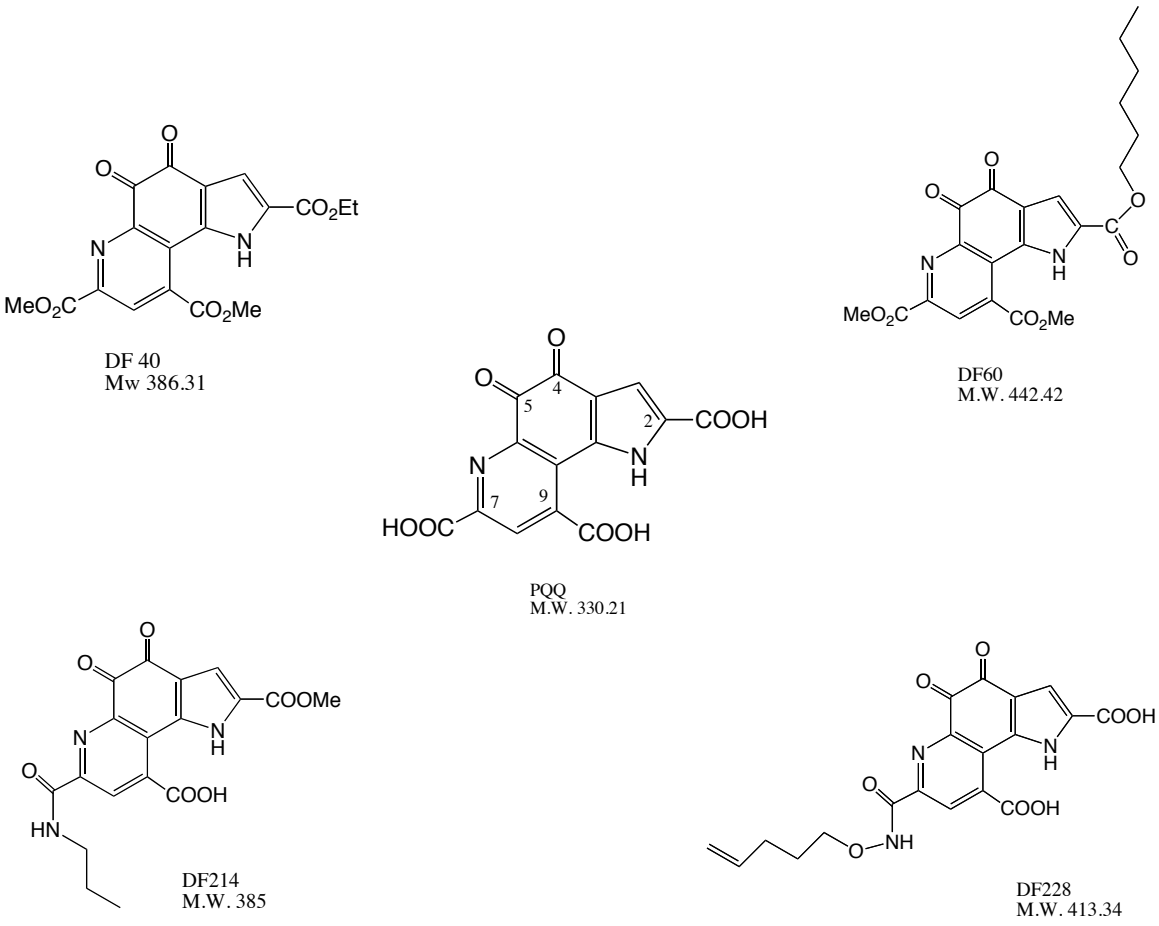

Figure 4.2. PQQ and PQQ derivatives examined in this work.

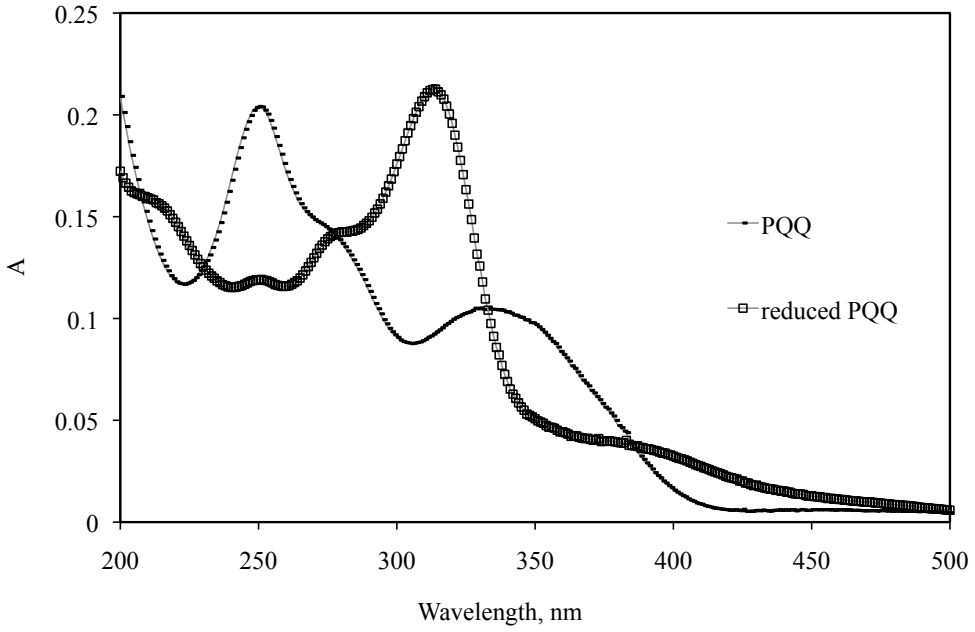

Figure 4.3. UV spectra overlap for PQQ and $NaBH_4$ reduced PQQ.

(a)

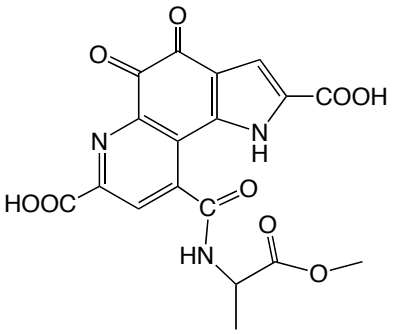

(b)

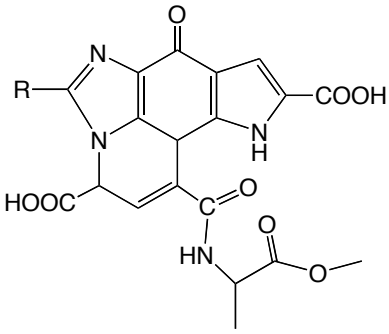

Figure 4.4. The desired PQQ-alanine methyl ester (a) and the synthesized IPQ adduct (b) of PQQ-alanine methyl ester. (Note that the alanine methyl ester can be bonded to any one of the three PQQ carboxyl groups.).

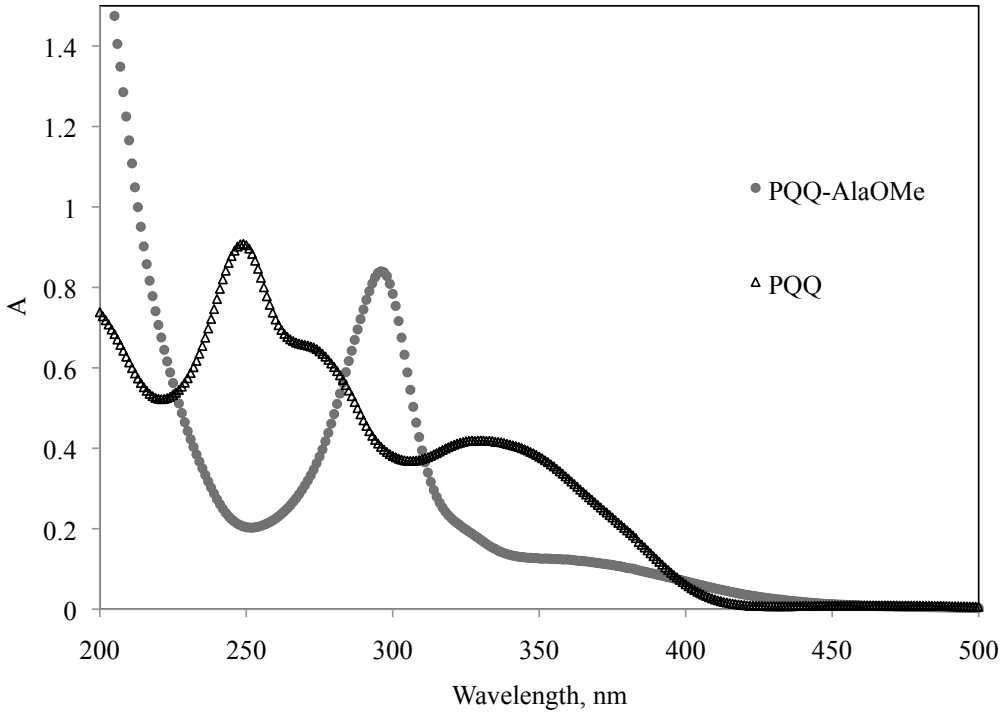

Figure 4.5. UV-Vis spectra comparison of PQQ and PQQ-alanine methyl ester conjugate.

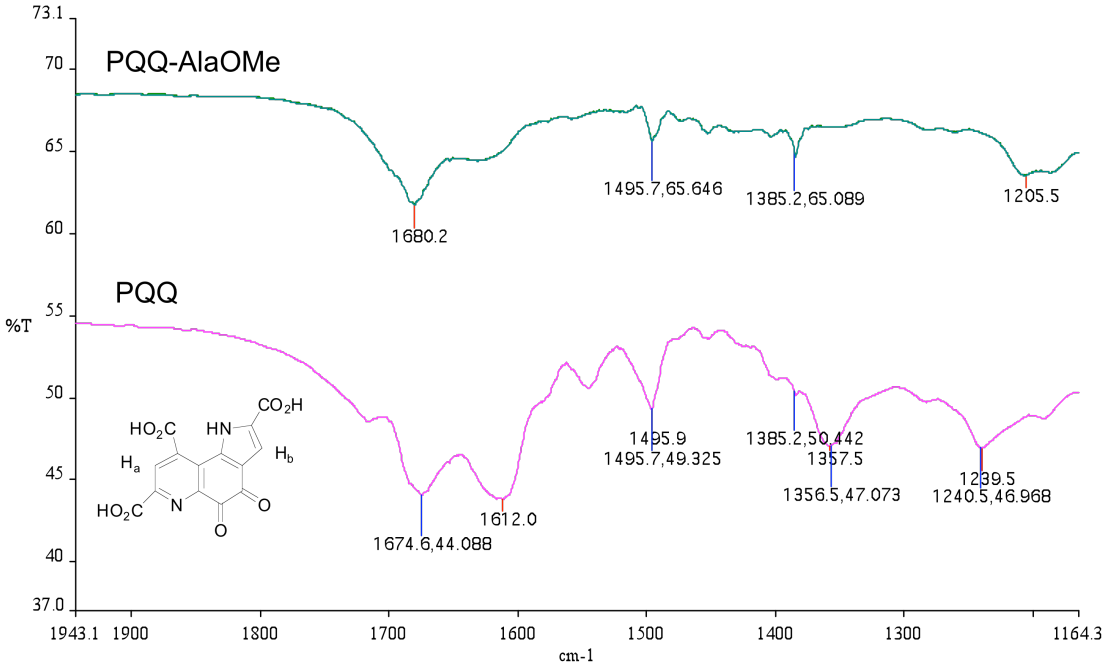

Figure 4.6. FT-IR spectra comparison of PQQ and PQQ-alanine methyl ester conjugate.

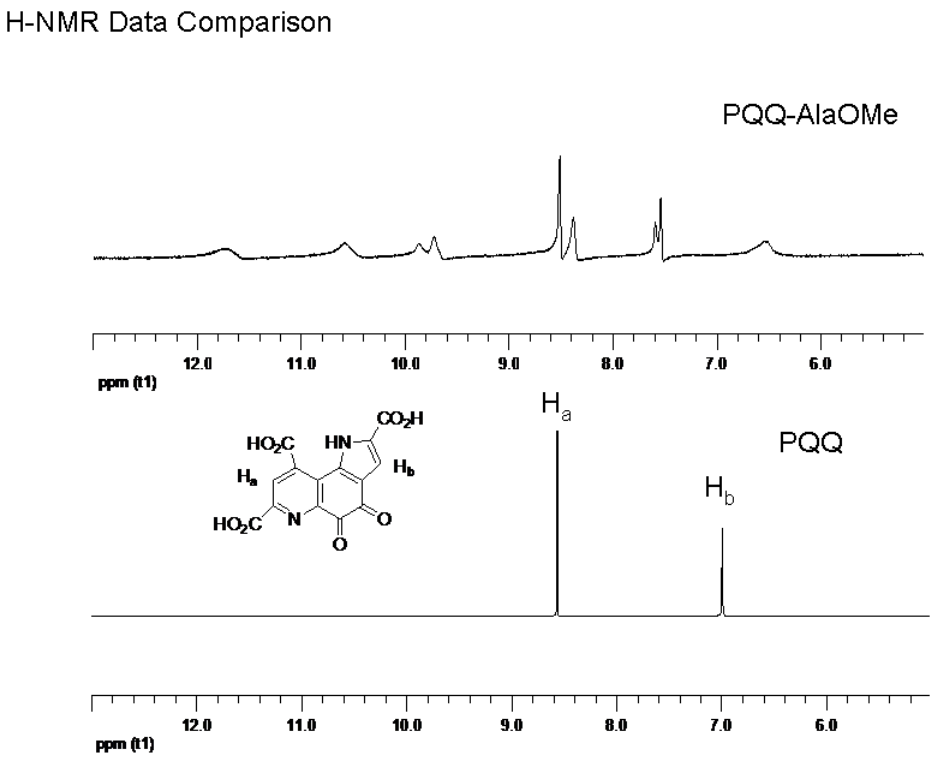

Figure 4.7. Proton NMR spectra of PQQ and PQQ-alanine methyl ester conjugate.

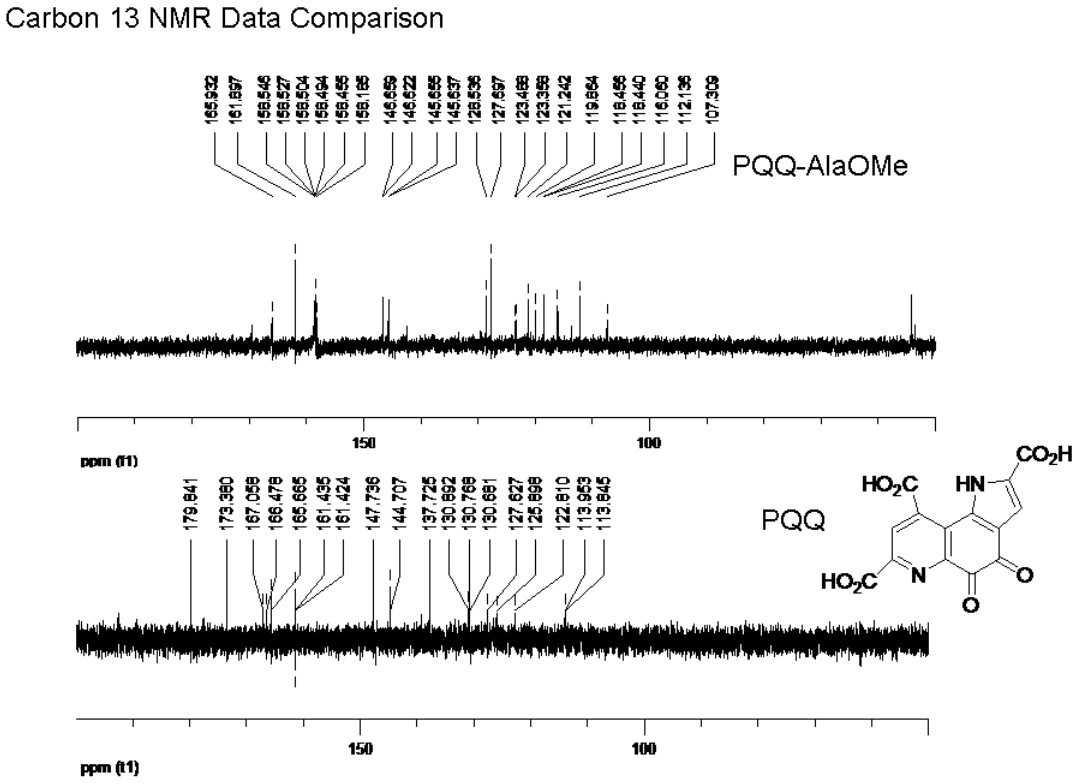

Figure 4.8. C13-NMR spectra of PQQ and PQQ-alanine methyl ester conjugate.

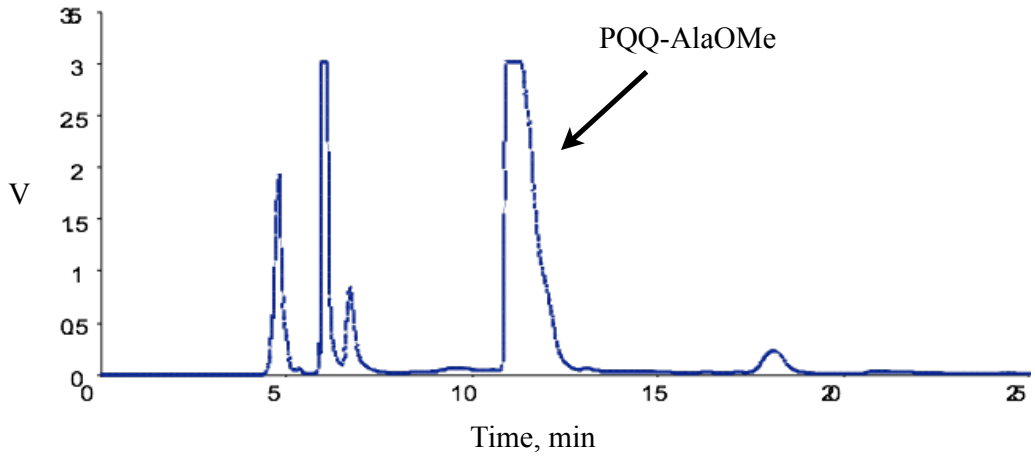

Figure 4.9. HPLC chromatogram showing the isolation of PQQ-alanine methyl ester conjugate.

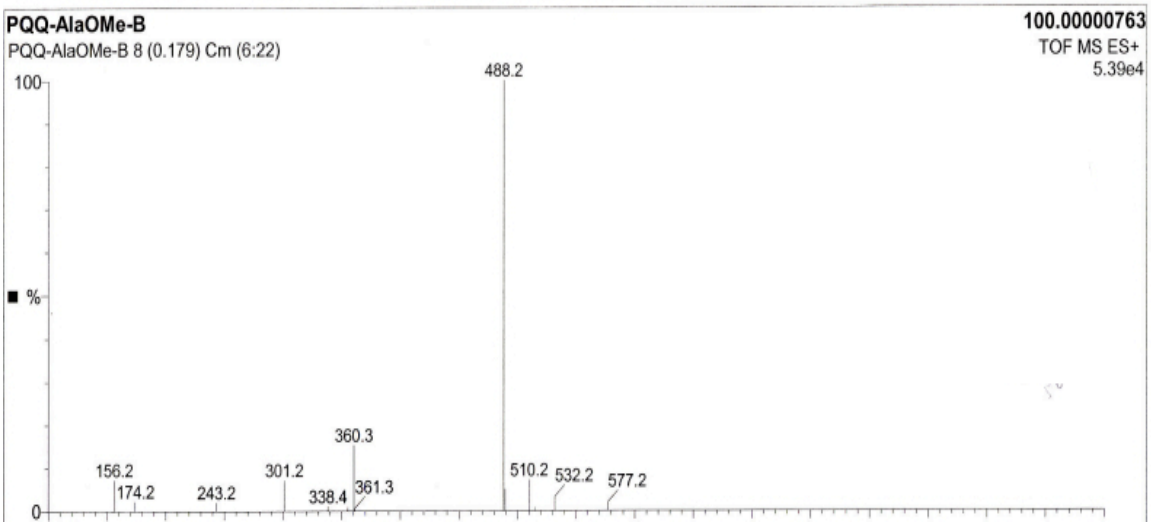

Figure 4.10. Mass spectrum of HPLC purified PQQ-alanine methyl ester conjugate.

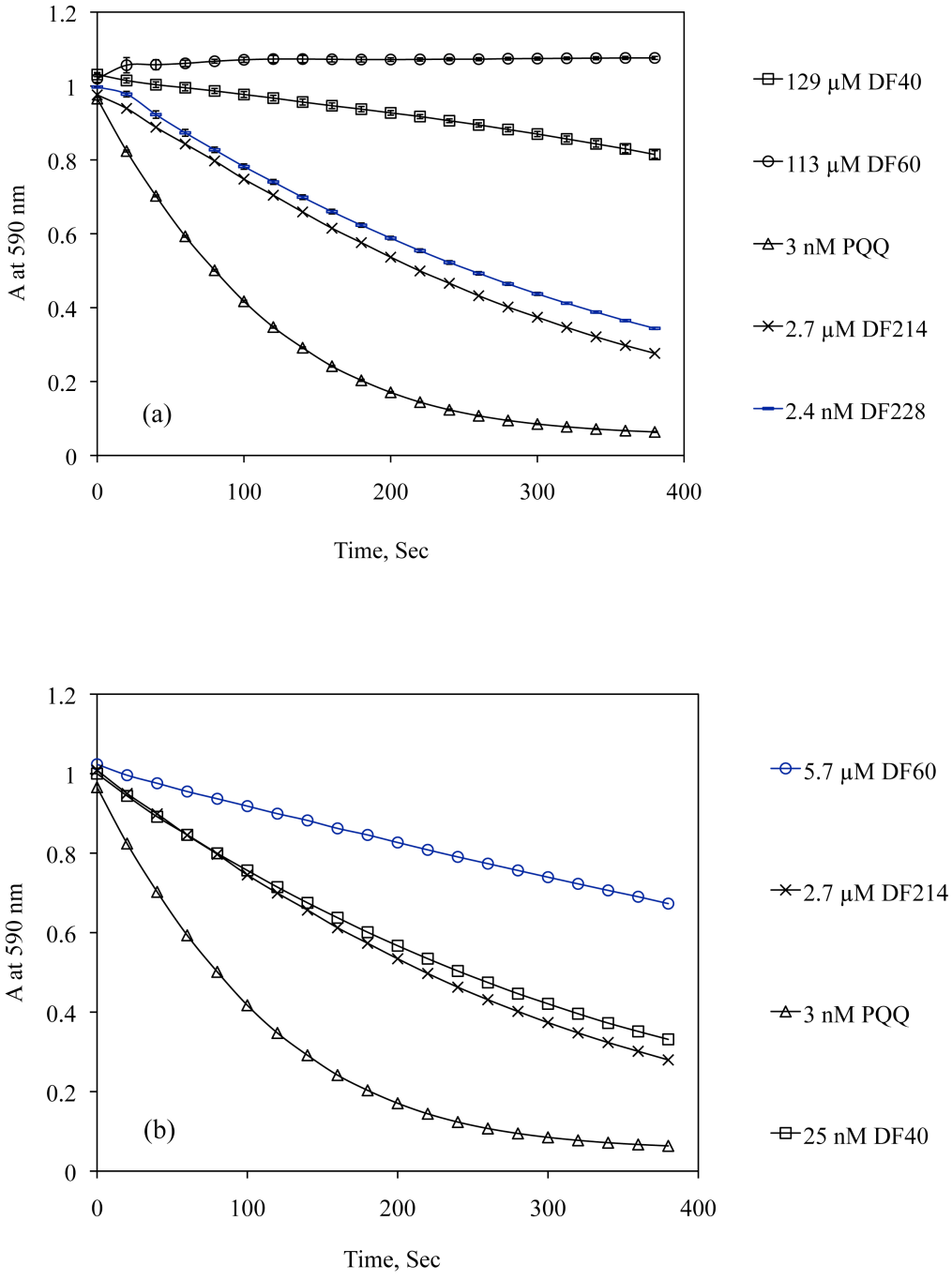

Figure 4.11. Biological activities of PQQ deriviatives measured with the GDH reconstitution assay before (a) and after (b) NaOH treatment.

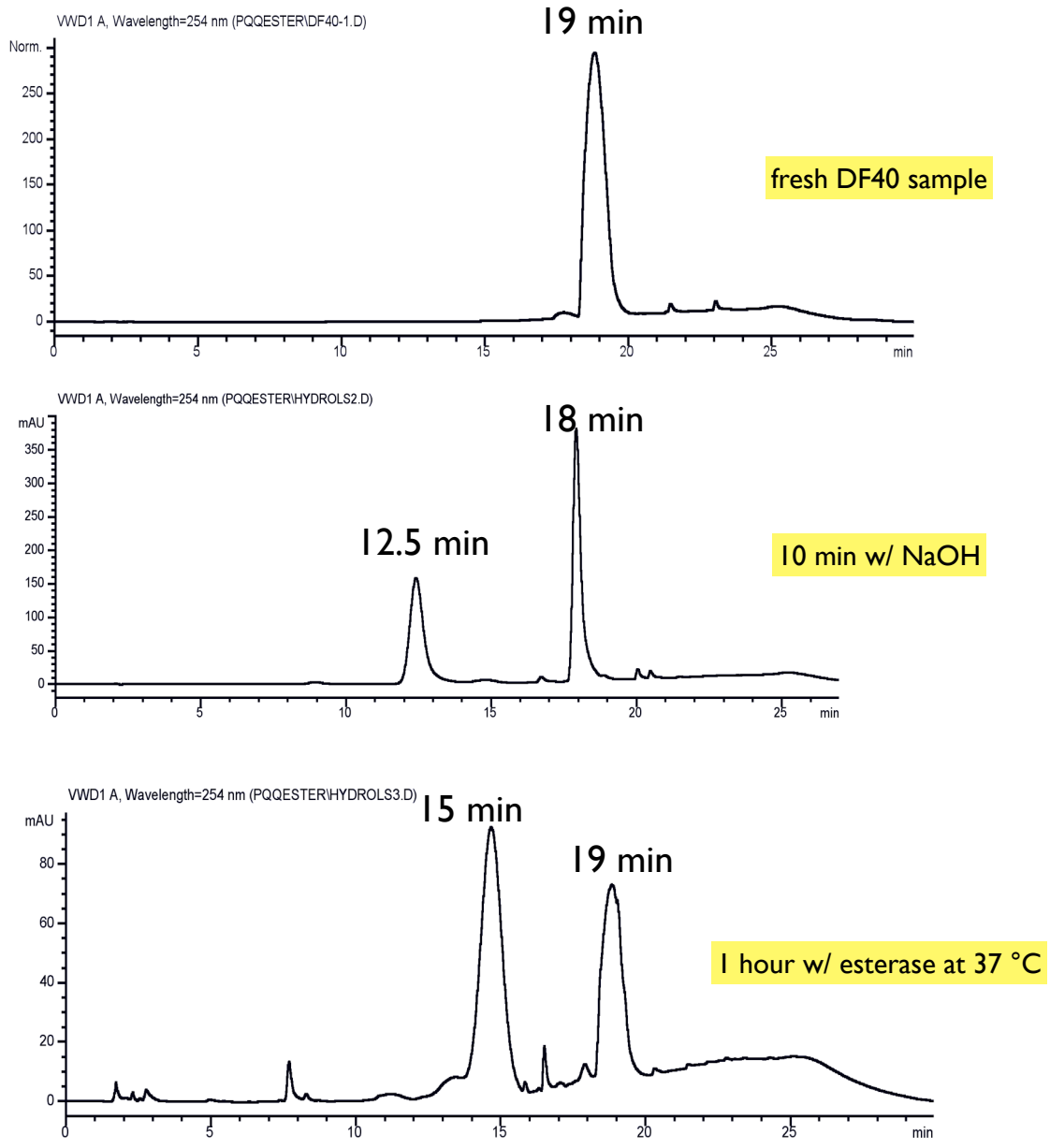

Figure 4.12. HPLC separations of the hydrolysis product under the treatment with NaOH or esterase.

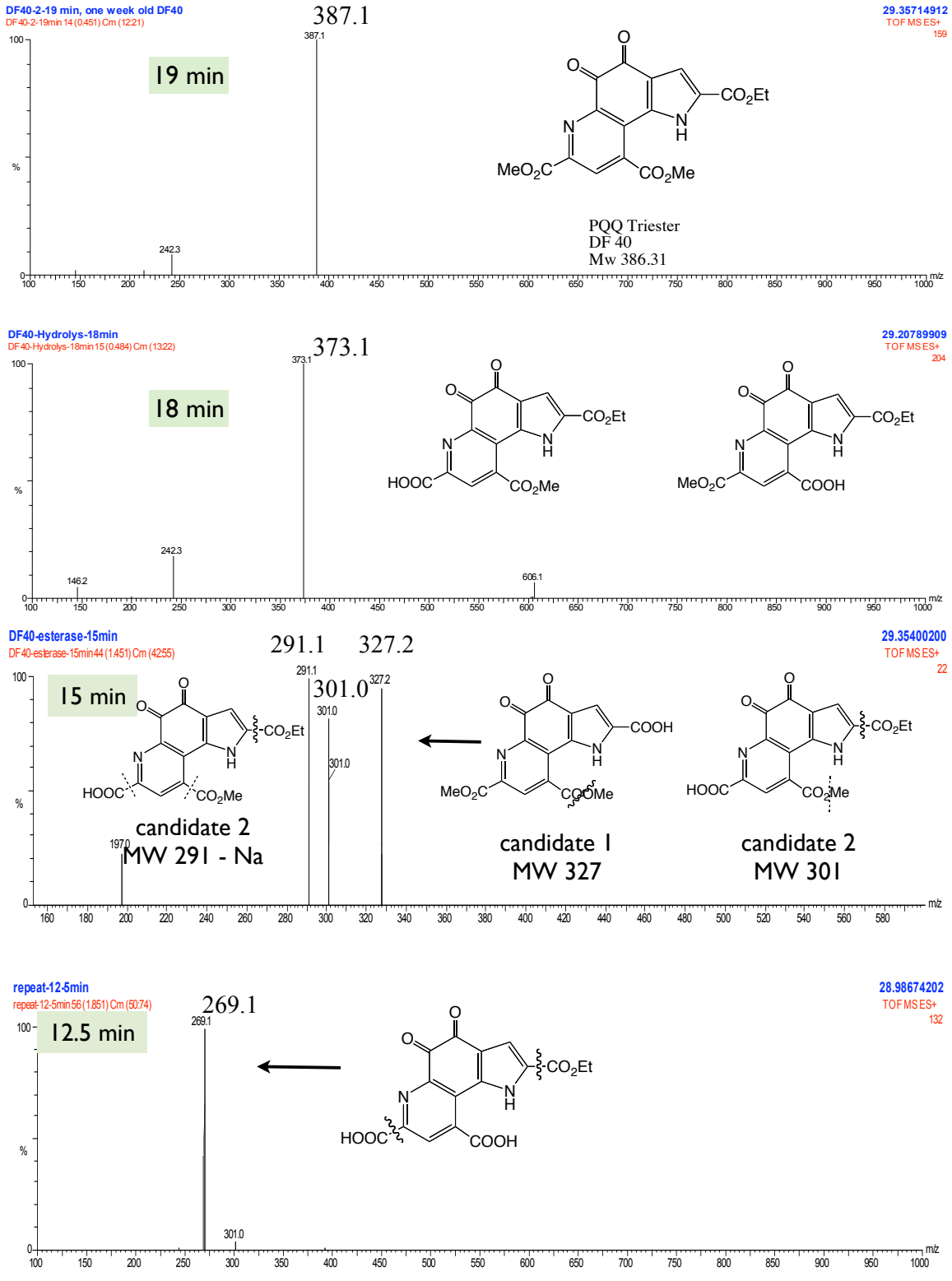

Figure 4.13. Mass spectra of HPLC isolated hydrolyzed PQQ derivatives with possible fragmentation patterns illustrated.

4.5. References

(1) Voet, D.V.; Voet, J.G. *Biochemistry*, John Wiley & Sons, Inc.; Part III and IV, 2004.

(2) Wittek, M.; Sturmer, M.; Doerr, H.; Berger, A. *Expert Rev. Mol. Diagn.* **2007,** *7*, 237-246.

(3) Choi, S.J.; Szoka, F.C. *Anal. Biochem.* **2000,** *281*, 95-97.

(4) Malik, A.; Rudolph, R.; Sohling, B. *Anal. Biochem.* **2005,** *340*, 252-258.

(5) Mouratou, B.; Rouyre, S.; Pauillac, S.; Guesdon, J.L. *Anal. Biochem.* **2002,** *309*, 40-47.

(6) Steinrucke, P.; Aldinger, U.; Hill, O.; Hillisch, A.; Basch, R.; Diekmann, S. *Anal. Biochem.* **2000,** *286*, 26-34.

(7) Tolun, G.; Myers, R.S. *Nucleic Acids Res.* **2003,** *31*, e111.

(8) Trubetskoy, V.S.; Hagstrom, J.E.; Budker, V.G. *Anal. Biochem.* **2002,** *300*, 22-26.

(9) Fonteh, P.; Keter, F.; Meyer, D.; Guzei, I.; Darkwa, J. *J. Inorg. Biochem.* **2009,** *103*, 190-194.

(10) Ohtsuka, K.; Maekawa, I.; Waki, M.; Takenaka, S. *Anal. Biochem.* **2009,** *385*, 293-299.

(11) Forrest, H.; Salisbury, S.; Sperl, G. *Biochim. Biophys. Acta* **1981,** *676*, 226-229.

(12) Dekker, R.; Duine, J.; Frank, J.; Eugene, J.; Verwiel, J.; Westerling, J. *Eur. J. Biochem.* **1982,** *125*, 69-73.

(13) Duine, J.A.; Frank, J.; Jongejan, J. *Anal. Biochem.* **1983,** *133*, 239-243.

(14) Mure, M.; Itoh, S.; Ohshiro, Y. *Tetrahedron Lett.* **1989,** *30*, 6875-6878.

(15) Sleath, P.; Noar, J.; Eberlein, G.; Bruice, T. *J. Am. Chem. Soc.* **1985,** *107*, 3328-3338.

(16) Mure, M.; Nii, K.; Inoue, T.; Itoh, S.; Ohshiro, Y. *Perkin transactions. 2* **1990,** 315-320.

(17) Vankleef, M.; Jongejan, J.; Duine, J. *Eur. J. Biochem.* **1989,** *183*, 41-47.

(18) Mitchell, A.; Jones, A.D.; Mercer, R.;Rucker, R. *Anal. Biochem.* **1999,** *269*, 317-325.

(19) Nozaki, S. *Chem. Lett.* **1997,** 1-2.

(20) Jongejan, A.; Jongejan, J.; Hagen, W. *J. Comput. Chem.* **2001,** *22*, 1732-1749.

(21) Duine, J.; Frank, J.; Verwiel, P. *Eur. J. Biochem.* **1980,** *108*, 187-192.

(22) Shinagawa, E.; Matsushita, K.; Nonobe, M.; Adachi, O.; Ameyama, M.; Ohshiro, Y.; Itoh, S.; Kitamura, Y. *Biochem. Biophys. Res. Co.* **1986,** *139*, 1279-1284.

CHAPTER 5

PREPARATION AND CHARACTERIZATION OF HEMIN CONJUGATES FOR PROTEASE ASSAYS AND HOMOGENEOUS BINDING ASSAYS USING RECONSTITUTION OF APO-HORSERADISH PEROXIDASE AS A SIGNAL GENERATOR

5.1. Introduction

The development of a biosensor or bioassay requires two essential components in the system: molecular recognition and signal transduction. The appropriate molecular recognition employs natural biological proteins (binding proteins (1-3), antibodies (4), DNAs and RNAs (5, 6)) or artificially designed synthetic polymers (aptamers (7, 8) and molecularly imprinted polymers (MIP) (9, 10)). Signal transduction includes optical methods (11-14), electrochemical methods (15, 16), and mass analysis such as those based on quartz crystal microbalances (QCM) (17, 18). Traditionally, a homogeneous protease assay is based on an enzyme-substrate interaction where the enzyme acts directly on a peptide substrate to cleave the peptide into fragments. Thus, the detection methods, as discussed in detail in Chapter 4, for protease assays focus on measuring the change induced by the action of substrate cleavage. A homogeneous binding assay, on the other hand, involves a competition between free analyte molecules and the same analyte molecule or its derivatives labeled with a signal modulator such as an enzyme (see Chapter 3).

In this chapter, an enzyme amplification system is examined that is composed of an apo-horseradish peroxidase (apo-HRP) and its prosthetic group – hemin. The feasibility of an optical detection method has been examined by introducing varying concentrations of free hemin to a fixed amount of apo-HRP in the presence of 3,3',5,5'-tetramethylbenzidine (TMB), a chromogenic substrate for HRP. Due to its potential real-time and ultra-sensitive assay capabilities, this new approach is expected to be useful for developing a host of new optical and electrochemical assays to detect low levels of both proteases and small biologically important molecules. First, in a similar manner as described in Chapter 4, the assay system is applied for real-time detection of protease (trypsin as a model) activity by employing a specially designed substrate probe that possesses a substrate cleavage site for trypsin. Second, the assay system is examined for the development of a homogeneous binding assay based on the concept of the apo-enzyme reactivation immunoassay (ARIS). To date, the ARIS has exclusively employed the FAD-GOx system and it has been applied for the analysis of a series of analytes, including theophylline (19), TNT (20, 21), progesterone (22), and some therapeutic drugs (23, 24). However, quantification was based on the amount of hydrogen peroxide produced by the FAD-GOx system. A second enzyme system, HRP, is coupled to provide a means to detect the hydrogen peroxide produced. Herein, efforts are directed to develop an ARIS system directly with the hemin-HRP system, using thyroxine (T4) as a model analyte.

Thyroxine is a major thyroid hormone secreted by the follicular cells of the thyroid gland, acting as a reservoir for its active form – triiodothyronine (T3). T4 is very important in the regulation of metabolic rate and in the diagnosis of thyroid diseases (25).

A number of efforts have been made to develop a functional assay for T4 in a biological matrix such as blood serum (26, 27). Many of them require a separation system (e.g., affinity HPLC column (28) or microfluidic channels modified with antibodies (29)) coupled with a post-column detection system, such as time-resolved fluorescence (TRF) (30), an enzymatic reaction, or electrochemiluminescence (ECL). In this study, the development of a potentially simple (homogeneous) and more convenient (colorimetric, 96-well plate) method is attempted.

5.2. Experimental

5.2.1. Apparatus. A Perkin-Elmer dual beam spectrophotometer (Model: Lamda 35; Boston, MA) was used for recording UV-Vis spectra. A Micromass LCT Time-of-flight (TOF) interfaced with electrospray ionization (ESI) and a Micromass TofSpec-2E matrix-assisted, laser-desorption Time-of-Flight Mass spectrometer (MALDI-TOF MS) were used for obtaining sample mass spectra. An HP Agilent 1050 HPLC system equipped with a varying wavelength UV detector and a C-18 reversed phase column (Waters Symmetry, 5 μm, 150 mm) was used for isolation/purification of the PQQ conjugates. A Labsystems Multiskan RC 351 microplate reader was used to monitor the color change as a result of the enzymatic reaction in a 96-well plate.

5.2.2. Reagents. All solutions were prepared with Millipore (18.2 MΩ Milli-Q) water. Polypropylene 96-well microtiter plates and acetonitrile were purchased from Fisher Scientific (Pittsburgh, PA). Hemin chloride, inactivated horseradish peroxidase (apo-HRP), 3,3',5,5'-tetramethylbenzidine (TMB), trifluoroacetic acid (TFA), triisopropyl silane (TIS), analine methylester (AlaOMe) hydrochloride salt, N-ethyl-N′-(3-dimethylaminopropyl)carbodiimide (EDC), N,N'-dicyclohexylcarbodiimide (DCC), N-

hydroxysucciniimde (NHS), dimethylformamide (DMF), diisopropylethylamine (DIPEA), N-(tert-butoxycarbonyl)glycine 6-(boc-amino)hexanoic acid (Boc-C6-COOH), 1-methylimidazole, L-thyroxine, and anti-thyroxine antibody were purchased from Sigma-Aldrich (St. Louis, MO). 1-Hydroxybenzotriazole (HOBt) and the model peptide (H-R(Pbf)FK(Boc)LR(Pbf)R(Pbf)FAR(Pbf)R(Pbf)R(Pbf)VR(Pbf)R(Pbf)A-Rink amide resin) were purchased from Peptides International (Louisville, KY).

5.2.3. Preparation and Characterization of Hemin-AlaOMe

Approximately 1 mg of hemin was dissolved in fresh DMF with 35.6 μmole of EDC (2 eq.), 0.54 mg of HOBt (0.1 eq.) and 0.2 μL of DIPEA (5.74M). The mixture was stirred at room temperature for 20 min. Then, an aliquot of 250 μL of AlaOMe (4.97 mg, 2 eq.) was added to the above mixture. The reaction was allowed to proceed under ambient conditions for 4 h, followed by HPLC isolation and MS analysis. The isolated samples were lyophilized and dissolved in 50 mM, phosphate buffer, pH 6.0.

In order to evaluate the reconstituted HRP activity for the prepared derivatives, a colorimetric assay was developed to monitor the free hemin or hemin derivatives. Briefly, in 200 μL of 50 mM, phosphate buffer, pH 6.0, 10 μL 0.5 mg/mL apoHRP and 20 μL of hemin or hemin derivatives of varying concentrations were mixed and incubated for 2 min before an aliquot of 40 μL of TMB/hydrogen peroxides substrate system was added for the color development. The reaction was monitored at 443 nm.

5.2.4. Preparation and Characterization of the Hemin-peptide Conjugate

The peptide purchased was intentionally left on the resin beads with appropriate protection of side chains. Prior to reaction, 100 mg of the resin was pre-soaked in approximately 500 μL of DMF. As illustrated in the reaction scheme shown in Figure

5.1, about 50 mg of hemin was dissolved in ~ 1 mL of DMF with EDC (2.2 eq.), HOBt (0.1 eq.) and 20 μL of DIPEA (5.74 M). The activation was allowed to proceed for 20 min at room temperature. Then, the activated hemin mixture was combined with the pre-soaked resins and the reaction mixture was shaken at 700 RPM for 16 h. After that, the resin beads were moved to a fritted glass funnel and were washed extensively with large volumes of organic solvents: DMF, DMF with 5% acetic acid, dichloromethane (DCM), acetone with 10% acetic acid, and finally with DMF and DCM. The peptide was deprotected and cleaved off the resin by reacting the washed resins with a cleavage "cocktail" solution containing TFA, TIS and deionized water (95: 2.5: 2.5, v:v:v) for 1.5 h. The filtrate was collected and the resins were further washed with 100 mL of methanol. The filtrates were combined and subjected to the rotary evaporator until the peptide was completely dried. The peptide was further washed and precipitated with cold ether and dried by flowing nitrogen over the sample. The resulting crude hemin conjugated peptide was then dissolved in 5 mL of deionized water for further HPLC purification and MS analysis. The purified hemin-peptide conjugate was evaluated in the HRP reconstitution assay as described above.

5.2.5. Preparation and Characterization of the Hemin-T4 Conjugates

Preparation of the NHS ester of Boc-C6-COOH

A 231.5 mg sample of Boc-C6-COOH (1 mmole) was dissolved in 3 mL of freshly distilled THF with 115.1 mg of NHS (1 eq.). While stirring, 2 mL of THF solution containing 206.4 mg of DCC (1 eq.) was added and the reaction mixture was stirred for 48 h. The reaction mixture was then subjected to rotary evaporation for THF

removal. About 5 mL of DMF/MeCN (4:1) mixture was used to dissolve the Boc-C6-NHS.

Preparation of the NHS ester of Boc-Gly

Boc-Gly-NHS was prepared in the same manner as described above, where 175 mg of Boc-Gly (1 mmole), 206 mg of DCC (1 eq.), and 110 mg of NHS (1 eq.) were used.

Preparation of C6-T4 conjugate and Gly-T4 conjugate

Approximately 38 mg (50 μmole) of T4 was dissolved in 500 μL of 1-methylimidazole and 200 μL of the prepared Boc-C6-NHS was added. The reaction mixture was stirred overnight, followed by chloroform extraction after adjustment to neutral pH by adding HCl. The collected chloroform layer was mixed with TFA (1:1) and the deprotection reaction was allowed to proceed overnight. The deprotected C6-T4 was collected and redissolved in 3 mL of acetonitrile after the rotary evaporation of TFA and chloroform. The preparation of the Gly-T4 conjugate was carried out in the same manner.

Preparation of Hemin-T4, Hemin-Gly-T4 and Hemin-C6-T4

The direct conjugation of hemin with T4 was carried out by reacting 33 mg (50 μmole) of hemin with 38.5 mg (1 eq.) of T4 (dissolved in 500 μL of 1-methylimidazole) in the presence of 9.5 mg of EDC (0.5 eq.) and 5.8 mg of NHS (0.5 eq.). The reaction mixture was stirred overnight. The conjugation of hemin with Gly-T4 and C6-T4 was conducted in the same manner where 6.6 mg of hemin, 40 μL of 1-methylimidazole, 1.9 mg of EDC and 1.2 mg of NHS were used with 500 μL of the prepared Gly-T4 and C6-T4, respectively. The resulting crude hemin-T4 derivatives were then subjected to HPLC

purification and MS analysis. The purified hemin-T4 derivatives were evaluated in the HRP reconstitution assay as described above. The concentrations of hemin derivatives were estimated using the molar extinction coefficient of hemin.

5.2.6. Trypsin Assay Based on the Prepared Hemin-peptide Conjugate

The trypsin assay was carried out first by mixing ~11 pmole of the purified hemin-peptide for 20 min with varying concentrations of the freshly prepared trypsin. Then, 10 μL of 1 mg/mL of aprotinin, a potent inhibitor of trypsin, was used to quench the reaction. The reaction mixture was incubated for 5 min followed by the addition of HRP and the substrate system containing TMB and hydrogen peroxide as described earlier. The color change was monitored at 443 nm.

5.2.7. Evaluation of the ARIS for T4 Based on the Prepared Hemin-T4 Conjugates

5.2.7.1. Antibody Work-up

First, about 400 μL of 1 mg/mL anti-thyroxine antibody (anti-T4) was loaded onto a Sephadex G-25 column, which was pre-equilibrated with 50 mM phosphate buffer, pH 6.0. After equilibration, the eluant of the first bed volume was collected. Then, the collected anti-T4 was treated with a saturated solution of ammonium sulfate. The fractional precipitation method was used to divide the antibody into 3 fractions: P1 (0-40% ammonium sulfate), P2 (40-70%), P3 (above 70%). The precipitated antibody fractions were reconstituted with 1 mL of 50 mM phosphate buffer, pH 6.0, followed by dialysis using an Amicon centrifuge tube with a filter inset (5,000 MWCO). Further, one portion (100 μL) of the desalted anti-T4 was directly subjected to membrane dialysis (10K MWCO) for 3 consecutive days with fresh buffer (50 mM phosphate buffer, pH

6.0) changed each day. The resulting dialyzed antibody (P4) and other purified antibodies (P1, P2, and P3) were collected and stored at 4 ºC until use.

5.2.7.2. ARIS Assay

Briefly, in the first step, the purified hemin-C6-T4 and anti-T4 were mixed together followed by the addition of apo-HRP and the substrate system containing TMB and hydrogen peroxide. In the second step, the antibody was incubated with free T4 first. Then, the mixture was incubated with the hemin-C6-T4 before addition of the apo-HRP and its substrate. At the same time, the control experiments, where hemin-C6-T4 was reacted with apo-HRP and anti-T4 was reacted with apo-HRP, were carried out to monitor the positive or negative signals.

5.3. Results and Discussion

5.3.1. Hemin-HRP Reconstitution Assay

Hemin is practically insoluble in water, thus the preparation of hemin standard solutions started by dissolving hemin in DMF, followed by dilution with aqueous buffers to the desired concentrations. Due to its hydrophobic nature, hemin appeared to be very "sticky" to various solid surfaces, including glass and polymers. Therefore, a fresh stock solution of hemin was prepared just before a given set of experiments. The dose-response of the hemin-HRP assay, as shown in Figure 5.2, was obtained by the addition of varying concentrations of hemin to the mixture of the apo-HRP and the TMB substrate system. Analysis for the replicates of 3 samples could be readily achieved with the standard deviations less than 5%. The sensitivity of the assay was demonstrated with the lowest concentration of 50 pM attempted and the linear detection range up to 500 pM.

5.3.2. Isolation and Characterization of Hemin Derivatives

5.3.2.1. Hemin-AlaOMe and Hemin-peptide

The AlaOMe was used as a model compound to study the conjugation behavior of hemin. Substitution at a single propionate group is desired because these groups are critical in stabilizing the position of the hemin when combined with the apo-HRP. However, two equivilents of AlaOMe were used in the experiment in order to obtain a higher yield of the desired mono-substituted hemin derivative. As shown in Figure 5.3a, three major peaks (Peak 1, Peak 2, and Peak 3) were found around 20 min, using HPLC to separate the reaction mixture. The identities of the three peaks were confirmed with ESI-MS: Peak 1 corresponds to free hemin; Peak 2 corresponds to the mono-substituted hemin-AlaOMe; and Peak 3 corresponds to the di-substituted hemin-AlaOMe. The conjugation efficiency was also evaluated by injecting the reaction mixture at a fixed time interval (1 h, 2 h, and 4 h).

The hemin-peptide was purified and characterized in the same manner as described above and the mass to charge ratio was found to be a mono-substituted derivative as well (Figure 5.4). HPLC isolations of the conjugation reaction products (hemin-AlaOMe and hemin-peptide) were compared with the one of free hemin (Figure 5.3b). The mono-substituted hemin-AlaOMe eluted later than free hemin because of the increase in hydrophobicity. On the other hand, the hemin-peptide eluted earlier than hemin because the peptide possesses multiple charges resulting from protonations of the side chain amines on the arginine and the lysine residues. The biological activities of the hemin-AlaOMe and the hemin-peptide were evaluated in the hemin-HRP reconstitution assay. The results are summarized in Table 5.1 with a comparison of retention times of the hemin conjugates. The hemin-peptide showed almost no activity as compared to ~

4.4% of the regenerated HRP activity with the hemin-AlaOMe. The long peptide chain probably hindered the reactivation of the hemin-peptide with the apo-HRP.

5.3.2.2. Hemin-T4 Conjugates

The preparation of NHS esters followed a modified procedure from the literature (31). The reagent 1-methylimidazole was used not only as a solvent to dissolve the thyroxine but also as a base in the coupling reaction. The NHS ester formation, T4 conjugation, Boc deprotection, and finally hemin conjugation were all followed with HPLC and MS confirmation. The isolated hemin-T4 conjguates were dissolved in MeCN/H_2O (50:50 v:v) and their UV-Vis spectra were compared to the one of free hemin (Figure 5.5). Their biological activities in the hemin-HRP reconstitution assay were evaluated and a summary of the residual activity of the hemin-T4 conjugates are shown in Table 5.2, together with their HPLC retention time comparisons. Hemin-C6-T4 showed the best residual activity followed by the hemin-Gly-T4 and then the hemin-T4. The activity was dependent on the length of the spacer between the hemin and the T4 residue. Due to the flexibility and the allowed distance of T4 from the active center of HRP, hemin-C6-T4 was less sterically hindered.

5.3.3. Hemin-HRP Reconstitution – Based Trypsin Assay

As shown in Table 5.1, the hemin-AlaOMe species was still active in reconstituting apo-HRP to holo-HRP while the presence of the peptide tail on the hemin completely inhibited the HRP activity. Therefore, a cleavage of the peptide by trypsin is expected to restore the HRP activity. Some preliminary experiment results (data not shown) suggested that the apo-HRP itself was susceptible to the proteolytic hydrolysis of the trypsin. Thus, an inhibitor of trypsin, aprotinin (32), was used in the assay to quench

the trypsin activity after the incubation of the trypsin with the hemin-peptide. A control experiment for the aprotinin was carried out and no interefering effects were found in the hemin-HRP assay with the use of aprotinin (Figure 5.6). A dose-response of the trypsin assay is shown in Figure 5.7, where the trypsin concentration as low as 0.1 μg/mL was detected. The relatively high detection range could result from a number of reasons: residual acetonitrile remaining with the hemin-peptide could decrease the HRP activity; the length of the cleavage products of the hemin-peptide could range from 5 to 10 amino acids, depending on positions of the Arg/Lys residues in the peptide; the resulting cleaved hemin-peptide had a limited ability to reactivate the apo-HRP. Even though one arginine group was intentionally placed at a position where the hemin was directly conjugated, it will probably be very difficult for the trypsin to act on this position because of the steric hinderance by the bulky hemin molecule.

5.3.4. Hemin-HRP Reconstitution – Based ARIS for T4

Sodium azide was used as an additive with the commercially available antibody in order to prevent bacterial growth. It was removed from the antibody matrix using a desalting column and dialysis methods (centrifuge aided or via passive diffusion) because of its inhibitory effect on the peroxidase activity. The resulting antibody showed a significant false positive response (data not shown) when incubated with the apo-HRP and TMB substrate system, while incubation of the antibody with the TMB substrate system did not show any response. This suggested that the antibody mixture must have been contaminated with a substance bearing hemin-like activity. The antibody was further purified using a fractional precipitation method, and the resulting antibody fractions (P1 to P4) were incubated with the apo-HRP followed by the addition of the

TMB substrate system. The result, as shown in Figure 5.8, demonstrated that the antibody fractions still gave the false positive response although in a much reduced fashion. Further, the antibody fractions were examined with the hemin-C6-T4 (the best candidate for activity regeneration). The P2 fraction was found to have the best inhibition (62%) (Figure 5.9) of the hemin-C6-T4's ability to activate apo-HRP. Then, in the presence or absence of free T4, the activity of the hemin-C6-T4 was monitored after the incubation with the diluted (50 fold) P2 antibody fraction. As shown in Figure 5.10a, more than 80% inhibition was obtained when the hemin-C6-T4 was incubated with the P2 as compared to the one without the P2 incubation. The diluted P2 gave almost no significant positive response. However, when a solution of free T4 was incubated with the P2 first and then the hemin-C6-T4, followed by addition of the apo-HRP and its substrate system, no regenerated signal was obtained (Figure 5.10b). One control experiment with free hemin and the P2 fraction further suggested that the inhibitory effect seen before was not due to the binding of the P2 to the T4 portion of the hemin-C6-T4, but rather due to the non-specific interaction between the hemin and the P2 (Figure 5.11).

5.4. Conclusions

In this study, the feasibility of a homogeneous trypsin assay and ARIS immunoassay were investigated using the hemin-HRP reconstitution as a signal generator. The hemin-HRP reconstitution assay was shown to be very sensitive with the detection range in the pM range. The chemical modification of the hemin was mainly focused on the linkage through one of its propionate groups via the amide bond formation. The synthetic hemin derivatives were successfully prepared and characterized

with HPLC and MS. The biological activities of these derivatives were evaluated in the hemin-HRP reconstitution assay and residual activities of these derivatives were compared. Unfortunately, for the trypsin assay, a more carefully designed peptide appears to be needed to achieve not only better residual activity of the hemin derivative, but also more efficient proteolytic cleavage. For the ARIS assay, an alternative binding protein may be a better choice by avoiding the complex inhibitory effects from a serum-based antibody.

	Residual Activity	Retention Time in HPLC
hemin	n/a	20.2 min
hemin-AlaOMe	4.4%	20.8 min
hemin-peptide	0.04%	17.5 min

Table 5.1. Residual activities and retention times of hemin-AlaOMe and hemin-peptide compared to free hemin.

	Residual Activity	Retention Time in HPLC
Hemin-T4	~ 0.1%	7-8 min
Hemin-Gly-T4	~ 0.9%	10-11min
Hemin-C6-T4	~ 1%	12 min

Table 5.2. Comparison of the residual activities and retention times for hemin-T4 derivatives.

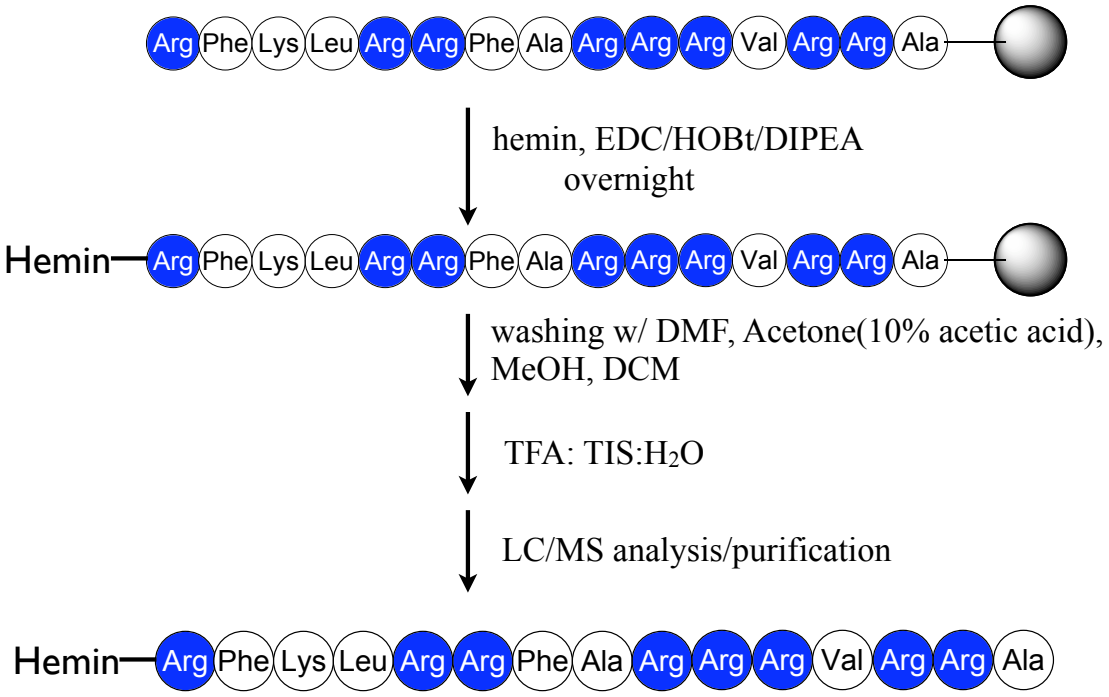

Figure 5.1. Solid-phase on-resin conjugation reaction scheme of the hemin-peptide.

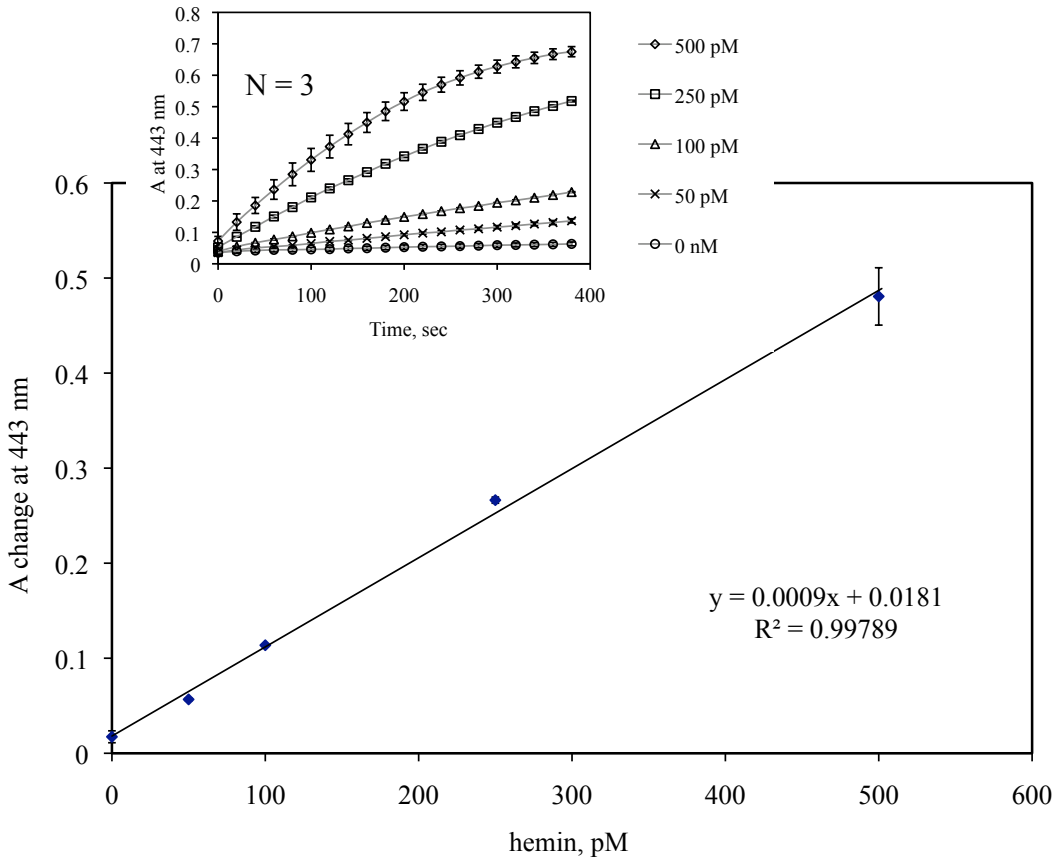

Figure 5.2. Hemin dose-response in the apo-HRP reconstitution assay (insert: the real time monitoring of the color change).

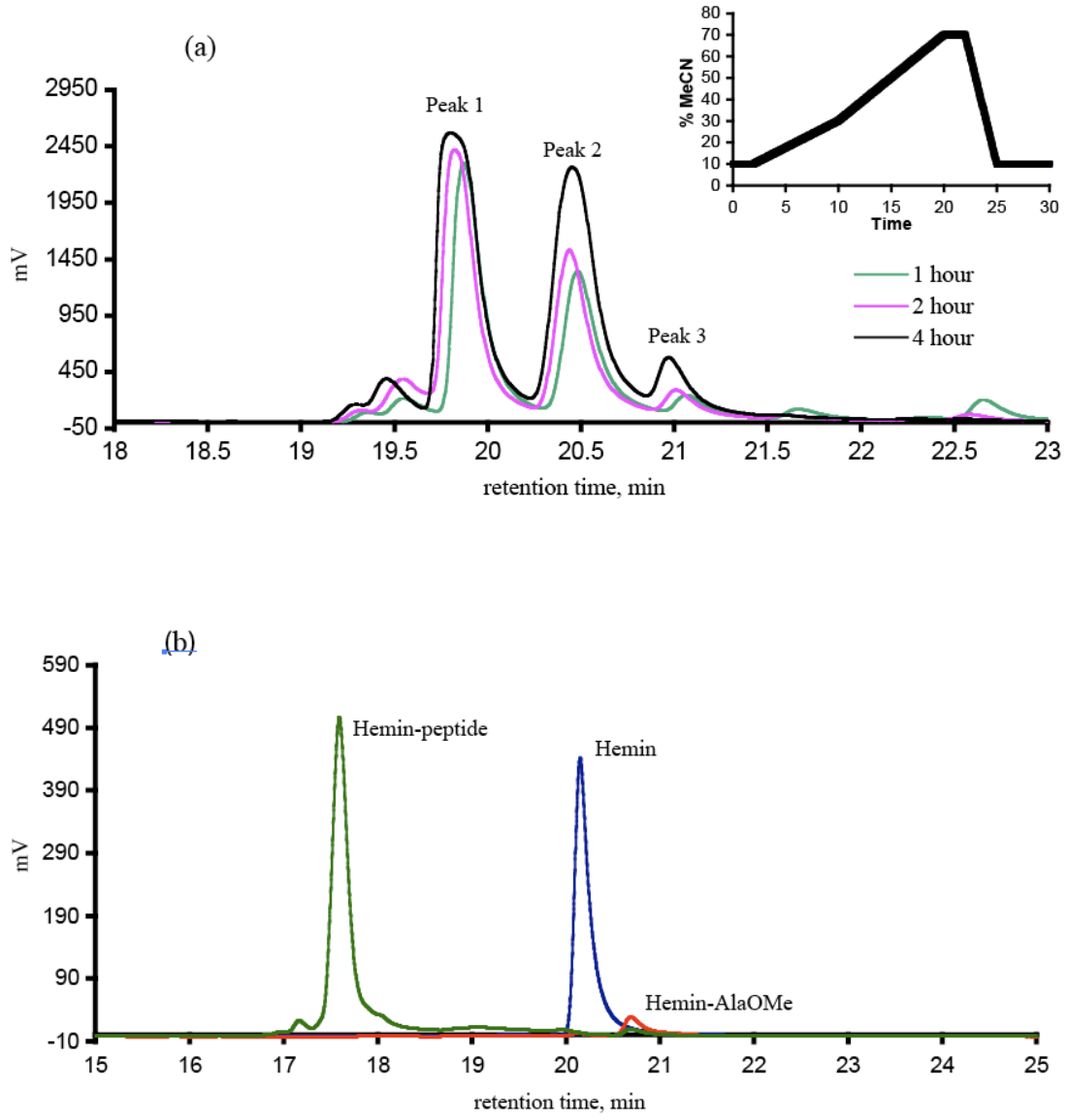

Figure 5.3. (a) HPLC separation at the fixed time intervals (see text for details) for the hemin-alanine methylester derivatives (inset represents a typical gradient setting.); (b) Overlay of the HPLC chromatograms for hemin, hemin-AlaOMe, and hemin-peptide.

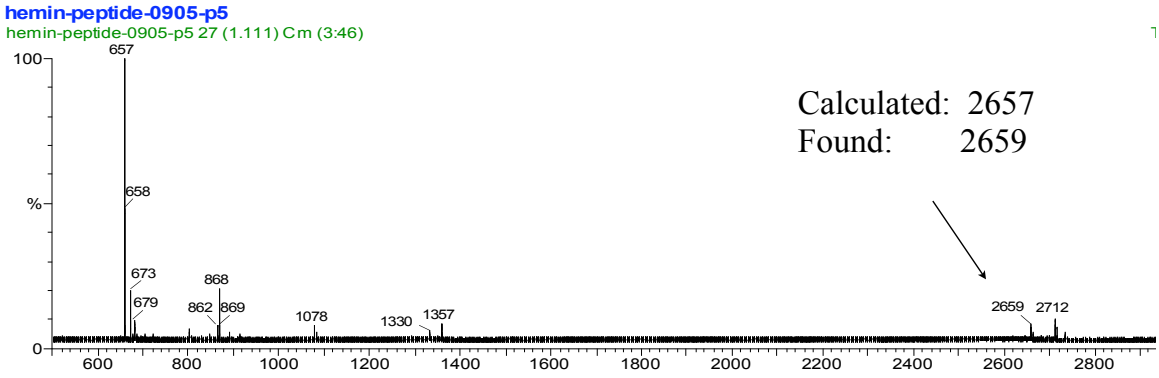

Figure 5.4. MS spectrum of the hemin-peptide conjugate.

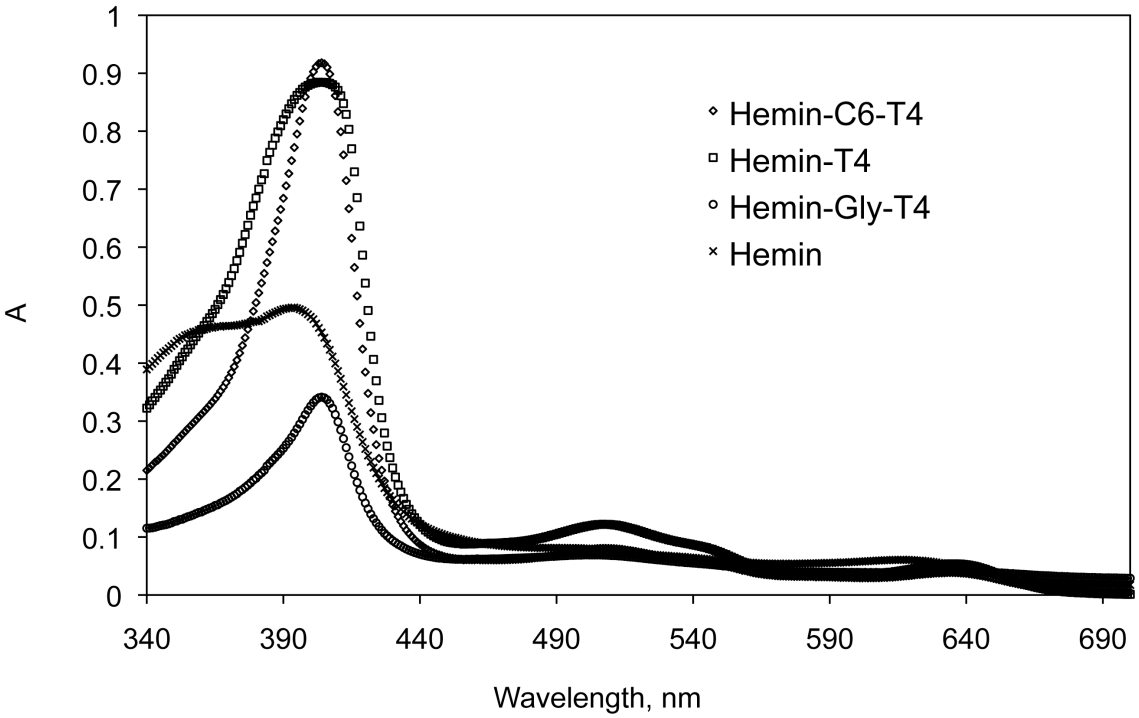

Figure 5.5. UV-Vis spectra comparison of the hemin-T4 derivatives

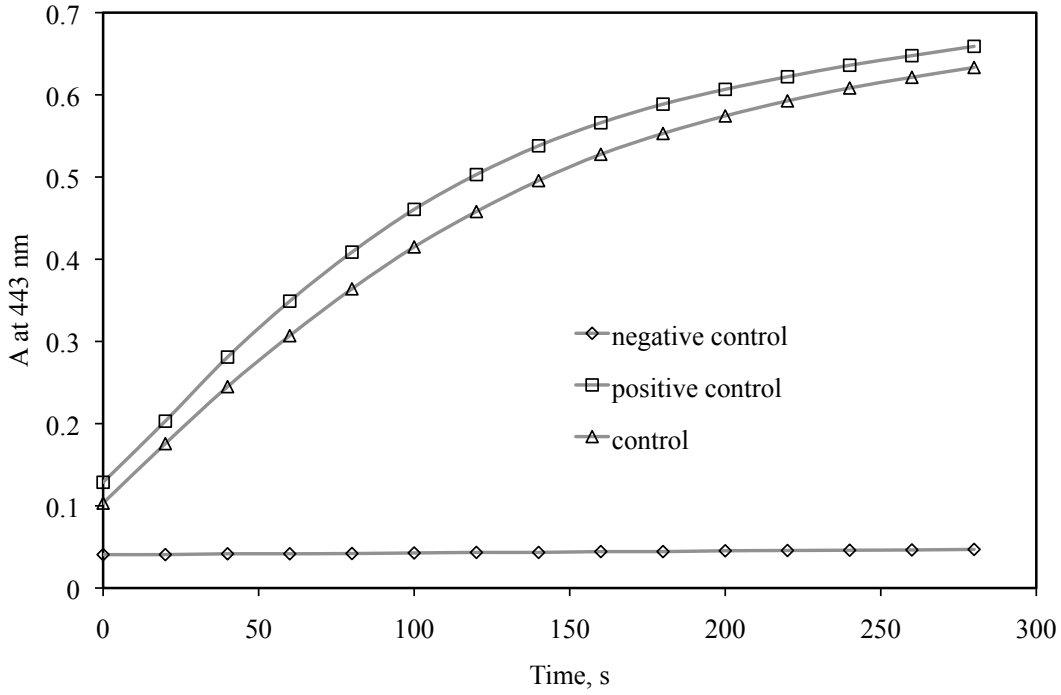

Figure 5.6. Aprotinin effects on the hemin-HRP assay: negative control (apo-HRP + aprotinin); positive control (apo-HRP + hemin + aprotinin); control (apo-HRP + hemin)

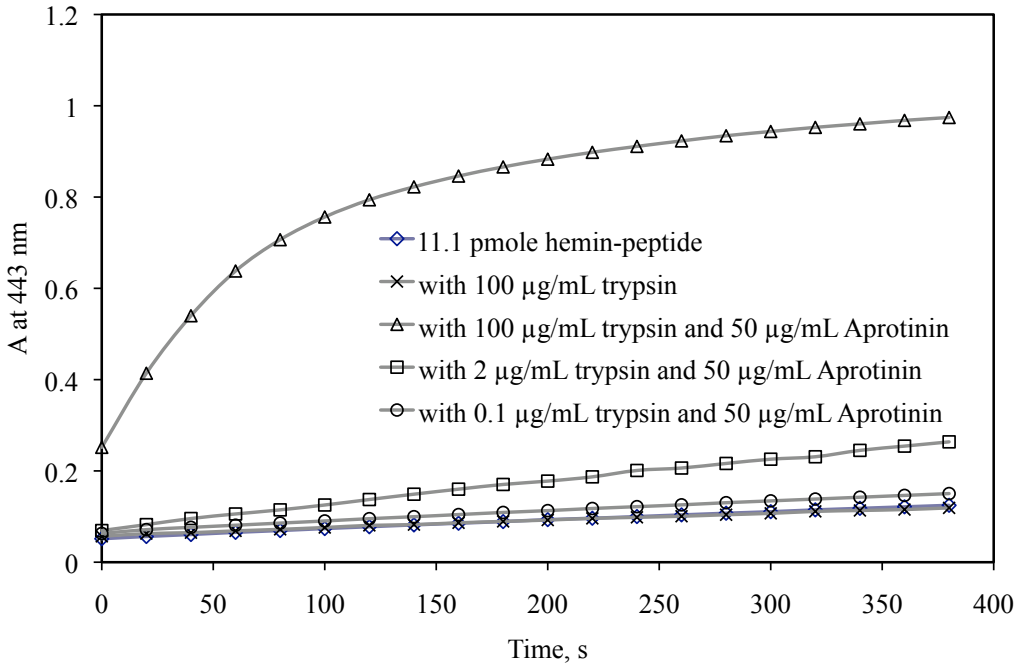

Figure 5.7. Regeneration of HRP activity after incubating the hemin-peptide substrate with varying concentrations of trypsin.

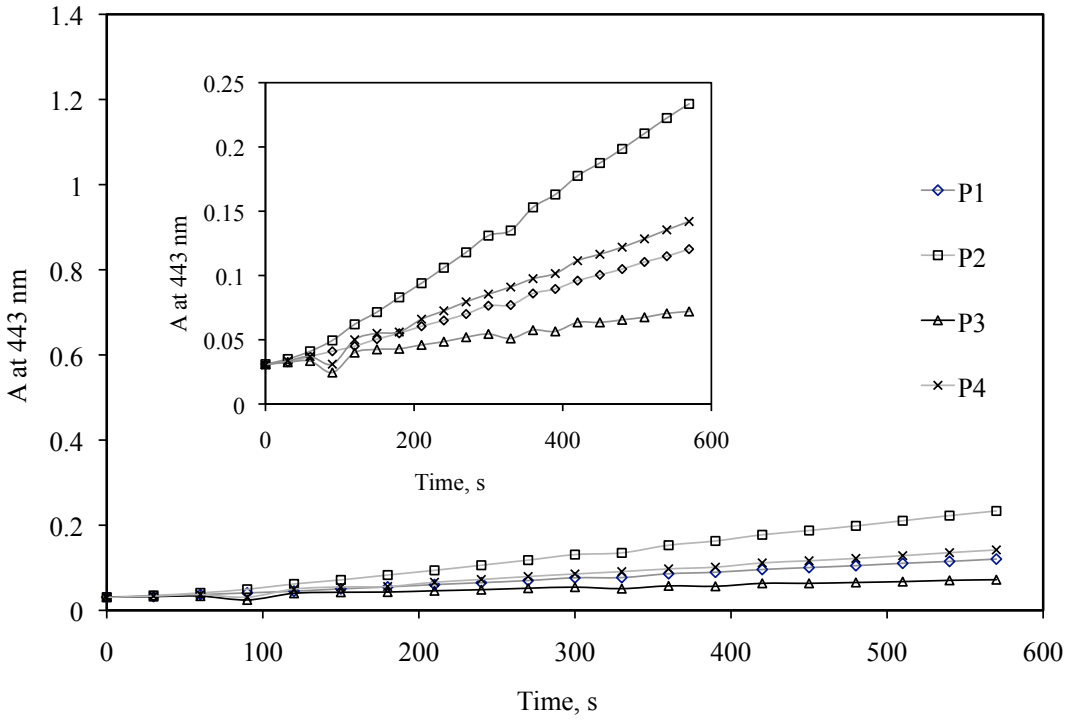

Figure 5.8. The antibody fractions after ammonium sulfate precipitation evaluated with the apo-HRP reconstitution assay (insert: TMB oxidation monitored at 443 nm).

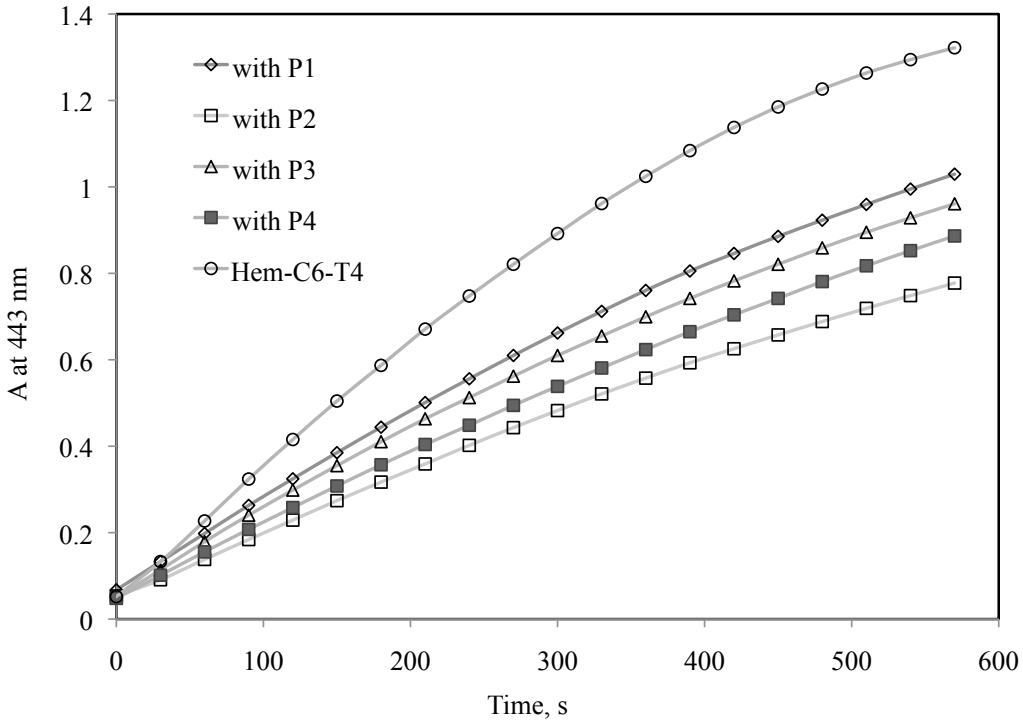

Figure 5.9. Antibody fractions evaluated for the binding efficiency in the presence of the hemin-C6-T4 conjugate.

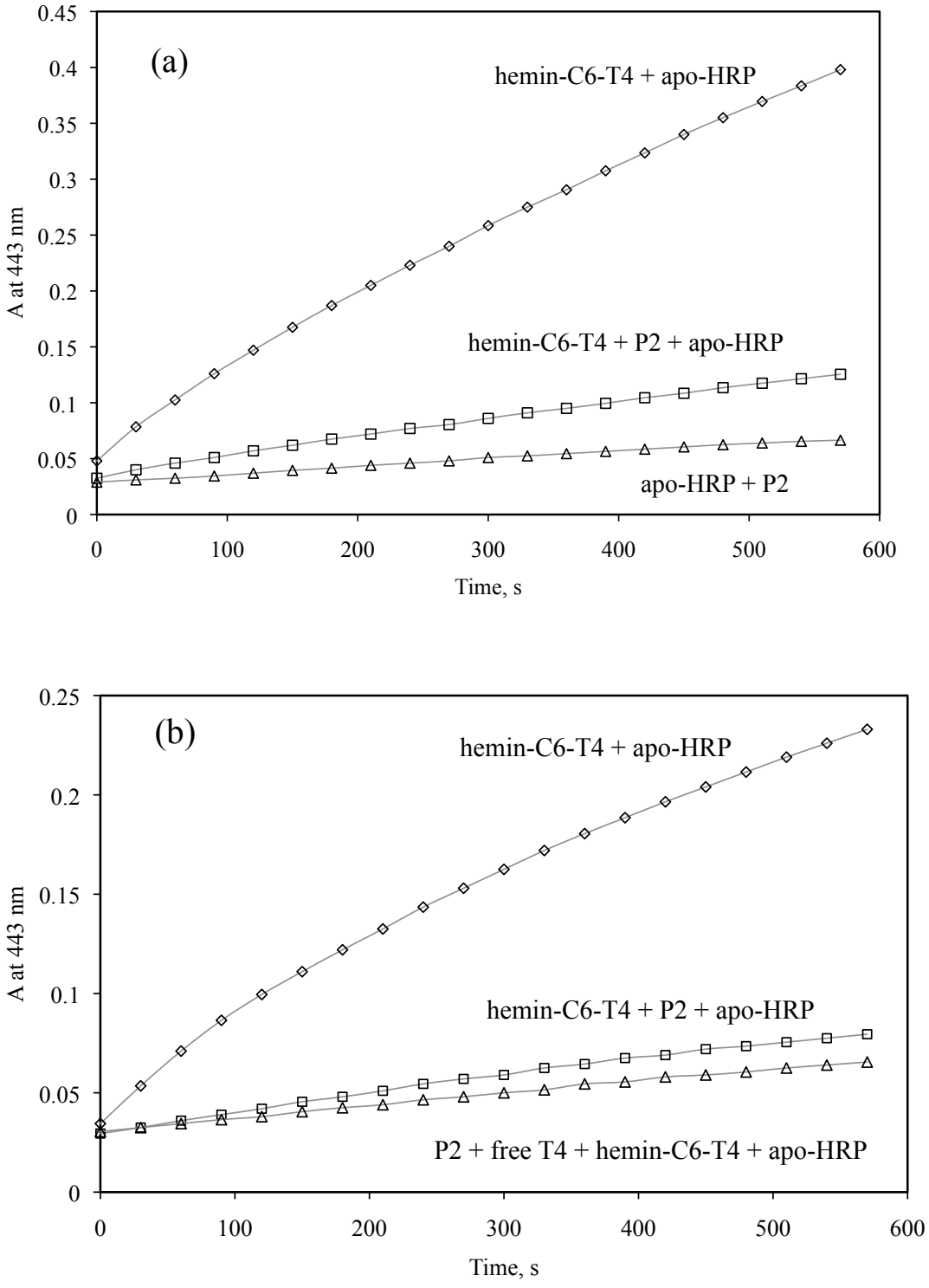

Figure 5.10. ARIS assay for free thyroxine (T4).
(a) Binding of the hemin-C6-T4 with the anti-T4 antibody inhibited the reconstitution of the apo-HRP;
(b) In the presence of free T4, the regeneration of the HRP activity was investigated.

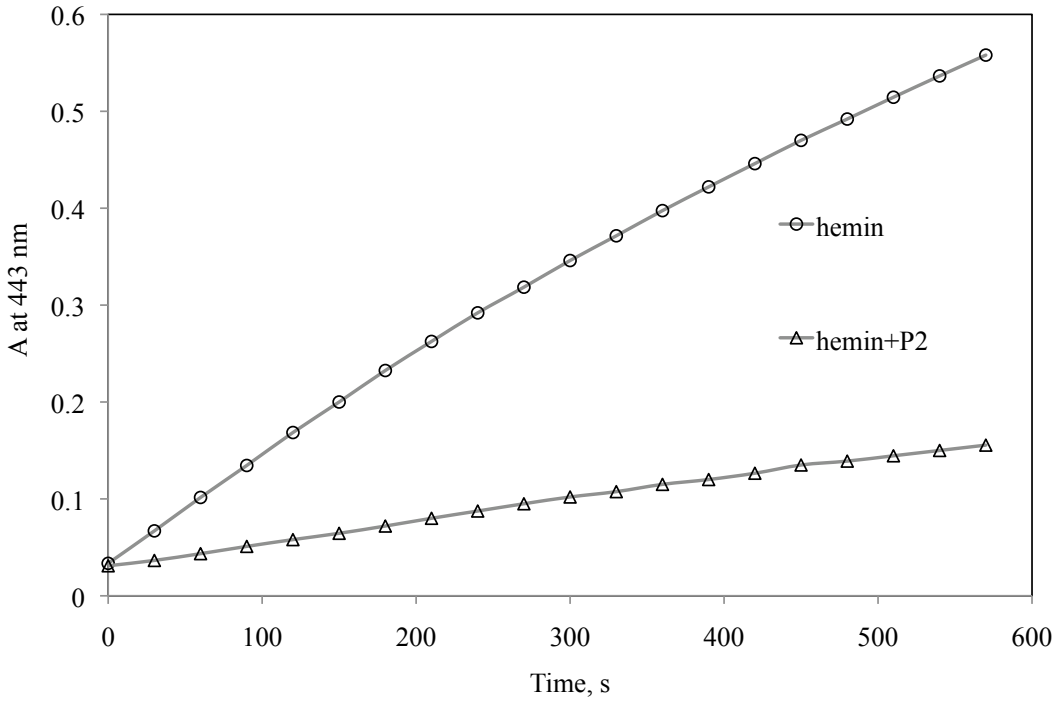

Figure 5.11. Inhibitory effect of the P2 antibody fraction for free hemin evaluated in the apo-HRP reconstitution assay.

5.5. References

(1) Hrebicek, T.; Cichna-Markl, M. *J. Sol-gel Sci. Technol.* **2005,** *36*, 275-283.

(2) Nygren-Babol, L.; Sternesjo, A.; Jagerstad, M.; Bjorck, L. *J. Agr. Food Chem.* **2005,** *53*, 5473-5478.

(3) Rao, A.K.; Creager, S. *Anal. Chim. Acta* **2008,** *628*, 190-197.

(4) Li, X.; Yang, X.; Zhang, S. *Trend Anal. Chem.* **2008,** *27*, 543-553.

(5) Roglin, L.; Altenbrunn, F.; Seitz, O. *Chembiochem* **2009,** *10*, 758-765.

(6) Thieme, D.; Neubauer, P.; Nies, D.; Grass, G. *Appl. Environ. Microbiol.* **2008,** *74*, 7463-7470.

(7) Centi, S.; Messina, G.; Tombelli, S.; Palchetti, I.; Mascini, M. *Biosens. Bioelectron.* **2008,** *23*, 1602-1609.

(8) Pultar, J.; Sauer, U.; Domnanich, P.; Preininger, C. *Biosens. Bioelectron.* **2009,** *24*, 1456-1461.

(9) Kempe, H.; Kempe, M. *Anal. Chem.* **2006,** *78*, 3659-3666.

(10) Urraca, J.; Moreno-Bondi, M.C.; Orellana, G.; Sellergren, B.; Hall, A. *Anal. Chem.* **2007,** *79*, 4915-4923.

(11) Hemmila, I.; Laitala, V. *J. Fluoresc.* **2005,** *15*, 529-542.

(12) Szollosi, J.; Damjanovich, S.; Matyus, L. *Cytometry* **1998,** *34*, 159-179.

(13) Thaler, M.; Buhl, A.; Welter, H.; Schreiegg, A.; Kehrel, M.; Alber, B.; Metzger, J.; Luppa, P. *Anal. Bioanal. Chem.* **2009,** *393*, 1417-1429.

(14) Wiltschi, B.; Knoll, W.; Sinner, E.K. *Methods* **2006,** *39*, 134-146.

(15) Shah, J.; Wilkins, E. *Electroanalysis* **2003,** *15*, 157-167.

(16) Wang, J. *Biosens. Bioelectron.* **2006,** *21*, 1887-1892.

(17) Boujday, S.; Gu, C.; Girardot, M.; Salmain, M.; Pradier, C.M. *Talanta* **2009,** *78*, 165-170.

(18) Uludag, Y.; Piletsky, S.; Turner, A.; Cooper, M. *FEBS J.* **2007,** *274*, 5471-5480.

(19) Morris, D.; Ellis, P.; Carrico, R.; Yeager, F.; Schroeder, H.; Albarella, J.; Boguslaski, R.; Hornby, W.; Rawson, D. *Anal. Chem.* **1981,** *53*, 658-665.

(20) Dosch, M.; Weller, M.; Bückmann, A.; Niessner, R. *Fresenius. J. Anal. Chem.* **1998,** *361*, 174-178.

(21) Heiss, C.; Weller, M.; Niessner, R. *Anal. Chim. Acta* **1999,** *396*, 309-316.

(22) Posthuma-Trumpie, G.A.; Van, D.B., WAM; Van, D.W., DFM; Schaaper, W.; Korf, J.; Van, B. *Biochim. Biophys. Acta (Proteins Proteom.)* **2007,** *1774*, 803-812.

(23) Miles, M.V.; Tennison, M.; Greenwood, R.; Benoit, S.; Thorn, M.; Messenheimer, J.; Ehle, A. *Ther. Drug Monit.* **1990,** *12*, 501-510.

(24) Schroeder, H.; Johnson, P.; Dean, C.; Morris, D.; Smith, D.; Refetoff, S. *Clin. Chem.* **1986,** *32*, 826-830.

(25) Weitzel, J. *Thyroid Hormone and Mitochondrial Biogenesis* Henry Stewart Talks (London); 2007.

(26) Gu, J.; Soldin, O.; Soldin, S. *Clin. Biochem.* **2007,** *40*, 1386-1391.

(27) Wang, X.; Chen, H.; Lin, J.M.; Ying, X. *Int. J. Biol. Sci.* **2007,** *3*, 274-280.

(28) Oates, M.R.; Clarke, W.; Zimlich, A.; Hage, D. *Anal. Chim. Acta* **2002,** *470*, 37-50.

(29) Murphy, B.; He, X.Y.; Dandy, D.; Henry, C. *Anal. Chem.* **2008,** *80*, 444-450.

(30) Wu, F.; Xu, Y.; Xu, T.; Wang, Y.; Han, S.Q. *Anal. Biochem.* **1999,** *276*, 171-176.

(31) Yang, H.; Lopina, S. *J. Biomater. Sci. (Polym. Ed.)* **2003,** *14*, 1043-1056.

(32) Werle, M.; Takeuchi, H. *Int. J. Pharm.* **2009,** *370*, 26-32.

CHAPTER 6

CONCLUSIONS AND FUTURE DIRECTIONS

6.1. Conclusions

The primary focus of this dissertation research was to explore not only some fundamental aspects of the interactions between the apo-enzymes and their prosthetic groups, but also their direct applications in immunoassays, binding assays, and protease assays. These experiments unveiled the potential of utilizing these types of signal transduction mechanisms for bio-analytical applications and suggested the possible synthetic modifications of prosthetic groups in order to afford better usability.

The optimization of the reconstitution assay for PQQ and apo-GDH was introduced in Chapter 2, where the PQQ was designed to be a rate limiting reagent and all other reagents were in excess. The feasibility of using PQQ-doped polymeric nanoparticles as an antibody label was also examined thoroughly. The relatively hydrophilic PQQ was converted to a hydrophobic TDMA salt of PQQ (PQQ-TDMA) and was successfully loaded into the PMMA nanospheres after the initial experiments found the most suitable polymeric material for this purpose. Secondly, acetonitrile was found to be the best solvent to release the PQQ from the PMMA spheres and the activity of GDH was retained better in the presence of this solvent as compared to other organic solvents. Further, the surface of the PQQ loaded PMMA particles (PMMA-PQQ) was functionalized by physically adsorbing a binder protein – NeutrAvidin. The

NeutrAvidin-coated PMMA-PQQ particles were further characterized with a biotinylated microtiter plate, where biotin-BSA was covalently linked to the surface. In the presence of free biotin, the NeutrAvidin-coated particles were prevented from reacting with the immobilized biotin. The dynamic range for the detection of free biotin was dependent on the surface coverage of the NeutrAvidin on the particles and the number of particles participating in the competition reactions. The linear detection range was found to be 2 – 10 nM biotin. Finally, the PMMA-PQQ particles were also evaluated to develop a sandwich immunoassay for CRP with a detection limit of 220 pg/mL using the optimized surface antibody coverage, compared to 3.1 ng/mL before such optimization.

In Chapter 3, the GDH-PQQ reconstitution assay system was adapted for an enzyme-based homogeneous competitive binding assay. The concept was demonstrated using biotin/avidin as a model and biotinylated GDH as a signal modulator. The prepared biotinylated GDH conjugates were fully characterized in terms of the mole ratios of biotin to GDH, the residual activities of the conjugates, and inhibition in the presence of added avidin and free PQQ. The dose dependence and the incubation time effect of avidin were investigated and optimized. The biotin-GDH conjugate with the most residual activity and the highest avidin inhibition was chosen for the optimization of the homogeneous competitive binding assay for biotin. The detection range of the assay is dependent on the amount of avidin present in the reaction, which is dependent on the minimum amount of the biotin-GDH required for a detectable signal. Both an equilibrium saturation method and a sequential saturation method were examined, and both yielded a detection limit of less than 10 nM of biotin.

A feasibility study requiring the modification of PQQ by its conjugation with an oligomer substrate started with a simple esterified amino acid, alanine methylester (AlaOMe), and was described in Chapter 4. The reactivity of the C-5 carbonyl resulted in unwanted side products of the conjugation reaction, even with in situ $NaBH_4$ reduction of the quinone groups prior to the conjugation reaction. The HPLC purified PQQ conjugate was characterized via FT-IR, UV-Vis, ESI-MS, and NMR (proton and C13). The conjugate was concluded to be a mixture of analogues of PQQ-AlaOMe: one of the three possible carboxyl groups reacted with the AlaOMe while the C5 carbonyl formed an iminoquinone (IPQ) with the AlaOMe. Further studies were also carried out with new PQQ esters and derivatives synthesized by Barry & Associates (Dexter, MI). Their biological activities in the GDH assay were evaluated and compared to the esters treated by forced hydrolysis, using NaOH or an esterase. A significant increase in the biological activity of the PQQ ester, DF40, was further studied using HPLC and MS. The C9 ester was found to hydrolyze first, followed by the hydrolysis at the C7 position with NaOH treatment. The free carboxyl groups at these two sites were responsible for the change in the GDH activity. The biological activities for the prepared PQQ derivatives, DF214 and DF228, with the C9 or C2 and C9 free carboxyl groups, respectively, suggested that the best conjugation site of PQQ is at the position of C7 carboxyl group.

In Chapter 5, an alternative prosthetic group-enzyme system, hemin-HRP, was studied for its potential applications in a protease assay and an immuno-binding assay, particularly the one based on the reconstitution of hemin with the apo-HRP. The hemin-HRP reconstitution assay was optimized for detection of free hemin in the sub-nM range. The hemin conjugates of AlaOMe, a 15-mer peptide, and thyroxine (T4), with various

spacers (glycine and hexyl) or without spacers, were successfully prepared and characterized via HPLC and MS. Their biological activities in the hemin-HRP assay were evaluated and compared. In order to maintain the catalytic function of the hemin, only one of the propionate groups was used to form the derivatives. The hemin-peptide was empolyed as a substrate probe in a homogeneous trypsin assay. Because of the proteolytic effect of trypsin toward the HRP, aprotinin was used to inhibit the trypsin activity after the incubation was completed. A dose-response curve of the trypsin activities was demonstrated with the lowest trypsin concentration of 0.1 μg/mL. However, a better design of the substrate peptide appears to be critical in further developing this homogeneous trypsin assay. The best candidate of the prepared hemin-T4 derivatives was found to be hemin-C6-T4 in terms of the most residual HRP reconstitution activity. Due to the complex nature of the anti-thyroxine antibody, some "work-up" procedures were carried out in order to further purify it. With extensive dialysis and ammonium sulfate precipitations, the best antibody fraction was selected and used in further development of an ARIS assay. However, the ARIS assay was not successful due to the inhibitory effect of the antibody itself to the hemin-HRP assay.

6.2. Future Directions

The experimental results described in this dissertation (Chapters 2 and 4) revealed the potential in developing ultra-sensitive assays based on chemically modified PQQ. In addition to the rapid colorimetric detection as demonstrated in Chapters 2 and 3, the synthesized PQQ derivative DF228, of which the C7 carboxyl group was extended via a hydroxamate linkage, was found to retain almost half of the activity as free PQQ. Future applications derived directly from these findings are discussed below.

6.2.1. DNA Derivatized PQQ Probe for Real-Time Polymerase Chain Reaction (PCR) Assay

PCR assays have become increasingly important in recent years. The main applications involve molecular diagnostics (1), pharmaco-genomics (2), and microbial detection such as pathogen (3) and biological warfare agent detection (4, 5), particularly with some slow growing microorganisms or ones that cannot be cultured. Besides their high specificity, the high sensitivity of PCR assays has become one of most important features that have attracted much attention. However, major drawbacks of traditional PCR include the possible cross contamination of the sample by the post-PCR handling and tedious end-point quantification using gel separation/chemical staining of the PCR-amplified target DNA. Recently, considerable research efforts have been directed on the development of real-time PCR assays. Nonspecific real-time detection is realized by use of double strand intercalation and minor groove binding dyes (6, 7). Site-specific real-time detection involves the use of separate primers and probes. Most of them employ fluorescence based detection, such as molecular beacons (8), Scorpion (9), SYBR Green (10), and TaqMan assays (11). However, expensive instrumentation for fluorescence detection can prevent wider use of these techniques. A cumulative fluorescence background signal associated with FRET detection methods also influences the true detection limit of such assays.

An enzyme amplified PCR assay can be developed based on the concept of a PQQ-oligomer substrate. Similar to a 5' nuclease fluorescence assay (12), synthesized oligonucleotide probes that are covalently attached with PQQ can target specific regions

of a DNA target. Upon the hydrolysis action of DNA polymerases, PQQ molecules are released and participate in the amplified enzyme system as illustrated in Figure 6.1.

6.2.2. Small Molecule Derivatized PQQ for the Development of ARIS Based on GDH-PQQ Reconstitution Assay

To develop a biosensor or bioassay for low molecular weight species, one common approach is based on oxidation of analytes by specific enzymes. This has led to the development of a whole range of enzyme-based electrochemical sensors for these analytes, e.g., electrochemical sensors for glucose (13), lactate (14), and glutamate (15). When no selective enzymatic reaction is available for an analyte, an interaction between the analyte and the analyte-specific antibody forms the basis of the current immuosensors, including electrochemical sensors and optical sensors, as discussed in detail in Chapter 5. The ARIS assay system combines molecular recognition, e.g., competition between free analytes and analyte-prosthetic group conjugates for binding sites of analyte-specific antibodies, and signal transduction mechanisms, e.g., recombination of the analyte-prosthetic group and the apo-enzyme of the prosthetic group. Although not very commonly used, the ARIS assay system (16) possesses some advantages over the traditional enzyme (whole enzyme) linked homogeneous competitive binding assays, such as high sensitivity, fast read-out time, and potentially a short requisite incubation time.

The present ARIS systems, as discussed in Chapter 5, are all based on FAD-GOx reconstitution and the signal detection relies on a second enzyme (HRP) coupled with this reaction. In order to establish a simpler and sensitive assay scheme, a direct signal

detection of the competitive binding reaction is desired (see Figure 6.2). Such a concept was proposed with the hemin-HRP reconstitution based ARIS assay in Chapter 5. However, the assay for thyroxine was not successful because of the inhibitory effect of the anti-thyroxine antibody and the potential problems associated with the hydrophobicity of hemin. These problems could be circumvented if the PQQ derivatized reagent is developed and further optimized for ARIS in two ways: firstly, the GDH is a relatively stable enzyme compared to HRP; secondly, the hydrophilicity of PQQ will help with the water solubility of the synthesized PQQ-small molecule derivatives, since most of drugs, vitamins, and hormones are hydrophobic in nature. As already demonstrated in Chapter 5, the length of a spacer between PQQ and a target molecule must first be optimized to retain the residual enzymatic activities of the PQQ-small molecule conjugates. The optimized PQQ-small molecule conjugate will then be evaluated with an antibody toward the target molecule. Since the solubility of PQQ is quite good, unlike hemin in the HRP assay system, the PQQ-small molecule conjugate is expected to be free of any inhibitory effect in the presence of an antibody or protein. Another advantage of the PQQ-GDH system over the present FAD-GOx system is that the specific activity of GDH (17) is higher than GOx (18). Therefore, higher signal amplification should be observed with the PQQ-GDH system.

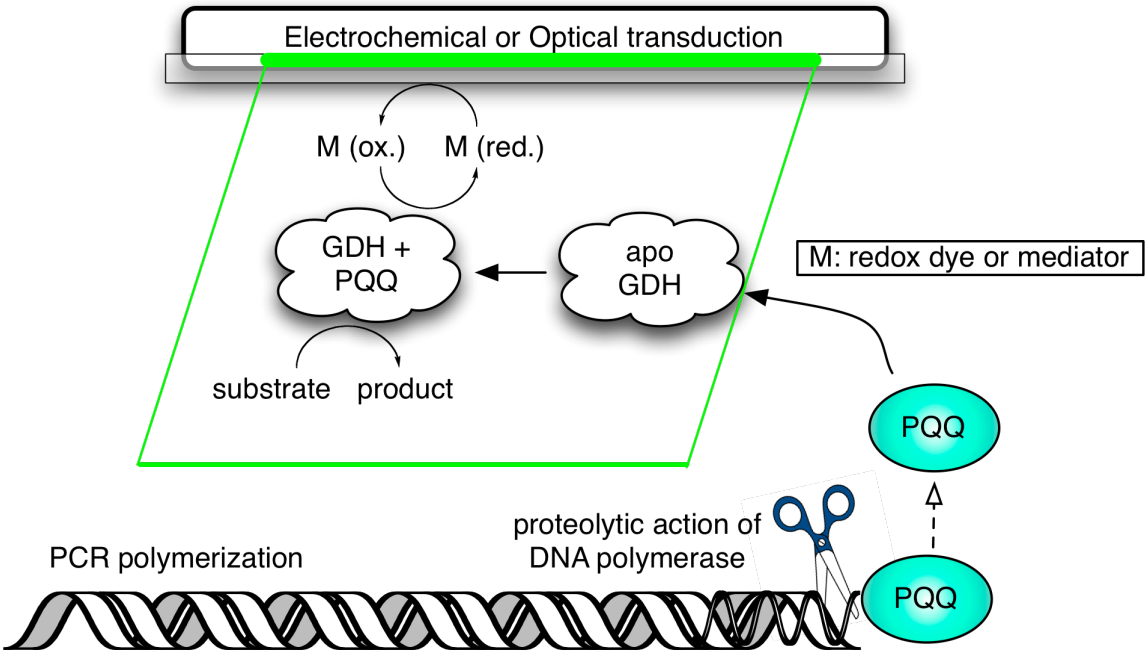

Figure 6.1. Real time PCR based on the DNA derivatized PQQ as a probe.

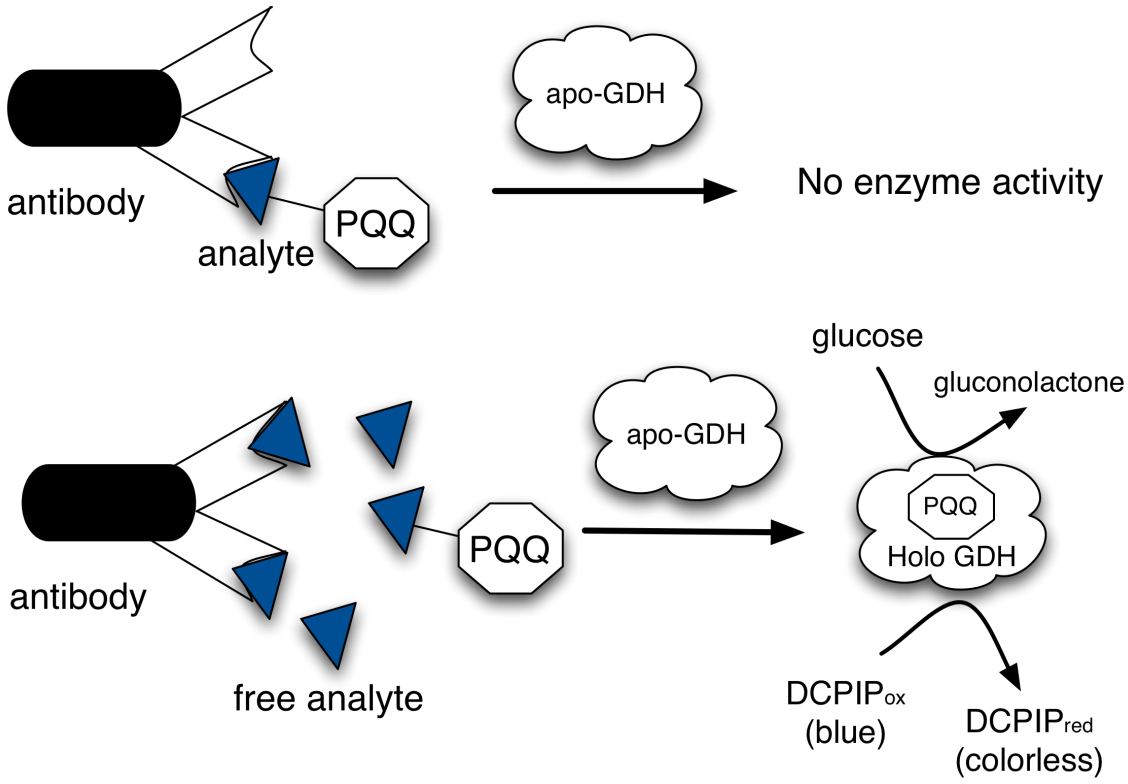

Figure 6.2. Schematic of ARIS based on the GDH-PQQ reconstitution assay.

6.3. References

(1) Sontakke, S.; Cadenas, M.; Maggi, R.; Diniz, P.; Breitschwerdt, E. *J. Microbiol. Meth.* **2009,** *76*, 217-225.

(2) Schweitzer, B.; Kingsmore, S. *Curr. Opin. Biotechnol.* **2001,** *12*, 21-27.

(3) Gurukumar, K.; Priyadarshini, D.; Patil, J.; Bhagat, A.; Singh, A.; Shah, P.; Cecilia, D. *Virol. J.* **2009,** *6*, ARTN 10.

(4) Hindson, B.; Mcbride, M.; Makarewicz, A.; Henderer, B.; Setlur, U.; Smith, S.; Gutierrez, D.; Metz, T.; Nasarabadi, S.; Venkateswaran, K.; Farrow, S.; Colston, B.; Dzenitis, J. *Anal. Chem.* **2005,** *77*, 284-289.

(5) Kane, S.; Letant, S.; Alfaro, T.; Krauter, P.; Mahnke, R.; Legler, T.; Raber, E. *J. Microbiol. Meth.* **2009,** *76*, 278-284.

(6) Bengtsson, M.; Karlsson, H.; Westman, G.; Kubista, M. *Nucleic Acids Res.* **2003,** *31*, ARTN e45.

(7) Mao, F.; Leung, W.; Xin, X. *BMC Biotechnol.* **2007,** *7*, ARTN 76.

(8) Li, X.; Song, C.; Zhao, M.; Li, Y. *Anal. Biochem.* **2008,** *381*, 1-7.

(9) Whitcombe, D.; Theaker, J.; Guy, S.P.; Brown, T.; Little, S. *Nature Biotechnol.* **1999,** *17*, 804-807.

(10) Reynisson, E.; Lauzon, H.L.; Magnusson, H.; Hreggvidsson, G.; Marteinsson, V. *J. Environ. Monitor.* **2008,** *10*, 1357-1362.

(11) Giulietti, A.; Overbergh, L.; Valckx, D.; Decallonne, B.; Bouillon, R.; Mathieu, C. *Methods* **2001,** *25*, 386-401.

(12) Gut, M.; Leutenegger, C.; Huder, J.; Pedersen, N.; Lutz, H. *J. Virol. Methods* **1999,** *77*, 37-46.

(13) Wang, J. *Electroanalysis* **2001,** *13*, 983-988.

(14) Rahman, M.; Shiddiky, M.; Rahman, M.; Shim, Y. *Anal. Biochem.* **2009,** *384*, 159-165.

(15) Isik, S.; Castillo, J.; Blochl, A.; Csoregi, E.; Schuhmann, W. *Bioelectrochemistry* **2007,** *70*, 173-179.

(16) Posthuma-Trumpie, G.A.; Van, D.B., WAM; Van, D.W., DFM; Schaaper, W.; Korf, J.; Van, B. *Biochim. Biophys. Acta (Proteins Proteom.)* **2007,** *1774*, 803-812.

(17) Razumiene, J.; Vilkanauskyte, A.; Gureviciene, V.; Barkauskas, J.; Meskys, R.; Laurinavicius, V. *Electrochim. Acta* **2006,** *51*, 5150-5156.

(18) Kelly, R.L. and Adinarayana, R. C. *Arch. Microbiol.* **1986**, *144*, 248-253.